ABSTRACT

KIM, TAE-HYUNG. Transcription Factor Sp2 Regulates Growth, Differentiation, and Tumorigenesis of Epidermal Stem Cells. (Under the direction of Jonathan M. Horowitz).

Transcriptional regulation requires the collaboration of a variety of proteins, including sequence-specific DNA-binding proteins. Sp proteins are sequence-specific DNA-binding proteins encoded by nine genes that control the expression of a constellation of mammalian genes including genes required for cell-cycle control, differentiation, and development. De-regulation of Sp protein abundance and/or activity has been associated with a variety of maladies, including cancer, however direct evidence implicating any given Sp-family member has been lacking. Although the biochemical and functional properties of many Sp proteins are well-understood others, such as Sp2, have received relatively little attention. Prior to the initiation of the work to be reported here, little was known about the requirement for Sp2 for mammalian development nor was it known if the de-regulation of Sp2 plays an important role in tumorigenesis. A major goal of the research to be described was to determine whether Sp2 over-expression is oncogenic.

To initiate these studies, I generated transgenic mouse lines that over-express an epitope tagged mouse Sp2 cDNA in epidermal progenitor cells. Two transgenic mouse lines were identified and termed Sp2-A and Sp2-C. An additional transgenic mouse line, termed Sp2-NotI, was generated that over-expresses a mutated Sp2 protein that lacks DNA binding activity. The integration sites for the transgenes carried by Sp2-A and -C mice were determined to be on mouse chromosomes 6 and 5, respectively. Transgene integration occurred within an intergenic region of chromosome 6, whereas integration on

chromosome 5 resulted in the disruption of Latrophilin 3 (Lphn3). Lphn3 encodes a brain-specific G protein-coupled receptor of uncertain functional significance. Transgene expression in Sp2-C animals is ten-fold greater than that in Sp2-A mice and three-fold greater than in Sp2-NotI mice. Sp2-A, Sp2-C, and Sp2-NotI hemizygous animals are viable and fertile. Sp2-A and Sp2-NotI hemizygotes develop alopecia following weaning, whereas Sp2-C animals do not. Sp2-A and -C homozygotes perish prior to post-natal day 13 due to a severe disruption of the epidermal differentiation program. Sp2-C hemizygotes are at increased risk of developing tumors following exposure to environmental carcinogens and are extremely susceptible to wound-induced neoplasia. In contrast, (i) Sp2-NotI animals are more resistant to tumorigenesis induced by chemical carcinogens than wild-type littermates, and (ii) Sp2-A and Sp2-NotI hemizygotes exhibit delayed wound healing.

Primary keratinocyte cultures prepared from each transgenic strain were characterized for their growth properties *in vitro*. In contrast to cultures prepared from wild-type animals, primary keratinocyte cultures derived from transgenic animals proliferate poorly and are characterized by large numbers of apoptotic cells. Cell-cycle analyses revealed that the majority of Sp2-A, -C, and -NotI keratinocytes are arrested in all cell-cycle compartments, and DNA synthetic capacity is reduced significantly relative to wild-type keratinocytes. When these *in vitro* data are taken together with *in vivo* results, I conclude that Sp2 over-expression is a "driver" of tumorigenesis and that Sp2 regulates the proliferation and differentiation of epidermal progenitor cells. Moreover, I speculate that that Sp2 may be a useful target for anti-cancer therapeutics.

Transcription Factor Sp2 Regulates Growth, Differentiation, and Tumorigenesis of Epidermal Stem Cells

by
Tae-Hyung Kim

A dissertation submitted to the Graduate Faculty of
North Carolina State University
in partial fulfillment of the
requirements for the Degree of
Doctor of Philosophy

Comparative Biomedical Sciences

Raleigh, North Carolina

2011

APROVED BY:

_____	_____
Dr. John M. Cullen	Dr. Robert C. Smart
_____	_____
Dr. Jonathan M. Horowitz Chair of Advisory Committee	Dr. Troy H. Ghashghaei

DEDICATION

Если жизнь тебя обманет…

Алекса´ндр Серге́евич Пу́шкин,
(1799–1837)

Если жизнь тебя обманет,
Не печалься, не сердись!
В день уныния смирись:
День веселья, верь, настанет.

Сердце в будущем живет;
Настоящее уныло:
Всё мгновенно, всё пройдет;
Что пройдет, то будет мило.

IF BY LIFE YOU WERE DECEIVED…

Aleksandr Sergeyevich Pushkin
(1799–1837)

If by life you were deceived,
Don't be dismal, don't be wild!
In the day of grief, be mild
Merry days will come, believe.

Heart is living in tomorrow;
Present is dejected here;
In a moment, passes sorrow;
That which passes will be dear.

BIOGRAPHY

Tae-Hyung Kim was born (June 9, 1979) and raised in Seoul, South Korea.

Education

2006 – Present	North Carolina State University, Raleigh, NC Department of Molecular Biomedical Sciences Laboratory of Dr. Jonathan M. Horowitz, Ph.D. Graduate program in Comparative Biomedical Sciences
2003 – 2005	Seoul National University, Seoul, South Korea Department of Biochemistry and Molecular Biology Laboratory of Dr. Jeong-Sun Seo, M.D., Ph.D. Graduate program in Molecular Genomic Medicine M.S. in Medicine, 2005
1998 – 2002	Sungkyunkwan University, Suwon, South Korea Department of Biological Sciences B.S. in Biology, 2002

ACKNOWLEDGEMENTS

I would like to thank my advisor, Dr. Jonathan Horowitz, for his guidance and continuous support that nurtured me as a scientist. I acknowledge that without his help, this study would have not been finished.

I also would like to thank my committee members, Dr. John Cullen, Dr. Robert Smart, and Dr. Troy Ghashghaei, for their valuable advice and support.

Lastly, I would like to thank my family and friends for their loves and support.

TABLE OF CONTENTS

LIST OF TABLES

LIST OF FIGURES

Chapter 1

1. Introduction

1.1 General introduction to mammalian transcription factors

Gene expression is regulated at multiple levels, including transcriptional initiation, mRNA degradation, and protein translation. Transcription is tightly regulated by numerous proteins that together ensure that genes are expressed at the correct time in the proper place. One class of proteins responsible for the regulation of transcription is typified by transcription factors that bind DNA specifically. Sequencing of the human genome revealed approximately 20,000 - 25,000 protein-coding genes (1), and sequence-specific DNA-binding proteins form the second largest functional category (2). Sequence-specific DNA-binding proteins are sub-divided into structurally distinct families based on the precise structural motifs utilized to bind DNA. The largest family of sequence-specific DNA-binding proteins in the human genome, represented by some 700 genes (3% of total protein-coding genes), bind to DNA via structural motifs termed zinc-"fingers" (3). The Cys_2-His_2 sub-class of zinc-"finger" proteins are the most common DNA-binding motif found in humans (2, 4). Indeed, analysis of genes encoded by the human genome revealed approximately 900 members of the Cys_2-his_2 sub-class of zinc-“finger” proteins amongst more than 2,000 hypothetical genes that encode transcriptional activators including Cys_2-His_2 zinc-“finger”, Homeo box, Helix-loop-helix DNA binding, Basic leucine zipper (bZIP), Forkhead transcription factors and so on in the human genome (5). The reason why there is a difference between 700 and 900 in the number of estimation of zinc-“finger” proteins is those estimations are based on various algorithms used in different references. One family of mammalian Cys_2-His_2 zinc-"finger" proteins is encoded by the Sp/XKLF (specificity protein/Krüppel-like factor) family of

mammalian transcription factors. The Sp/XKLF family is comprised of two major subgroups, the Sp proteins (nine members) and the KLFs (17 members), the latter sub-family deriving its name due to sequence homology with the *Drosophila* gap gene *Krüppel* (6, 7). Sp/XKLF-family members share an evolutionarily-conserved DNA-binding domain at their respective carboxy-termini, whereas other portions of these proteins are considerably more diverse.

Sp1 is the first mammalian transcription factor to be cloned (8, 9). Its name initially referred to the requirement for the use of Sephacryl and phosphocellulose columns for purification, however the "Sp" designation soon reflected its designation as Specificity protein 1 (10). Closely related proteins were identified subsequently and named Sp2, Sp3 (SPR-2), and Sp4 (SPR-1) (11, 12). In addition to Sp1-4, smaller proteins sharing a similar DNA-binding domain were identified and named Sp5, Sp6 (KLF14, Epiprofin), Sp7 (Osterix), Sp8 (mBtd), and Sp9 (13-18). Previous studies have reported that Sp- family members are expressed widely in mammalian tissues. Sp1 is expressed ubiquitously in mouse embryos (19). Saffer *et al.* reported that Sp1 expression is variable during mouse development based on the analysis of Sp1 mRNA in 11 tissues from age of 5 to 64 post-natal days. In addition, Sp1 is highly expressed in developing hematopoietic cells, neural tissues in fetus and spermatids suggesting that Sp1 may play a role in differentiation (19). Like Sp1, Sp3 is expressed ubiquitously in early mouse embryos (20). Recently our lab reported that Sp2 is expressed in 16 adult mouse tissues using RT-PCR analysis although often at relatively low levels, and variably (skin, stomach, intestine are low whereas thymus is high) (21). Unlike Sp1 and Sp3, Sp4 is expressed in a tissue-specific manner. Sp4 is expressed predominantly in

brain, testis, epithelial tissues, and developing teeth (10, 20). Sp5-9 are also expressed widely in mouse tissues. Additional details regarding the expression of Sp proteins will be discussed in section 1.4.1.

1.2 Biochemical and functional properties of Sp family members

1.2.1 Structural and functional properties of the DNA-binding domain

Members of the Sp family of transcription factors share a highly-conserved carboxy-terminal DNA binding domain (Figure 1) (22). The DNA binding domain consists of three Cys_2-His_2 zinc "fingers" that are required for high-affinity interactions with GC-rich promoter elements, e.g., GC-box (5'-GGGGCGGGG-3') and GT/CACC-box (5'-GGTGTGGGG-3'), often in close proximity to sites of transcriptional initiation (23). Each zinc-"finger" contains 21-23 amino acids that are separated from one another by seven-amino acid spacers, which are also highly conserved. A single zinc ion is chelated by each zinc-"finger" (Figure 1). Crystal structures of the DNA-binding domains of Sp proteins have not as yet been reported. However, X-ray crystallographic studies of TFIIIA, a related zinc-"finger" protein, and a Zif268 protein-DNA complex have suggested that zinc-"fingers" bind to the G-rich strand of the nine base pair recognition sequence in a 3'-to-5' fashion (7, 24). DNA-binding studies have shown that Sp proteins have similar affinities for their cognate GC-rich sites, e.g. Sp1 exhibits an equilibrium dissociation constant (K_d) of 410-530pM for its consensus-binding site (5'-GGGGCGGGGC-3') and Sp2 binds its consensus-binding site (5'-GGGCGGGAC-3') with a K_d of 225pM (25, 26). The amino-acid sequences of the three zinc-"fingers" of Sp1, Sp3, Sp4, and Sp5 are highly conserved (more than 90%) whereas Sp2 and Sp6 exhibit less

sequence homology, 75% and 85%, respectively (7, 10, 27). Even though the overall amino-acid sequences of the three zinc-"fingers" carried by Sp proteins is well conserved, subtle amino acid differences within the zinc-"fingers" account for differences in the DNA-binding specificity of each family member (7). It is not known whether sequence variations in the inter-"finger" linker region contributes to the sequence specificity of Sp proteins. Most Sp-family members encode nuclear localization sequences adjacent to, or within the zinc-"finger" motif. (28, 29).

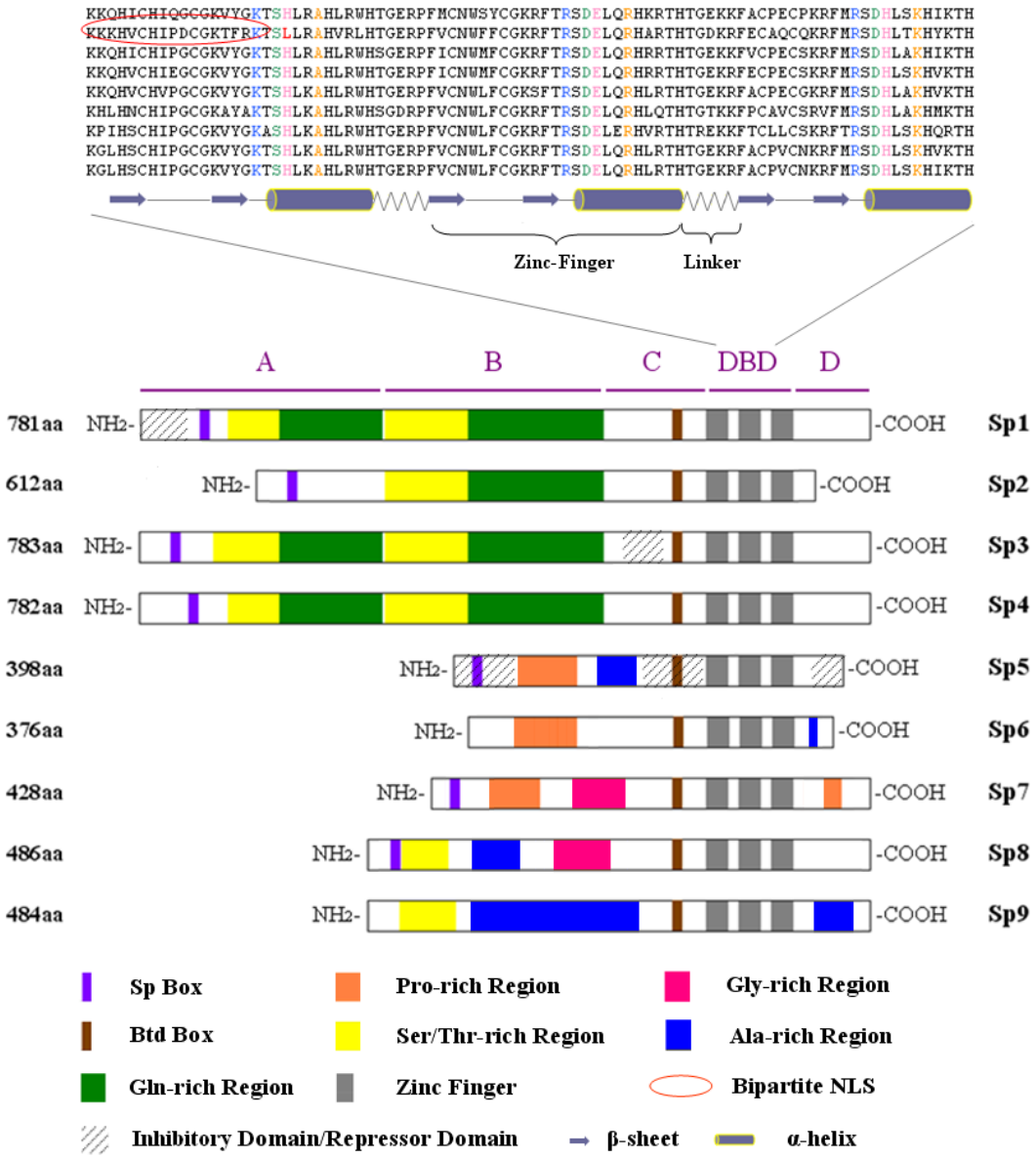

Figure 1 Conserved domains in Sp transcription factors. The *trans*-activation domain consists of domains A, B and C. The A and B domains carry alternating serine/threonine-rich and glutamine-rich regions and the C domain contains highly charged amino acids. The Cys_2His_2 zinc-"fingers" of the DNA-binding domain (DBD) consists of highly-conserved zinc-"finger" and linker sequences. The carboxy-terminal D domain is required for multimerization of Sp proteins. Sp1, Sp3, and Sp5 encode "inhibitory domains" that antagonize *trans*-activation.

1.2.2 Structural and functional properties of the *trans*-activation and multimerization domains

Four structurally-distinct regions flanking the DNA-binding domain, termed domains A, B, C, and D have been defined in Sp-family members and their contributions to Sp1-4 transcriptional activity have been analyzed (Figure 1). Domains A and B are encoded at the extreme amino-terminus of Sp proteins and in Sp1, 3, and 4 consist of sub-regions that feature alternating glutamine- (~25% glutamine) and serine/threonine-rich (~50% serine and threonine) residues (30). In contrast, Sp2 encodes only domain B. The glutamine-rich sub-domains are believed to be responsible for *trans*-activation whereas the functions of the serine/threonine-rich sub-domain are less understood (31). The serine/threonine-rich regions of Sp1 have been reported to be targets of glycosylation that regulate protein/protein interactions (32, 33). Domain C is adjacent to the first zinc-"finger" and contains the so-called Buttonhead (Btd) box as well as highly-charged amino acids. The presence of the Btd box distinguishes Sp-family members from XKLF proteins. Little is known about the precise functional significance of the Btd box, however it is likely that it is functionally important since it is conserved in Sp-related factors in *Drosophila* and *C. elegans* (22). Domain C encodes numerous charged amino acids and is well conserved among Sp-family members (22, 30, 34). Domain D is located at the extreme carboxy-terminus and has been shown to be required for multimerization of Sp1 and synergistic *trans*-activation (35). Another structural feature of many Sp proteins is that they share a stretch of 13 amino acids, termed the Sp box, at their amino termini. The function(s) of the Sp box has not as yet been elucidated. The *trans*-activation domains of Sp5-9 have not

been defined, although they share many of the domains and sub-domains carried by other members of the Sp family (36). It is worth noting that Sp1, Sp3, and Sp5 encode "inhibitory domains" that function to antagonize *trans*-activation. The Sp1 "inhibitory domain" is encoded at the extreme amino-terminus (amino acids 1-82) (37, 38), whereas a functionally analogous domain in Sp3 is encoded within the C domain (amino acids 547-559) (39, 40).

1.3 Regulation of the Sp transcription factor family

Sp1 is the best characterized member of the Sp family. Sp1 acts as a *trans*-activator of both proximal promoter elements as well as distal enhancers (41). Sp1 *trans*-activation has been reported to be regulated by a variety of post-translational modifications. For example, phosphorylation of Sp1 by Akt in phosphatidylinositol-3-kinase (PI3K) pathway increases vascular endothelial growth factor (VEGF) expression in several prostate cancer cell lines (42). In addition to PI3K, various kinase pathways, e.g., mitogen-activated protein kinase (MAPK), cyclin A- dependent kinase, and protein kinase C (PKC), have been reported to play a role in phosphorylation of Sp1 (36). Glycosylation of Sp1 results in the repression of *trans*-activation without affecting DNA-binding activity *in vitro* (43). Acetylation is also reported to play a role in the induction of Sp1 *trans*-activation in pancreatic cancer cell lines. Treatment of cancer cell lines with trichostatin A (TSA), an inhibitor of histone deacetylases, increased Sp1 acetylation and transcription of the transforming growth factor beta type II receptor (TbetaRII) (44). The amino-terminus of Sp1 has been reported to be subject to cleavage by proteasome-dependent degradation at Leu^{56} and Leu^{57} (45). Recently, Sp1 was reported to be sumoylated *in vivo* with a high-probability sumoylation consensus motif,

$VK^{16}IE^{18}$, and sumoylation of this lysine residue is critical to prevent proteasome-dependent cleavage of this domain. As a result, sumoylation of Sp1 inhibits Sp1-dependent transcription due to increased stability of the negative regulatory domain of Sp1 (46). In addition to the aforementioned post-translational modifications, the activities of Sp proteins are regulated by protein/protein interactions (47). For example, Sp1 forms homotypic multimeric complexes as well as heterotypic interactions with numerous nuclear proteins such as the TATA-box binding protein (TBP) and TBP-associated factors (TAFs), which can result in transcriptional activation (31, 36).

Sp3 is another well-studied member of the Sp-family and its characterization has revealed properties not shared by Sp1 or other members of the Sp family. Sp3 has been termed a bifunctional transcription factor in that it has been reported to *trans*-activate or repress the transcription of target genes. Sp3 function is complicated, however, by the fact that the Sp3 gene encodes three functionally distinct isoforms: a full-length protein termed Sp3 (110-115kDa) and two smaller isoforms (60-70kDa) termed M1 and M2 that are synthesized via internal translational initiation (48). M1 and M2 function as potent transcriptional repressors or are transcriptionally inactive in certain promoter settings (48, 49). All three isoforms carry a lysine residue (K539) embedded within a consensus sumoylation motif and this lysine is the major site of sumoylation *in vivo*. Mutations that prevent sumoylation of M1/M2 *in vivo* convert these Sp3 isoforms into transcriptional activators, whereas an analogous mutation in Sp3 only marginally increases transcriptional activity (48). Sumoylation of Sp3 has been reported to modulate its sub-nuclear localization

(50). Although the precise mechanism that accounts for transcriptional repression by M1/M2 following sumoylation is still unknown, it is believed that sumoylation recruits co-repressors that are then tethered to DNA via the Sp3 DNA-binding domain. In addition to sumoylation, activity of Sp3 can be regulated by acetylation. Repression of transcription by Sp3 can be histone deacetylase (HDAC) dependent or independent (51, 52). As for Sp1, *trans*-activation by Sp3 has been reported to be enhanced by acetylation *in vivo* (53, 54).

1.3.1 Biochemical and functional properties of Sp2

Sp2 carries the least conserved DNA binding domain (75% amino acid identity) amongst Sp-family members, and binds a nonameric consensus DNA-binding sequence (5'-GGGCGGGAC-3') with high affinity (225pM) *in vitro* (7, 26, 27, 55). In keeping with the contention that Sp-family members have distinct DNA-binding specificities, Sp1 and Sp3 exhibit significantly less affinity for the Sp2 consensus sequence (700pM and 8.9nM, respectively) (26). In the absence of *bona fide* Sp2 target genes, artificial promoter constructs, such as dihydrofolate reductase (DHFR), have been utilized to assess Sp2 transcriptional activity (26). The DHFR promoter is regulated by Sp1/Sp3 *in vivo* via four well-characterized GC-rich promoter elements (56). To assess Sp2 transcriptional activity, these four elements were mutated to generate consensus Sp2-binding sites and the transcriptional activity of this "Sp2-specific" DHFR reporter gene was examined in transient co-transfection assays with a Sp2 expression vector. Co-expression of Sp2 led to a mild increase in DHFR reporter activity, whereas the co-expression of Sp1 or Sp3 led to robust levels of transcription. Indeed, Moorefield *et al*. reported that transient over-expression of

Sp1 resulted in a 300-fold induction of DHFR promoter activity. Transient over-expression of Sp3 resulted in a 200-fold induction, whereas Sp2 transfection resulted in little changes in DHFR transcription (26). To determine if one or more portions of Sp2 limited its capacity to stimulate transcription, a series of Sp1/Sp2 chimeras were created by swapping analogous portions of Sp2 with those of Sp1 and examined in transient co-transfection assays with the "Sp2-specific" DHFR reporter gene. These chimera experiments revealed that both the Sp2 *trans*-activation and DNA-binding domains were negatively regulated *in vivo*. Consistent with these results, little or no Sp2 DNA-binding activity was detected in many human and mouse cell lines examined *in vitro* protein/DNA-binding assays. When taken together, these results indicate that Sp2 is functionally distinct from other Sp-family members and suggest that Sp2 may have a unique role in cell physiology (26).

Given the widespread expression of Sp2 and yet the surprising absence of detectable Sp2 DNA-binding activity, experiments were performed to compare its subcellular localization with that of other Sp-family members. Western blots of mechanically-fractionated cell extracts indicated that virtually all Sp2 protein is associated with the nuclear matrix, whereas Sp1/Sp3 are localized in both soluble and insoluble nuclear fractions (57). To confirm this result, the subcellular localization of an EYFP-Sp2 fusion protein was determined in COS-1 cells. This EYFP-Sp2 fusion localized to discrete nuclear foci that are stably associated with the nuclear matrix and that are distinct from promyelocytic (PML) oncogenic domains (PODs). Deletion analyses indicated that a 37 amino acid sequence (amino acids 513-549) spanning the first zinc-"finger" of Sp2 is

required for nuclear matrix association. These amino acids are the most divergent amongst Sp-family members, perhaps accounting for Sp2's unique subnuclear localization (57).

Recently, *socs1* was identified as a Sp2 target gene in mouse and human cells (58). Suppressors of cytokine signaling (SOCS) proteins are negative regulators of signaling directed by the Janus-family of kinases (JAK) and signal transducers and activators of transcription signaling (STAT) proteins (59, 60). SOCS1, one of eight members of the SOCS gene family, is a critical regulator of IFN-γ signaling and is transcribed rapidly after stimulation by various cytokines (58). The mouse *socs1* promoter carries a Sp2 consensus sequence proximal to an interferon regulatory factor binding element (IRF-E), and Sp2 and IRF-1 were reported to physically interact on the *socs1* promoter. Using Sp2 siRNAs, the authors reported that Sp2 is required for the transcriptional expression of *socs1* after IFN-γ stimulation in both mouse and human cells (58). To my knowledge, this study is the first to reveal a target gene (*socs1*) and a binding partner (IRF-1) of transcription factor Sp2.

1.4 The roles of Sp-family members in animal development and cancer

1.4.1 Development

With the completion of human genome project, thousands of potential Sp1 target genes were predicted based on frequency of Sp1 consensus binding sites in the genome. In reality, however, it is very likely that this is an over-estimate of the true number of Sp1 target genes. Cawley *et al.* reported a functional screen in which 353 Sp1 binding sites were identified on human chromosomes 21 and 22 based on chromatin immunoprecipitation and

high density oligonucleotide arrays (61). In some instances, predicted Sp1 target genes have been validated experimentally. Vascular endothelial growth factor (VEGF) is a key mediator of angiogenesis. The human VEGF promoter encodes three potential Sp1-binding sites, and Sp1 and Sp3 were shown to physically interact with these sites in nuclear extracts using gel "super-shift" assays (62). DNA methyltransferases (DNMTs) play pivotal roles in the development of cancer (63), and the promoters of two DNMTs (DNMT3A and DNMT3B) encode several Sp1-binding sites. Physical interaction between these binding sites and Sp1/Sp3 was also confirmed by in gel-"shift" assays (64). Since angiogenesis and DNA methylation are critical events during development, those reports imply that Sp1 plays pivotal roles in animal development. I will describe more evidences that Sp1 is required for the development below.

Consistent with its necessity for the regulation of many target genes, elimination of Sp1 in mouse embryos via Cre-mediated recombination results in the retardation of development due to a broad range of abnormalities, and all embryos perish *in utero* by embryonic day 10 (E10). To determine if the requirement for Sp1 is cell autonomous, Sp1-null embryonic stem cells were injected into wild-type blastocysts and the contribution of nullizygous cells to the developing embryo was analyzed. Chimeric embryos developed normally at early stages, but Sp1-null cells declined rapidly after embryonic day 11 (65). These results indicate that Sp1 is an essential gene *in vivo* and is required cell autonomously. Surprisingly, however, deletion of Sp1 had little or no effect on the viability or proliferation of mouse embryo fibroblasts *in vitro*. Moreover, many Sp1 target genes continued to be

expressed in these cells. Thus, although required absolutely *in vivo* other Sp-family members can compensate for the loss of Sp1 *in vitro*.

To evaluate the requirement for Sp2 for animal development, two approaches have been adopted. First, the zebrafish Sp2 orthologue was cloned and shown to be closely-related to human and mouse Sp2 with respect to sequence, sub-cellular localization, and function (66). Zebrafish Sp2 was shown via RT-PCR to be a maternally-inherited transcript in unfertilized eggs, and zygotic transcription of zebrafish Sp2 begins 3 hours after fertilization. *In situ* hybridization confirmed that zebrafish Sp2 is expressed at the earliest stages and throughout development, as well as in adult tissues (66). To determine whether Sp2 is an essential gene, zebrafish Sp2 was eliminated by microinjection of embryos with gene-specific morpholinos. Morpholinos that prevent splicing of Sp2 message or translation resulted in the arrest of zebrafish development in gastrulation (66). Second, recent studies from our lab as well as another group have shown that Sp2 is essential for mouse embryogenesis (67)(Haifeng Yin, personal communication). Sp2-null embryos survive until E9.5 of gestation whereas $Sp2^{wt/ko}$ embryos develop normally. In contrast to results for Sp1, conditional elimination of Sp2 in cultures of mouse embryo fibroblasts leads to growth arrest (67). These data further strengthen the notion that the functions of Sp-family members may only partially overlap. The precise role(s) of Sp2 in the regulation of cell physiology and development remains to be determined.

Sp3 does not appear to be required for the completion of mouse development, however newborn nullizygotes invariably perish 10 mins after birth due to respiratory failure. Additionally, Sp3 nulls exhibit dental deficiencies due to defective expression of ameloblast-specific transcripts, skeletal defects due to insufficient numbers of osteoblasts, and deficiencies of T and B lymphocytes as well as erythrocytes. (68-71).

In contrast to Sp1 and Sp3, Sp4 is expressed in a tissue-specific manner. Sp4 is expressed beginning on mouse embryonic day 9 in the posterior neuropore. As development proceeds, Sp4 is expressed highly in the central nervous system and Sp4 expression is maintained predominantly in the brain in adults but is also detectable in epithelial tissues, testis, and teeth. Sp4 deficient mice exhibit normal development *in utero*, but two-thirds of newborn mice perish within four weeks of birth due to unknown causes. Surviving Sp4 deficient animals show growth-retardation and defects in reproduction. Sp4 nullizygous males fail to breed in spite of normal spermatogenesis, and the onset of sexual maturation in Sp4 nullizygous females is delayed. The failure of males to mate is probably due to abnormal reproductive behavior even though the structure and histology of tissues responsible for reproductive behavior, such as the hypothalamus and the vomeronasal organ, are normal (11, 72, 73).

Sp5 expression is remarkably dynamic throughout mouse development. Two distinct expression patterns have been identified: expression during gastrulation and a second wave of expression during organogenesis. During early gastrulation, Sp5 expression is detected in

the primitive streak and expression is confined to the central nervous system, somites, and pharyngeal regions in later stages of gastrulation. During organogenesis (subsequent to E8), Sp5 is detected largely in the developing brain and spinal cord (13, 74). Sp5 nullizygotes do not exhibit obvious developmental abnormalities, suggesting that its functions are supplanted by other Sp-family members. In this regard it is worth mentioning that Sp5 shares little sequence similarity to other Sp-family members outside of the DNA binding domain (20, 74).

Sp6, also called KLF14, is expressed in many adult mouse tissues (e.g., skeletal muscle, kidney, testis, lung, spleen, brain, liver, and heart) as detected by RT-PCR (14). Sp6 generates two distinct transcripts, termed Sp6 and epiprofin, differing in their utilization of alternative non-coding exons (75). During mouse development Sp6 and epiprofin transcripts are expressed largely in embryonic dental epithelium, in differentiated odontoblasts of newborns, in the inner root sheath of hair follicles, and in the apical ectodermal ridge of developing limbs (76). Sp6 null mice exhibit severe alopecia, reduced body weight, defective teeth, mild forms of syndactyly and oligodactyly, and defective lung alveolarization (77).

A Sp7 cDNA was isolated from mouse osteoblasts and named Osterix (Osx) (15). Soon after, its human orthologue and alternatively-spliced isoforms were identified (78, 79). A longer isoform encodes a 431-residue protein whereas a shorter isoform encodes a 413-residue protein lacking amino-terminal residues. The short isoform is most abundant in humans. Human and mouse Sp7 share 95% amino acid sequence identity. Although low

level expression of Sp7 is detected in a variety of tissues (e.g., testis, heart, brain, placenta, lung, pancreas, ovary, and spleen), Sp7 expression in humans is largely confined to osteoblasts and chondrocytes of all endochondral and membranous bones (78, 79). Consistent with its expression pattern, Sp7 plays an important role in osteoblast differentiation and bone formation. Sp7/Osx null mice do not form cortical bone or bone trabeculae. Newborn homozygous null animals have difficulty breathing, rapidly become cyanotic, and die within 15 mins after birth (15). Since Sp7/Osx null osteoblasts express Runx2/Cbfa1 (a transcription factor required for bone formation) and Sp7/Osx is not expressed in Runx2/Cbfa1 null mice, it is likely that Sp7/Osx is a Runx2/Cbfa1 target gene (15).

Sp8 was originally identified as the murine orthologue of *Drosophila* Buttonhead (Btd) and termed mouse Btd (mBtd) (18). The human orthologue has three exons, and two transcript variants have been identified that are conserved in mice and zebrafish. The Sp8 gene consists of two 5' UTR exons and a third exon containing all of the coding and 3' UTR sequences. Two isoforms carry distinct first exons (either exon 1 or 2) and a common second exon (exon 3); the larger isoform encodes a 508-residue protein and the smaller isoform encodes 490-residue protein (16, 80). Sp8 is detected in embryonic ectoderm and the primitive streak during gastrulation and is followed by restricted expression in the tail bud. Sp8 is expressed in the central nervous system during organogenesis and in the apical ectodermal ridge (AER) of limb buds. Consistent with its expression pattern, targeted deletion of Sp8 results in severe truncation of the posterior axial skeleton as well as defects

in anterior and posterior neuropore closure leading to exencephaly, spina bifida, and death at birth (80). Sp8/mBtd plays critical roles in early limb development and this role is well conserved in invertebrates and vertebrates (18, 20).

Sp9 is similar to Sp8 both in its structure and tissue-specific expression pattern. As for Sp8, mouse Sp9 is expressed in the AER and regulates limb outgrowth. Sp9 expression occurs in the midbrain/hindbrain boundary and in the AER of the developing limbs of chickens. In zebrafish, Sp9 is expressed in the forebrain, in the prospective midbrain/hindbrain boundary during early somitogenesis, and in the hindbrain and the apical fold of the developing pectoral fin in later stages. Fibroblast growth factor 10 (FGF10) is known to positively regulate Sp9 expression during vertebrate limb outgrowth (17, 81). Since mice nullizygous for Sp9 knockout have not been reported, phenotypes associated with Sp9 nullizygosity remain to be discovered.

When taken together, the results of gene targeting studies indicate that most Sp-family members perform unique and essential roles in animal development that cannot be supplanted by other Sp-family members or additional GC box-binding proteins.

1.4.2 Cancer

Sp proteins are responsible for the expression of a variety of genes required for cell-cycle progression, differentiation and development (31, 36, 82). A variety of evidence indicates that the de-regulated expression of Sp proteins may play a critical role in tumor

development, progression, and metastasis. However, most of these studies have focused on Sp1.

Wang and colleagues reported that Sp1 expression is increased in gastric tumor cells, that elevated Sp1 expression levels are correlated with increased mortality rates, and Sp1 protein expression levels in pancreatic cancers can be used as a prognostic marker (83, 84). In keeping with the earlier observation that Sp1 stimulates VEGF expression, the expression of VEGF is increased in pancreatic and gastric cancers (84, 85). In addition to VEGF, Sp1 over-expression is correlated with the up-regulation of a number of additional proteins that play important roles in tumorigenesis, including urokinase plasminogen activator (uPA) and its receptor (uPAR), the hepatocyte growth factor receptor (HGFR/MET), and the epithelial growth factor receptor (EGFR) (86-88). Sp1 protein expression is elevated in breast carcinomas, thyroid tumors, colon tumors, and epidermal tumors (86, 89-91). Lou *et al.* reported that human fibrosarcoma cell lines over-express Sp1 and formed tumors in athymic mice. Consistent with the need for continuous Sp1 over-expression to drive tumorigenesis, down-regulation of Sp1 protein expression in these human cells eliminated or reduced tumor formation (92). A more recent study reported that Sp1 is up-regulated in human gliomas and promotes MMP-2 mediated invasion, resulting in poor clinical outcomes (93). Taken together, these correlative studies indicate that deregulated expression and activation of Sp1 can play an important role in cancer development and progression.

Prior to beginning my thesis research, a single study reported a putative link between de-regulated Sp2 expression and tumorigenesis (94). Phan *et al.* reported that Sp2 expression is elevated in human prostate cancers and that Sp2 expression levels are correlated directly with tumor progression. In this pioneering study Sp2 expression was inversely correlated with that of carcinoembryonic antigen-related cell adhesion molecule 1 (CEACAM1), a tumor-suppressor gene that is down-regulated in several malignancies including prostate cancer (95, 96). Phan *et al.* reported that Sp2 was bound to the CEACAM1 promoter in a Dunning rat-derived prostate adenocarcinoma cell line and that CEACAM1 transcription was down-regulated by ectopic Sp2 expression in normal prostatic epithelial cells. Combined with evidence mentioned above that Sp2 is required for cell-cycle progression of mouse embryo fibroblasts, these results suggest that Sp2 over-expression can drive cell proliferation.

Sp3 has been reported to have a dual role as an inducer of apoptosis and as a marker of tumor aggressiveness (97). Essafi-Benkhadir *et al.* generated normal (Chinese hamster lung fibroblast) and tumor (colon carcinoma cells) cell lines that express an epitope-tagged full-length Sp3 protein under the control of a tetracycline-responsive promoter. The authors found that conditional expression of full-length Sp3 reduced tumor development in nude mice due to the induction of apoptosis. In addition, the authors reported that Sp3 is a caspase substrate and cleavage of Sp3 by caspases facilitated tumor cell survival (98). Interestingly, when Sp3 was over-expressed in established tumors it caused transient tumor regression followed by tumor progression, and tumor progression

coincided with re-accumulation of full-length Sp3. Lastly, patients with head and neck tumors showed poor prognosis for overall survival if full-length Sp3 was expressed highly (99).

Links between Sp4 expression and cancers have also been reported. Colon cancer cells treated with Cyclooxygenase 2 (COX-2) inhibitors, such as celecoxib (Cel), nimesulfide (NM) and NS-398, exhibit a marked reduction in the expression of vascular endothelial growth factor (VEGF). Abdelrahim *et al.* showed that decreased VEGF expression is accompanied by decreased levels of Sp1 and Sp4. Treatment with COX-2 inhibitors did not affect Sp1 or Sp4 mRNA levels, instead the degradation of these proteins was stimulated via increased ubiquitinylation. These results indicate that proteasome-dependent degradation of Sp1 and Sp4 plays a critical role in VEGF expression in colon cancer cells (100).

When taken together these results indicate that Sp proteins can impact tumor cell proliferation, and tentative links between de-regulated Sp protein expression and tumorigenesis have been noted. Prior to beginning my thesis research, however, direct evidence that any Sp protein is oncogenic was lacking.

1.5 Thesis aims

Prior to beginning my thesis research, evidence developed in the Horowitz lab indicated that (i) Sp2 is over-expressed in mouse skin squamous cell carcinomas and (ii) Sp2 over-expression is correlated directly with tumor progression. Taken together with

evidence (Phan *et al.*) linking Sp2 expression with human prostate cancers, I proposed to test the hypothesis that Sp2 over-expression is oncogenic. To test this hypothesis I generated transgenic mouse lines in which Sp2 expression is elevated in basal keratinocytes, the cell of origin of skin squamous cell carcinomas. I characterized gross phenotypes exhibited by the transgenic lines and showed that they are at increased risk of tumorigenesis elicited by environmental carcinogens. Perhaps more interestingly, I showed that some of these animals were susceptible to wound-induced papillomagenesis. Finally, I prepared primary mouse keratinocyte cultures from these transgenic animals to identify mechanisms underlying the regulation of their growth and differentiation. In the following chapters I will present biochemical, cellular, and genetic evidence indicating that Sp2 is an important player in the regulation of keratinocyte proliferation, differentiation, and tumorigenesis.

Chapter 2

2. Materials and methods

2.1 Transformation of bacterial cells

Competent DH5α cells were used for transformation. Plasmid DNAs to be amplified or ligation mixtures for cloning were combined with thawed competent cells and incubated on ice for 30 min. The competent cell/DNA mixture was heat-shocked at 42°C for 30 sec followed by incubation on ice for 2 min. After adding 250 µl of Super Optimal broth with Catabolite repression (SOC; 2% bacto-tryptone, 0.5% bacto-yeast extract, 10 mM NaCl, 2.5 mM KCl, 10 mM $MgCl_2$, and 20 mM Glucose) media, cells were incubated at 37°C on a rotating platform (200 RPM) for 1 hr followed by spreading on LB plates prepared with appropriate antibiotics (Kanamycin or Ampicillin, depending on the plasmid). PCR products were cloned using StrataClone™ PCR (Stratagene, #240205) or StrataClone™ Blunt PCR (Stratagene, #240207) cloning kits. In brief, 2 µl of each PCR product was added to 3 µl of StrataClone™ Cloning Buffer and 1 µl of StrataClone™ Vector Mix was added and mixed by gentle pipetting followed by incubation at room temperature for 5 min. The ligation mixture was added to StrataClone™ SoloPack competent cells and transformed as described above.

2.2 Primary keratinocyte cultures

Protocols for the preparation and maintenance of mouse primary keratinocytes were adopted and modified from the literature (101, 102). In brief, 1-2 day old newborn mice were euthanized by asphyxiation with CO_2. Dead mice were rinsed with ice-cold 70% ethanol and legs and tail were trimmed. A longitudinal dorsal incision is made from the tail to the snout and the skin is removed by pulling from the back legs towards the snout. To

dissociate the epidermis from dermis, skin samples were incubated with 5 ml of trypsin solution (0.25% trypsin in Hank's Balanced Salt Solution(HBSS) without calcium and magnesium; 5.33 mM KCl, 0.441 mM KH_2PO_4, 4.17 mM $NaHCO_3$, 137.93 mM NaCl, 0.338 mM Na_2HPO_4, 5.56 mM D-Glucose, and 0.0266 mM Phenol Red) per 60 mm dish overnight at 4°C. After overnight trypsin digestion, the epidermis was separated from the dermis using forceps and collected in 50 ml sterile tubes. Skin samples (up to 7) obtained from animals with identical genotypes were combined in single 50 ml sterile tubes, incubated with 5 ml of complete medium per skin sample [complete medium is EMEM (BioWittaker, #06-174G), 10% non-chelexed fetal bovine serum (Sigma, #F2442), EGF 10 ng/ml (Invitrogen, #113247-051; Stock: 40 µg/ml in phosphate-buffered saline without calcium and magnesium (PBS w/o Ca^{2+} and Mg^{2+})) containing 1% Antibiotic-Antimycotic Solution (Gibco, #15240-062)], and keratinocytes were released from the epidermis by gentle rocking at room temperature for 30 min. The epidermis and intact basement membrane was removed from the 50ml tube after rocking and the keratinocyte suspension was poured through a cell strainer (Falcon, #35-2350) sitting on top of a 50 ml centrifuge tube. Following filtration, keratinocytes were collected by centrifugation at 1,500 rpm for 5 min at 4°C. The supernatant was removed and the cell pellet was resuspended with 0.5 ml of complete medium per skin sample. Resuspended cells were kept on ice and cell concentration was determined using a hemocytometer. Appropriate numbers of cells were then plated onto as desired with complete medium as shown in the following table:

Table 1 Number of cells plated and volume of media added in culture plate or dish.

Plate or Dish	Number of cells	Complete Medium
96 well plate	5×10^4 cells/well	200 µl/well
6 well plate	1×10^6 cells/well	2 ml/well
60 mm dish	2×10^6 cells/dish	4 ml/dish
100 mm dish	4×10^6 cells/dish	9 ml/dish

Plated cells were cultured under 5% CO_2 at 37°C for 6 hrs in a humidified incubator, rinsed once with PBS w/o $Ca2^+$ and $Mg2^+$, and fed with complete Keratinocyte-SFM media [500 ml of Keratinocyte-SFM, Gibco®, #10725; 2.5 µg of EGF supplement (Gibco®, #10450-013), 25 mg of bovine pituitary extract (Gibco®, #13028-014), 250 µl of Gentamicin (Gibco®, #15710-064, Stock: 10 mg of gentamicin in 1 ml of distilled water) and 0.05 mM $CaCl_2$]. Complete Keratinocyte-SFM media was changed every other day until cultures were used for experiments, and keratinocyte cultures were used for experiments prior to confluence and were not sub-cultured.

2.3 Mammalian cell lines

COS-7 and HEK293 cell lines were obtained from the Duke Cell Culture Facility (Duke University, Durham, NC, USA). Cells were cultured in Dulbecco's modified Eagle's medium (DMEM; Mediatech, Inc., Manassas, VA, USA) supplemented with 10% heat-inactivated fetal

bovine serum (FBS; Atlanta Biologicals, Norcross, GA, USA) and 50 μg/ml Pipracil. Cells were cultured under 5% CO_2 at 37°C in a humidified incubator.

2.4 Mammalian cell transfection

SatisFection™ Transfection Reagent (Stratagene, #04121) was used for transfection as instructed by the manufacturer. In brief, appropriate amount of plasmid DNAs were diluted into serum-free medium (6-well plate: 2 μg in 100 μl, 60 mm dish: 6 μg in 300 μl, 100 mm dish: 16 μg in 800 μl) and transfection reagent was also diluted into serum-free medium at a 1.5:1 ratio (μl reagent:μg DNA) in a separate tube. The diluted transfection reagent was added drop-wise to diluted DNAs, mixed by gentle pipetting, and this transfection mixture was incubated for 15 min at room temperature. The transfection mixture was added drop-wise to each well or dish of cells (at approximately 70% confluence) and the mixture was dispersed by gentle rocking. Cells were harvested after 36-72 hrs of incubation under 5% CO_2 at 37°C in a humidified incubator.

2.5 Cell proliferation and apoptosis assays

2.5.1 CyQUANT® assay

Cell proliferation was quantified using a proprietary colorimetric kit [CyQUANT® Cell Proliferation Assay Kit (Invitrogen, Eugene, OR, USA)]. Primary mouse keratinocytes prepared from mouse skin were plated in 96-well plates at 5×10^4 cells per well. Culture media was removed from wells on each day post-plating, cells were washed once with PBS, plates were stored at-70°C for at least 3 hrs, and frozen plates were warmed to room

temperature prior to lysis. Cells were lysed via the addition of 200 µl of CyQUANT® GR dye/cell-lysis buffer to each well and mixed by gentle pipetting. Samples were incubated for 5 min at room temperature while protected from light. Sample fluorescence was measured following this incubation using a spectrophotometer outfitted with appropriate excitation (485 nm) and emission (538 nm) filters.

2.5.2 MTT assay

Primary mouse keratinocytes prepared from mouse skin were plated in 96-well plates at 5×10^4 cells per well. Cells were cultured under standard conditions and quantified via the addition of 10× MTT ((3-(4,5-Dimethylthiazol-2-yl)-2,5-diphenyltetrazolium bromide) stock solution (6 mg/ml in culture media) to media to a final working concentration of 1×. Cells were incubated for 4 hrs at 37°C under 5% CO_2 and plates were then centrifuged at 750× g for 8 min at room temperature. Media was aspirated completely, 100 µl of lysis buffer (0.04 N HCl in isopropyl alcohol) was added to each well, and cells were incubated for 15 min at 20˚C. Crystals that were not dissolved by the lysis buffer during this incubation period were resuspended by gentle tapping and the addition of 100 µl of dH_2O per well. Cells were quantified using a spectrophotometer set to read light absorbance at OD_{570}, and OD_{650} was read as a reference absorbance reading. The reference absorbance was subtracted from the dye absorbance reading and the results were plotted.

2.5.3 Apoptotic DNA “laddering” assay

Genomic DNA was extracted from primary keratinocyte cultures essentially as described by Yeung *et al.* (103). In brief, cells were harvested and lysed with 500 µl of lysis buffer (50 mM Tris-HCl, pH 7.5, 1% Nonidet^{TM} P-40, 20 mM EDTA) by repeated pipetting. Cell debris and intact non-apoptotic nuclei were removed by centrifugation at 1,600×g for 5 min, and supernatants were extracted once with phenol:chloroform:isoamyl alcohol (25:24:1, pH 8.0, 500 µl). The aqueous phase was removed to a new tube and DNAs were precipitated via the addition of a cocktail containing 50 µl of 3M sodium acetate, 1 µl of nuclease-free glycogen (Roche Applied Science, Indianapolis, IN, USA), and 600 µl of isopropanol and incubation on ice for 5 min. DNAs were collected by centrifugation at 12,900× g for 10 min at 4°C and precipitates were washed once with 70% ethanol. DNA pellets were resuspended in 30 µl of 1× RNaseONE® buffer (Promega, Madison, WI, USA), 1 µl of RNase was added, and samples were incubated for 30 min at 37°C. DNA "ladders" were resolved on 1.8% agarose gels containing ethidium bromide.

2.5.4 Annexin V and propidium iodide staining

To quantify apoptotic and necrotic cells in primary keratinocyte cell cultures, a proprietary kit was employed [Alexa Fluor® 488 annexin V/Dead Cell Apoptosis Kit (Invitrogen, Eugene, OR, USA)] in which cells are stained with Alexa® Flour 488 annexin V and propidium iodide(PI) and separated by flow cytometry. In brief, cells were collected by trypsinization and washed once with ice-cold PBS. Cells were resuspended in 100 µl of 1× annexin-binding buffer and incubated with 5 µl of Alexa Fluor® 488 annexin V and 1 µl of PI (100 µg/ml) for 15 min at room temperature. Following incubation, 400 µl of 1× annexin-

binding buffer was added and mixed gently. Samples were kept on ice until analyzed by flow cytometry.

2.5.5 Flow cytometric analysis of cell cycle progression

Propidium iodide staining was performed prior to separation of cells into cell-cycle compartments by flow cytometry. Cells were treated with trypsin for 10 min at 37°C and harvested into 15 ml tubes that contained 1 ml of culture media and 10% FBS. After centrifugation at 800 rpm for 10 min at 4°C, cell pellets were resuspended with 300 µl of ice-cold PBS and fixed via the addition of 700 µl of 100% ethanol and incubation at -40°C overnight. After fixation, ethanol was removed by centrifugation at 800 rpm for 10 min at 4°C and cell pellets were resuspended in 300 µl of ice-cold PBS. For DNA staining, 10 µl of propidium iodide stock solution (5 mg/ml in dH_2O) was added to each cell sample and 50 µl of DNase-free RNase I (1mg/ml) was added to eliminate contaminating RNA. Samples were kept on ice until analyzed by flow cytometry.

2.5.6 Tritiated thymidine incorporation assay

To quantify DNA synthesis in primary keratinocyte cultures, [methyl-^{3}H]thymidine incorporation assays were performed. Mouse keratinocytes were plated in 6-well plates at 1×10^6 cells per well. On each subsequent day, 6 µl of [methyl-^{3}H]thymidine solution (PerkinElmer, 20 Ci/mmol)] was added to 2 ml of culture media in each well to a final concentration of 3 µCi/ml. After 2 hr of incubation at 37°C under 5% CO_2, cells were washed twice with ice-cold PBS and then washed once with 10% Trichloroacetic acid (TCA) solution.

To lyse cells, 1 ml of lysis buffer (0.2 N NaOH, 1% SDS) was added to each well and samples were incubated for 5 min at 37°C. Following incubation, 0.5 ml of each lysate was transferred to liquid scintillation vials and 60 µl of 100% TCA and 3.5 ml of ScintiSafe™ 30% Cocktail counting solution (Fisher, #SX23-5) were added to each vial. Samples were mixed by vortexing and radiolabeled DNA in each sample was quantified with a liquid scintillation counter (Wallac 1409).

2.6 Isolation of genomic DNA

A Maxwell®16 robotic DNA extractor (Promega, Madison, WI, USA) was employed to prepare genomic DNA from mouse tissues. Mouse tail clips or ear punches were processed using Maxwell®16 DNA Purification Kits (Promega, #AS1030) as instructed by the manufacturer. Genomic DNA was transferred to sterile eppendorf tubes and stored at 4 ˚C until required. To quantify the concentration of genomic DNA, 2 µl of DNA solution was examined using a NanoDrop® ND-1000 Spectrophotometer.

2.7 Isolation of total RNA

Total RNA was prepared from cultured cells or mouse tissues using Trizol® Reagent (Invitrogen, #15596-026). Cells were lysed with 1 ml of Trizol® Reagent by repeated pipetting and mouse tissues were homogenized with a hand-held Polytrone homogenizer. After incubation at room temperature for 5 min, 200 µl of chloroform was added to each RNA sample and mixed well by shaking followed by incubation at room temperature for 3

min. Lysates were clarified by centrifugation at 14,000 rpm for 15 min at 4°C. The aqueous phase was transferred to a new tube, 500 µl of isopropanol was added and mixed by inverting the tube. After incubation at room temperature for 5 min, RNA samples were centrifuged at 14,000 rpm for 10 min at 4°C. Pellets were washed once with 700 µl of 75% ethanol and air dried. RNA pellets were resuspended with 100 µl of DEPC-treated water and incubation at 55°C for 10 min. All RNA samples were quantified using a NanoDrop® ND-1000 Spectrophotometer and the quality of RNA was checked by gel electrophoresis.

2.8 Elution of DNAs from agarose gels

PCR products separated by size via gel electrophoresis were purified using a proprietary kit [QIAquick Gel Extraction Kit (QIAGEN, #28704)] as instructed by the manufacturer. In brief, DNA fragments in agarose gels were excised using a clean, sharp scalpel blade. The weight of each gel slice is measured in milligrams and 300 µl of Buffer QG are added per 100 mg of gel. The mixture is incubated at 50˚C for 10 min and tubes are inverted every 2-3 min. After the gel slice is dissolved, 1 gel volume of isopropanol is added and mixed by inverting the tubes. The mixture is transferred to a spin column and centrifuged for 1 min at 13,000 rpm. The column is then rinsed with 700 µl of Buffer PE and centrifugation for 1 min at 13,000 rpm. DNAs are eluted from columns by adding 50 µl of Buffer EB (10mM Tris-Cl, pH8.5) followed by centrifugation (1 min at 13,000 rpm) and collection of DNA into a collecting tube.

2.9 Polymerase chain reaction (PCR)

2.9.1 Thermal asymmetric interlaced (TAIL) polymerase chain reaction

Transgene integration sites were isolated by TAIL-PCR as described in Pillai *et al*. (104). In brief, genomic DNA was extracted from ear punches as described above. Gene Specific Primers (GSP) were designed to represent nested portions of mouse Sp2, each with a length of 21–24 nucleotides, a melting temperature of approximately 64°C and GC-content of 50–60%. A set of Arbitrary Degenerate (AD) primers were designed as specified in Pillai *et al*. The GSP and AD primer sequences are shown in Table 2.

Table 2 Sequences and T_m values of primers for TAIL-PCR. For Arbitrary Degenerate (AD) primers, random nucleotides such as N, S, and W are synthesized. *N*: any base, *S*: G or C, *W*: A or T.

Primers	Sequence (5' to 3')	T_m (°C)
GSP1	GTA CCC ATA CGA TGT TCC AGA T	61.4
GSP2	GAT CAA CTA GTC TGG GAG CCC	63.8
GSP3	GTT TCA GGT TCA GGG GGA GGT G	69.8
GSP4	CAG CTA CAC TCT CTG CAC GC	64.0
GSP5	GCA CAC AAA CTG CTG GCC TTG C	73.0
GSP6	CGT GTG CAC CAG GCA TTT GAT C	71.7
AD1	NGT CGA SWG ANA WGA A	46.8
AD2	TGW GNA GSA NCA SAG A	34.8
AD3	AGW GNA GWA NCA WAG G	36.3
AD4	STT GNT AST NCT NTG C	45.5
AD5	NTC GAS TWT SGW GTT	46.0
AD6	WGT GNA GWA NCA NAG A	34.8

Thermal cycling conditions for Primary TAIL-PCR were as follows: 94˚C (5 min), 10 cycles of [94˚C (10 sec), 64˚C (30 sec),72˚C (3 min)], 1 cycle of [94˚C (10 sec), 25˚C (3 min), 64˚C (2.5 min)], 15 cycles of [94˚C (10 sec), 64˚C (3 min), 72˚C (2.5 min), 94˚C (10 sec), 64˚C (3 min), 72˚C (2.5 min), 94˚C (10 sec), 44˚C (1 min), 64˚C (2.5 min)]. Secondary TAIL-PCR conditions were as follows: 94˚C (5 min) followed by 12 cycles of [94˚C (10 sec), 64˚C (3 min), 72˚C (2.5 min), 94˚C (10 sec), 64˚C (3 min), 72˚C (2.5 min), 94˚C (10 sec), 44˚C (1 min), 64˚C (2.5 min)]. Tertiary TAIL-PCR conditions were as follows: 94˚C (5 min) followed by 20 cycles of [94˚C (10 sec), 44˚C (1 min), 64˚C (2.5 min)]. Gene-specific primer binding sites within the Sp2 transgene are illustrated in Figure 2.

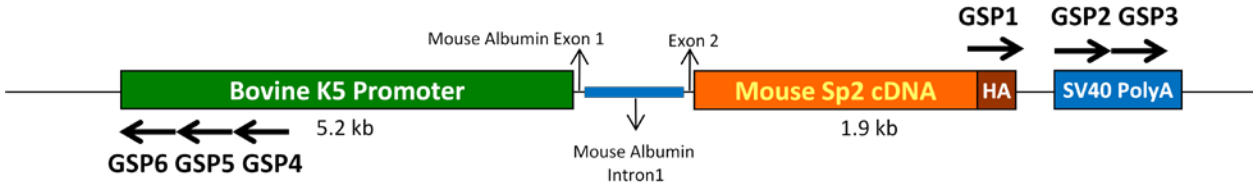

Figure 2 Gene specific primer binding sites for TAIL-PCR. GSP 4-6 primers bind to portions of the bovine keratin 5 promoter. GSP 1 primer binds to the HA epitope tag and GSP 2-3 primers bind to the SV40 PolyA tail.

For Primary TAIL-PCR, GSP1 and AD1-6 primer sets were used to amplify genomic DNA sequences 3' of the transgene integration site. GSP4 and AD1-6 primer sets were used to amplify genomic DNA sequences 5' of the transgene integration site. That is, I performed a total of 12 reactions on both ends of the integration sites (six reactions for the 3’ end and six reactions for the 5’ end). For subsequent nested PCR reactions (Secondary and Tertiary TAIL-PCR), I repeated the same reactions. Following the PCR, 10 µl of each reaction was examined by gel electrophoresis and staining with ethidium bromide. Primer sets that produced distinct amplification products were employed in a subsequent round of the PCR (Secondary TAIL-PCR) with nested primers. Once again, 10 µl of each PCR product was examined by gel electrophoresis and staining with ethidium bromide. Primer sets that produced distinct amplification products were then employed in a final round of Tail-PCR (Tertiary TAIL-PCR) and 10 µl of each PCR product was examined by gel electrophoresis and staining with ethidium bromide.

For all three rounds of TAIL-PCR, TITANIUM™ *Taq* DNA polymerase (Clonetech, #639210) was used as instructed by the manufacturer supplemented with 1 µl of 2.5 mM of dNTPs. Amplified PCR products resulting from each round of TAIL-PCR were purified by gel-elution and sub-cloned into a sequencing vector (pSC-A-amp/kan PCR cloning vector; StrataClone™, #240205) as described in Section 2.8. Resulting clones were analyzed by automated DNA sequencing using standard primers that anneal to plasmid sequences flanking each insert. Sequences obtained were compared with mouse genomic sequences using the BLAST search engine. Sequences that clearly showed junctions between mouse

chromosomal DNA and transgene sequences were identified and used to prepare maps of each transgene integration site (Figure 3). Mouse allele-specific primers were prepared from single-copy sequences flanking each transgene integration site, as well as sequences predicted to be disrupted by transgene integration, and the zygosity of transgenic mice was established by the PCR. The primer sequences are shown in Table 3.

Table 3 Primer lists of TAIL-PCR for both Sp2-Family A and C animals. Family A-F1 and Family A-R1 primers amplify a 383 base pair product for wild-type (non-transgenic) alleles. GSP6 and Family A-R1 primers amplify a 290 base pair product in animals carrying the Sp2-A transgene. Family C-F1 and Family C-R1 primers amplify a 427 base pair product of for wild type (non-transgenic) alleles. K5-F1 and Family C-R1 primers amplify a 611 base pair product in animals carrying the Sp2-C transgene.

Primers	Sequence (5' to 3')	T_m (°C)
Family A-F1	GGG TGA CTG AGG CAG AGT TTG	66.0
Family A-F2	CTC TTA TCA CTG CAT CCT CTC CC	65.0
Family A-F3	GGC CTT ATA AAC CGC AGT CCA G	67.4
Family A-R1	CAA GCA GTT CTG AGA CCT GCA C	66.3
Family A-R2	TGC ACC AAC CCT CTG TAG TCC	66.3
Family A-R3	AGA GTT AAC CTG AGT GCG GAG G	65.6
Family C- F1	GTT CTA AGC ACT AAC ATC ATC AGG CG	67.4
Family C- R1	GTT AGC TGA TAA CCT TTT GAA GAC CG	65.5
K5 F1	ACA TTG CAG CAC ATT GCA CAC TAT CC	71.4
Family C-F2	CAA GGA TCT GTT TTT ATG TAC ACC ACC	66.0
Family C-R2	TGT TAT GAA CAG AGT TAG AAG TTG CAA GAC	66.1

A

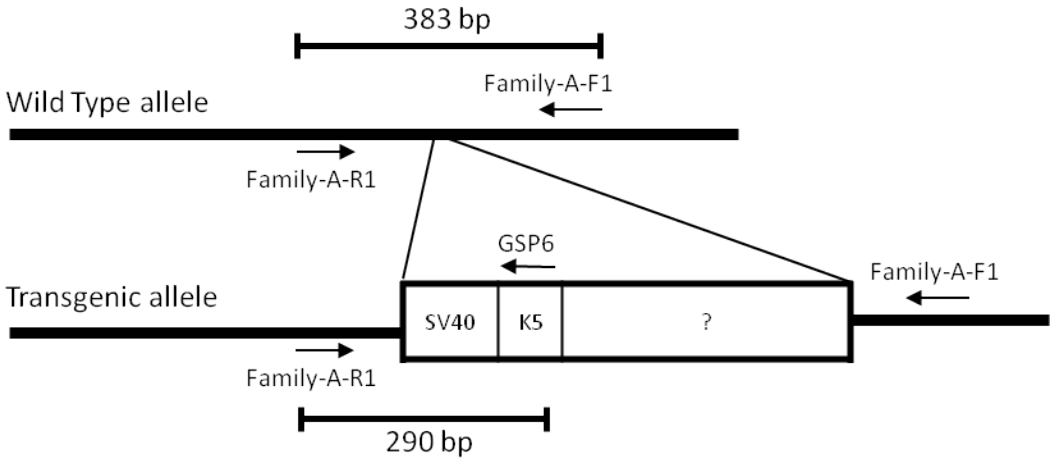

B

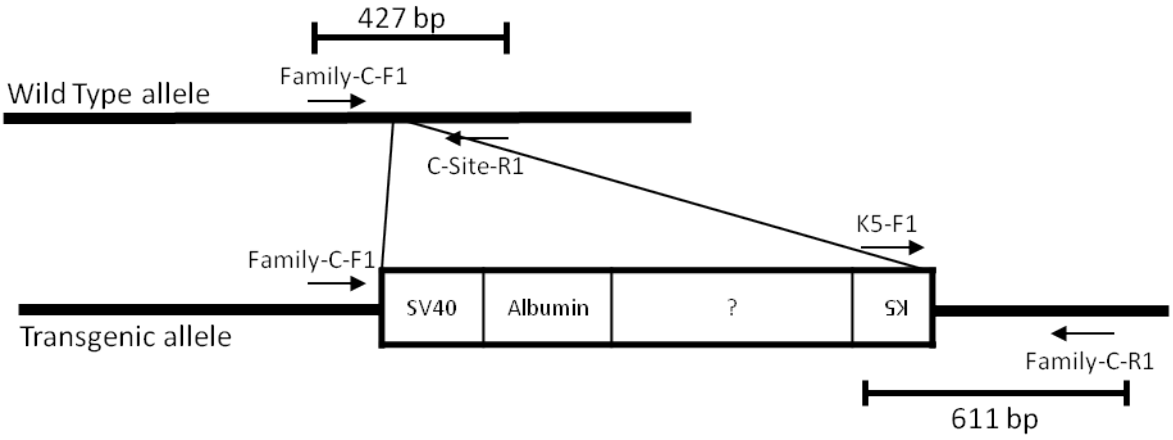

Figure 3 Schematic diagram of primer binding sites for allele specific genotyping. *A.* The Sp2-A integration site on mouse chromosome 6. Wild-type alleles produce a 383 bp amplified product whereas transgenic alleles produce a 290 bp product. *B.* The Sp2-C integration site on mouse chromosome 5. Wild-type alleles produce a 427 bp amplification product whereas transgenic alleles produce a 611 bp product. Each integration site contains a linear array of multimerized transgenes in various orientations relative to mouse chromosomal DNA (indicated by a question mark).

2.9.2 Reverse transcriptase-polymerase chain reaction

Total RNA was extracted from cells or tissues as described in Section 2.7 and 5 µg of total RNA was used as template to synthesize first strand cDNA. Total RNA was diluted in dH_2O to a final volume of 10 µl and mixed with 1 µl of 10 mM dNTPs and 1 µl of 0.5 µg/µl Oligo-(dT)12-18 Primer (Invitrogen, #18418-012). After incubation at 65°C for 5 min, this mixture was chilled on ice followed by the addition of 5 µl of 5× First-Strand Buffer [250 mM Tris-HCl (pH 8.3), 375 mM KCl, 15 mM $MgCl_2$] and 2 µl of 0.1M DTT. Following incubation at 42°C for 2 min, 1µl of SuperScript® III Reverse Transcriptase (Invitrogen, #18080-044) was added to the mixture and incubated for 50 min at 42°C. Reverse transcription was terminated by incubation at 70°C for 15 min and reactions were stored at 4°C until used as templates for the PCR. For subsequent PCRs, 2 µl of each cDNA mixture and 1µl of TITANIUM™ *Taq* DNA polymerase (Clontech, #639210) were combined and subjected to the following cycling conditions: GAPDH : 95˚C 1 min, 30 cycles of [95˚C 30 sec, 75˚C 30 sec, 68˚C 1 min], 68˚C 3 min, 4˚C hold; Sp2 : 95˚C 1 min, 35 cycles of [95˚C 30 sec, 75˚C 30 sec, 68˚C 1 min 30 sec], 68˚C 3 min, 4˚C hold; Keratin 5 : 94˚C 4 min, 30 cycles of [90˚C 30 sec, 65˚C 30 sec, 72˚C 30 sec], 72˚C 10 min, 4˚C hold; Keratin 14 : 94˚C 4 min, 30 cycles of [90˚C 30 sec, 65˚C 30 sec, 72˚C 30 sec], 72˚C 10 min, 4˚C hold; FoxN1 : 95˚C 1 min, 35 cycles of [95˚C 30 sec, 75˚C 30 sec, 68˚C 1 min 30 sec], 68˚C 3 min, 4˚C hold; ΔNp63α : 94˚C 4 min, 30 cycles of [90˚C 30 sec, 67˚C 30 sec, 72˚C 30 sec], 72˚C 5 min, 4˚C hold; TAp63 : 94˚C 4 min, 30 cycles of [90˚C 30 sec, 67˚C 30 sec, 72˚C 30 sec], 72˚C 5 min, 4˚C hold. Primers for these reactions are listed in Table 4.

Table 4 Primer lists for reverse transcriptase PCR.

Target genes	Primer sequence (5' to 3')	T_m (°C)	Product size
GAPDH	GAPDH F: CAA CTA CAT GGT CTA CAT GTT C	56.1	122bp
	GAPDH R: CTC GCT CCT GGA AGA TG	59.6	
Sp2	RPA 2F: CAA CAA CCT GGT GAA CAC CAG CGA TAT TG	75.0	429bp
	RPA 2R: GGT GTA CGG ATA TAA ACC TGG GTT GGT G	71.4	
Keratin 5	5'Krt5: AGG AGG CAG CAG CAT TGG TGT TGG CAG TGG C	84.5	584bp
	3'Krt5: GGA AGT CAG AAC CAG GAC AGA ATT TAG GTG	71.3	
Keratin 14	5'Krt14: AGA TCC GCA CCA AGG TCA TGG	70.4	204bp
	3'Krt14: GTG CAA CTC AGA AAA AGA AGC	60.6	
Keratin 14	5'Krt14-New: CTC CTC TGG CTC TCA GTC ATC C	66.5	228bp
	3'Krt14-New: GGG ACA ATA CAG GGG CTC TTC C	68.6	
FoxN1	Mouse FoxN1 forward: CCC CAG CCA GGA ACA CAA CCA	73.4	245bp
	Mouse FoxN1 reverse: GTG GCT GGT GAC CTT CGG C	70.5	
ΔNp63α	5'deltaNp63: TTG TAC CTG GAA AAC AAT G	55.9	447bp
	3'deltaNp63: GCA TCG TTT CAC AAC CTC G	64.3	
TAp63	5'Tap63: TCG CAG AGC ACC CAG ACA	67.4	612bp
	3'deltaNp63: GCA TCG TTT CAC AAC CTC G	64.3	

2.9.3 Quantitative real-time polymerase chain reaction

Expression levels of endogenous and transgene transcripts were determined by quantitative real-time (qRT)-PCR. First strand cDNA was synthesized as described in Section 2.9.2 and the QuantiTect® SYBR® Green PCR Kit (Qiagen, #204143) was used to amplify and quantify transcript abundance as instructed by the manufacturer. The 2x QuantiTect® SYBR® Green PCR Master Mix contains HotStarTaq DNA polymerase and QuantiTect SYBR Green PCR Buffer, fluorescent dye SYBR Green I, and Passive reference dye. This cocktail was supplemented with 2µl of template cDNA and 1µl of forward and reverse primers. The MyiQ™ single color real-time PCR detection system (Bio-Rad, Hercules, CA, USA) was used for thermal cycling (thermal-cycling conditions for all primer sets was: 95°C 15 min, 50 cycles of [95°C 10 sec, 59°C 1 min], followed by incubation at 4°C) and detection of signals. Amplification data was analyzed using iQ™5 software version 2.0. Target gene transcript levels were normalized to glyceraldehyde 3-phosphate dehydrogenase (GAPDH) transcript levels obtained in each sample via the subtraction of the C_t value of GAPDH from the C_t value for each target gene. Results were expressed as the fold-change in transcript levels. Primers used for qRT-PCR are shown in Table 5.

Table 5 Primer lists for quantitative real-time PCR.

Target genes	Primer sequence (5' to 3')	T_m (°C)	Product size
Endogenous mouse Sp2	RT-mSp2-F1: CCA GCC TAC CCC AAG GAA AC	66.6	119bp
	RT-mSp2-R1: GGG AGC CCT GAA TCT GAA GTA T	64.3	
Exogenous mouse Sp2	RT-mSp2-F2: TGT CAG AAG CGC TTC ATG AG	64.3	91bp
	RT-mSp3-R1: CTG GAA CAT CGT ATG GGT AC	59.3	
GAPDH	659: GGG TGT GAA CCA CGA GAA AT	63.7	120bp
	660: CCT TCC ACA ATG CCA AAG TT	63.7	
Mouse Sp2 Large (Exon3-4)	mSp2ex3F: ATG GCC GCC ACT GCT GCT GTC AGT CC	81.3	184bp
	mSp2ex4R: GGA CCA GTT TCC TTG GGG TAG GCT G	73.5	
Mouse Sp2 (Exon 5-6)	mSp2ex5F: AAT GGT GTC CAA GTC CAG GGT GTG CC	76.7	203bp
	mSp2ex6R: TTG GGA CAC GTG CAG GCC ATG CGC	83.3	
Filaggrin	Filaggrin-F: CAG GCG CTC TGG GGC GCG TCA	82.2	129bp
	Filaggrin-R: GCC TGA CTC TCG CTG ACC CC	70.8	
Loricrin	Loricrin-F: TCA TGA ATT TGC CTG AGG TTT C	64.9	95bp
	Loricrin-R: CAG AAC AGG ATA CAC CTT GAG C	62.6	
Keratin 1	Keratin 1-F: AGA TCA CTG CTG GCA AAC ATG G	68.3	138bp
	Keratin 1-R: TGA TGT TCT GCT GTA TTT GGG	62.4	
Keratin 5	K5-F: TCT GCC ATC ACC CCA TCT GT	67.9	173bp
	K5-R: CCT CCG CCA GAA CTG TAG GA	66.5	
Keratin 10	Keratin 10-F: CGC AAG GAT GCT GAA GAG TGG TTC	71.7	302bp
	Keratin 10-R: TGG TAC TCG GCG TTC TGG CAC TCG G	78.6	
Keratin 14	K14-F: AGC GGC AAG AGT GAG ATT TCT	64.2	106bp
	K14-R: CCT CCA GGT TAT TCT CCA GGG	65.6	

2.10 Preparation of transgene constructs

2.10.1 pTG1-K5-mSp2/HA

A full-length mouse Sp2 cDNA was synthesized from total RNA extracted from mouse heart and sequenced in its entirety to confirm its integrity. A 10 amino acid epitope tag derived from *Influenza* hemagglutinin(HA) was appended to the carboxy-terminus of the Sp2 open reading frame via the PCR with the following primers: 5'-GAA TTC AGA TCC GCC ACC ATG AGC GCA GAT CCA CAG ATG A-3' and 5'-CCC ACC TAG GCA CGA AGG GCT TGT ACC CAT ACG ATG TTC CAG ATT ACG CTA GCT GAA AGC TTG-3'. The integrity of this epitope-tagged mSp2 cDNA was confirmed by automated DNA sequencing and subcloned subsequently into pCMV4, a mammalian expression vector, generating pCMV4-mSp2/HA. COS1 cells were transfected with pCMV4-mSp2/HA and the expression of the epitope-tagged mouse Sp2 cDNA was determined by Western blotting with antibodies against Sp2 as well as HA. Once protein expression was confirmed, the epitope-tagged mSp2 cDNA was subcloned into plasmid pTg1 (a gift from the University of North Carolina Animal Models Core Facility). The bovine keratin 5 promoter was obtained from Dr. Robert C. Smart (NCSU) and inserted into pTg1 upstream of mSp2 cDNA sequences, creating the pTG1-K5-mSp2/HA transgene. The functionality of this expression construct was established via transfection of COS7 cells and Western blotting. The structure of pTG1-K5-mSp2/HA is illustrated in Figure 4

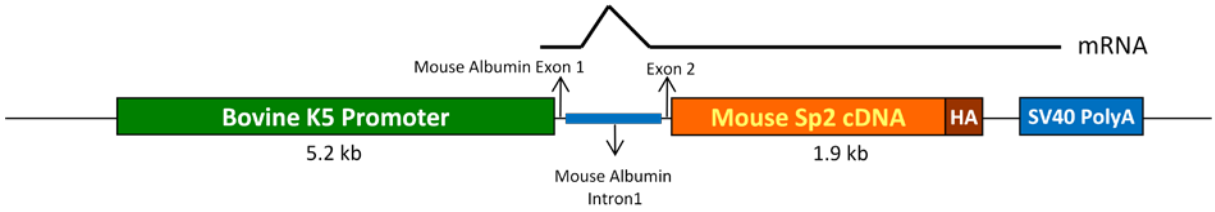

Figure 4 Sp2 transgene utilized to produce transgenic mice. The bovine keratin 5 promoter (5.2kb) drives transcription and mouse albumin-derived splicing sequences located upstream of the HA-tagged mouse Sp2 (1.9kb) cDNA are included to increase the efficiency of transgene expression. SV40-derived polyA signals are included at the 3' end of the Sp2 cDNA. The structure of the spliced mRNA produced by this construct is indicated above the transgene.

2.10.2 pTG1-K5-mSp2/HA-NotI

A transgene carrying an epitope tagged mouse Sp2 that is deficient in DNA binding activity was prepared from pSIN6.1CeGFPW-mSp2NotIHA-IRES by digestion with *KpnI* and *MluI*. A 1,832 base pair *KpnI* and *MluI* fragment was subcloned subsequently into pTg1 (a gift from the University of North Carolina Animal Models Core Facility) containing the bovine keratin 5 promoter. The integrity and functionality of this construct was confirmed by automated DNA sequencing as well as Western blotting. The structure and organization of this transgene construct is identical to that of pTG1-K5-mSp2/HA (Figure 4) except for the disruption of the Sp2 DNA binding motif. In this mutation, the DNA-binding domain was disrupted by insertion of 4 nucleotides (CCGG: NotI sequences) resulting in frameshift mutation of the following codons but producing intact HA tag in the end of carboxy-terminus. Therefore, the protein made by this construct cannot bind to DNA but has intact *trans*-activation domain of Sp2, intact NLS, and HA tag so that it can be localized in nucleus and be distinct from endogenous Sp2 proteins. More detail information is described in Section 4.7.

2.11 Labeling of proliferating cells *in vivo* with BrdU

A stock solution (10 mg/ml) of bromodeoxyuridine (5-bromo-2'-deoxyuridine, BrdU; Sigma, #B5002) was prepared in PBS. To label proliferating cells *in vivo*, animals were weighed and injected intraperitoneally with 10 µl of BrdU per gram of body weight 1 hr prior to euthanasia. BrdU solutions were prepared prior to injection and protected from

light. Following euthanasia dorsal skin was removed and fixed as described in Section 2.13 for immunohistochemical staining.

2.12 Western blotting of protein extracts prepared from mouse skin and primary keratinocyte cultures

Protein extracts from mouse skin were prepared as follows. Dorsal skin samples were grasped with forceps and incubated in a 60°C water bath for 10 sec followed by immediate cooling in ice water. The epidermis was scraped from whole skin using a spatula and placed in 1 ml of Western lysis buffer [150 mM NaCl, 1% NP40, 1% Sodium Deoxycholate, 0.1% Sodium Dodecyl Sulfate (SDS), 20 mM Tris-pH8.0, 5 mM Ethylenediaminetetraacetic acid (EDTA)] containing 1 mM Phenylmethylsulfonyl fluoride (PMSF), 1× Complete Mini EDTA-free Protease Inhibitor Cocktail (Roche, #11 836 170 001), and 1 mM Dithiothreitol (DTT). The epidermis was homogenized while on ice with a Polytron homogenizer, and homogenized samples were incubated on ice for 20 mins.

Protein extracts from primary keratinocyte cultures were prepared as follows. Cultured primary keratinocytes were rinsed once with ice-cold PBS and harvested with a cell scraper and 1 ml of PBS. Cells were pelleted at 13,000 RPM for 1 min at 25°C and resuspended with at least 150 µl of Western blotting lysis buffer. Genomic DNA was sheared by repeated passage through a 1 ml syringe outfitted with a 25G 5/8 needle.

Extracts from mouse skin and primary keratinocyte cultures were centrifuged at 14,000 rpm for 15 min at 4°C. Supernatants were transferred to new tubes and quantified using a BCA™ Protein Assay Kit (Pierce, #23227) as instructed by the manufacturer. Following quantification, 50 µg of protein was combined with SDS sample buffer (2% SDS, 80 mM Tris-pH6.8, 10% Glycerol, 0.002% Bromophenol blue and 5% beta-Mercaptoethanol) and boiled for 5 min. Proteins were resolved on polyacrylamide gels (4% stacking gel and 8% resolving gel) at 25 mA for the stacking gel and 40 mA for the resolving gel followed by transfer to Protran® nitrocellulose membranes (Whatman®, Dassel, Germany) at 70V for 45 min. Non-specific protein interactions were blocked via the incubation of membranes in 50 ml of blocking buffer (5% skim milk in TBS-T [50 mM Tris-pH7.5, 150 mM NaCl, 0.1% Tween®-20]) at room temperature for 30 min, and then incubated with primary antibodies diluted in antibody dilution buffer (0.5% skim milk in TBS-T) as indicated in the following table (Table 6).

Table 6 List of primary antibodies that are used for Western blotting.

Primary antibody	Catalog number	Dilution	Temperature	Incubation time
HA	SantaCruz, #sc-805	1:5,000	4°C	Overnight
Sp2	Sigma, #HPA003357	1:5,000	4°C	Overnight
Actin	SantaCruz, #sc-1616	1:5,000	Room temperature	1 hour
Keratin 1	Covance, #PRB-165P	1:10,000	Room temperature	1 hour
Keratin 5	Covance, #PRB-160P	1:10,000	Room temperature	1 hour
Keratin 10	Covance, #PRB-159P	1:3,000	Room temperature	1 hour
Keratin 14	Covance, #PRB-155P	1:10,000	Room temperature	1 hour
Loricrin	Covance, #PRB-145P	1:10,000	Room temperature	1 hour

Membranes were washed with TBS-T three times for 5 min each and then challenged with secondary antibodies as indicated in the following table (Table 7).

Table 7 List of secondary antibodies that are used for Western blotting

Secondary antibody	Catalog number	Dilution	Temperature	Incubation time
Anti-rabbit	Promega, #W401B	1:10,000	Room temperature	1 hour
Anti-goat	SantaCruz, #sc-2768	1:10,000	Room temperature	1 hour

Following incubation with secondary antibodies, membranes were washed with TBS-T three times for 5 min each and antigen/antibody complexes were detected using a chemiluminescent kit [Amersham^{TM} ECL^{TM} Western Blotting Analysis (GE Healthcare, #RPN2109)]. In instances where membranes were reprobed with additional primary antibodies, following chemiluminescent detection membranes was incubated with stripping buffer (2% SDS, 100 mM beta-Mercaptoethanol, 50 mM Tris-pH6.8) at 50˚C for 30 min. Stripped membranes were washed once with TBS-T for 5 min, incubated in blocking buffer for 30 min at room temperature, and then incubated with appropriate dilutions of primary antibodies.

2.13 Preparation of frozen and paraffin-embedded tissue sections

Frozen sections from mouse skin were prepared as follows. Mice were euthanized by cervical dislocation, hair was removed with an electric clipper, and dorsal skin samples

were collected using surgical scissors. Skin samples were trimmed to 1 cm by 1 cm using a scalpel blade, fixed with 4% paraformaldehyde at 4°C for 4 hrs, followed by incubation in 30% sucrose in PBS overnight at 4°C. Fixed tissues were placed in a plastic container, Tissue-Tek® O.C.T. compound (Sakura Finetek USA, Inc., Torrance, CA, USA) was added, and samples were stored at -80°C overnight. O.C.T.-embedded samples were mounted subsequently on specimen discs. Skin sections were prepared with a cryostat (Leica CM1850) set at 10 µm thickness and placed onto Fisherfinest Premium Frosted Microscope Slides (Fisher Scientific, Pittsburgh, PA, USA).

Paraffin-embedded sections from mouse skin were prepared as follows. Mice were euthanized by cervical dislocation, hair was removed with an electric clipper, and dorsal skin samples were collected using surgical scissors. Skin samples were fixed in 10% formaldehyde in PBS for 24 hrs, rinsed once with70% ethanol, and stored in 70% ethanol until they were transferred to specialists in the histology lab at the College of Veterinary Medicine at North Carolina State University for preparation of paraffin-embedded blocks and sectioning.

2.14 Immunohistochemistry

2.14.1 Immunohistochemical staining for Keratins, Loricrin, Green Fluorescent Protein (GFP), and HA

Paraffin-embedded sections on microscope slides were incubated at 64°C for 20 min prior to de-paraffinization and hydration via incubation in 100% xylene (three 4 min incubations), 100% ethanol (two 3 min incubations), and 95% ethanol (two 3 min incubations). Slides were washed twice for 5 min with PBS-T (0.1% Tween-20 in PBS) and endogenous peroxidases were blocked by incubation in 3% H_2O_2 for 10 min at room temperature. Slides were then washed twice for four min each with PBS-T and stained using proprietary kits [Vectastain® ABC Kit (Vector Laboratories, Inc., Burlingame, CA, USA)] manufactured for use with various primary antibody species as shown in the following table (Table 8).

Table 8 List of primary antibodies that are used for immunohistochemistry

Vectastain® ABC Kit	Primary antibody(s)	Antibody manufacturer	Dilution ratio
Rabbit	Keratin 1	Covance, #PRB-165P	1:3,000
	Keratin 5	Covance, #PRB-160P	1:3,000
	Keratin 6	Covance, #PRB-169P	1:3,000
	Keratin 10	Covance, #PRB-159P	1:1,000
	Keratin 14	Covance, #PRB-155P	1:3,000
	Keratin 15	Covance, #PCK-153P	1:3,000
	Loricrin	Covance, #PRB-145P	1:3,000
	HA	SantaCruz, #sc-805	1:3,000
Rat	Keratin 8	Gift from Dr. Robert Smart (105)	1:3,000
Mouse	GFP	SantaCruz, #sc-9996	1:3,000

Slides were incubated with blocking buffer [three drops of normal serum in 1% bovine serum albumin (BSA) in PBS-T] prepared with normal serum corresponding to the species in which biotinylated secondary antibodies were made. Following blocking at room temperature for 30 min, primary antibodies were diluted as shown in the above table, added dropwise to microscope slides, and incubated overnight at 4°C. Slides were washed twice with PBS-T for four mins each, and biotinylated secondary antibodies were prepared and applied to samples as instructed by the manufacturer. After incubation for 30 min at room temperature with secondary antibodies, sections were washed twice with PBS-T for five mins each, and sections were incubated with Vectastain® ABC Reagent for 30 min at room temperature. Sections were washed twice with PBS-T for four min each and then stained with DAB solution (Biogenex, #HK153-5K). DAB solution was removed by washing with dH_2O as soon as brown color development was apparent. Sections were counterstained with hematoxylin for 2 min and dehydrated 95% ethanol (twice for three min each), 100% ethanol (twice for three min each), and 100% xylene (three times for four min each). Finally, cover slips were affixed to slides with Permount® mounting solution (Fisher, #SP15-100).

2.14.2 Immunohistochemical staining for BrdU

Paraffin-embedded sections were de-paraffinized and hydrated with 100% xylene (three times for five min each), 100% ethanol (twice for three min each), and 95% ethanol (twice for three min each) followed by incubation in PBS for 5 min. Sections were incubated in 2N HCl for 30 min at 37°C, and washed with fresh boric acid-borate buffer (85% of 0.2 M

boric acid and 15% of 0.05 M sodium borate buffer) for 3 min at room temperature. Sections were digested with 0.01% trypsin [in 0.5 M Tris-HCl (pH7.8), 0.1% $CaCl_2$] for 3 min at 37°C, washed with dH_2O for 1 min, and endogenous peroxidases were blocked by incubation in 3% H_2O_2 for 10 min at room temperature. All subsequent steps (i.e., blocking, antibody applications, and DAB staining) proceeded as described in the previous section using a mouse anti-BrdU primary antibody (1:25, BD Biosciences, #347580).

2.15 Immunocytochemistry

Cells were cultured in six-well dishes that were pre-loaded with sterile glass cover slips. In preparation for antibody staining, culture media was aspirated from each well and cells were rinsed once with PBS, followed by incubation in 4% paraformaldehyde in PBS for 15 min at room temperature. Cover slips were washed with PBS three times for 5 min each and incubated in blocking buffer (5% normal serum from the same species as the secondary antibody to be utilized and 0.3% Triton X-100 in PBS) for 1 hr at room temperature. After blocking, cover slips were incubated with primary antibodies diluted in antibody dilution buffer (1% BSA and 0.3% Triton X-100 in PBS) overnight at 4°C. Cleaved caspase-3 (Cell Signaling, #9661S) was used to stain apoptotic cells. Cover slips were washed with PBS three times for 5 min each and incubated with a cocktail containing secondary antibodies (diluted 1:500 in antibody dilution buffer) as well as Alexa Fluor® 594 Phalloidin (1:40, Molecular Probes, Eugene, OR USA) and 4',6-diamidino-2-phenylindole (DAPI; 1:50,000 dilution from 14.3mM stock in dimethylformamide). After 1 hr of incubation at room temperature, cover slips were washed with PBS three times for 5 min each and rinsed once with dH_2O for 5 min.

Cover slips were affixed to microscope slides with Vectashield (Vector Laboratories, Inc., Burlingame, CA, USA).

2.16 *In vivo* tumorigenesis assay

2.16.1 Two-stage carcinogenesis

Mice were shaved under anesthesia at weaning (3 weeks old) and returned to their cages for two days. The dorsal skin of each mouse was painted with 200 nmoles (51.2 µg) of 7,12-Dimethylbenz[a]anthracene (DMBA) diluted in 200 µl of acetone to generate initiated cells. Two weeks after initiation, 6.8 nmoles (4.19 µg) of Phorbol-12-Myristate 13-Acetate (TPA) diluted in 200 µl of acetone was applied to dorsal skin twice a week for 20-25 weeks. Resulting papillomas were enumerated and monitored weekly until the size of any single papilloma reached 1 cm in diameter or the experiment was terminated. Papillomas were collected following euthanasia and processed for histology and/or immunohistochemical staining.

2.16.2 Wound-healing assay

Mice were anesthetized via isoflurane inhalation and their dorsal skins were shaved with an electric clipper. Four surgical wounds per mouse were made using a 4 mm diameter disposable biopsy punch (Miltex, Inc., York, PA, USA). Mice were monitored until recovered from anesthesia and returned to their cages. Wound healing was monitored and documented daily, and instances in which papillomas developed were noted. Experiments

were terminated when papillomas reached 1 cm in diameter or following papilloma degeneration.

2.17 Treatment with Tacrolimus (Protopic®)

Dorsal skins were shaved two days prior to painting with Tacrolimus (Protopic®; 0.1% tacrolimus ointment; Astellas Pharma Inc., Deerfield, IL, USA) and surgical wounding. On day one of each experiment, mice were anesthetized via isoflurane inhalation and painted with the Protopic® three hours prior to surgical wounding. Animals were painted once again with Protopic® seven days after wounding and monitored daily until the size of papillomas in untreated mice reached 0.5 cm in diameter or papillomas degenerated.

2.18 Statistical tests

Data is presented as average ± standard error. Statistical analysis was performed using software Microsoft Excel (Microsoft, Redmond, WA). For the student t-tests, *p*-values less than 0.05 were considered statistically significant.

Chapter 3

3. Mouse models of human cancers

Human cancers result from the accumulation of mutations that transform cells and block intrinsic and extrinsic tumor surveillance mechanisms. To understand the relative significance of any given mutation, it is often desirable to study its impact on cell proliferation in isolation. Indeed, such studies offer the opportunity to distinguish tumor-associated genetic defects that are functionally significant ("driver" mutations) from genetic aberrations that are merely associated with tumorigenesis ("passenger" mutations). Mice have been used extensively as models of human cancers for a number of reasons. First, they are small and relatively inexpensive to maintain. Second, mice breed relatively frequently (more than once a month), their gestation time is short (about 21 days), and their genomes can be genetically modified. Third, mouse genes are closely-related to their human counterparts. Approximately 99% of mouse genes have a homologue in the human genome (106, 107). Furthermore, the stepwise progression of human cancers is recapitulated in murine cancers (108). Finally, hundreds if not thousands of genetically modified mouse strains have been created and characterized and are readily available for inter-breeding. Many of these existing strains can be utilized to test specific hypotheses about mechanisms underlying tumorigenesis in a newly created strain of interest.

Palmiter and Brinster reported the creation of the first transgenic mouse strains (109). Subsequent advances in the genetic manipulation of gene expression have enabled researchers to regulate the expression of genes of interest both temporally and spatially *in vivo*. This technology is extremely powerful, yet transgenic mouse models also have several

inherent disadvantages. Transgenes integrate randomly within chromosomes and can disrupt endogenous genes inadvertently. Such gene disruptions can result in confounding phenotypes that can complicate the interpretation of phenotypes due to transgene function. Transgenic founders carry variable numbers of each transgene, and differences in gene dosage must be factored into the analysis of resulting phenotypes. Finally, limited numbers of tissue-specific promoters are available and thus it is often difficult to assess the functional significance of a gene of interest in the appropriate cell type. Despite these limitations, transgenic mouse strains have provided a great deal of insight into molecular mechanisms underlying tumor initiation, progression, and metastasis (for a detailed review, see (110)). For example: (1) tumor development has been shown to require multiple genetic alterations, such as loss of p53 and activation of any two of three oncogenes examined (c-myc, K-Ras, and Akt) (111). (2) Certain tumors require continuous expression of oncogenes (a phenomenon termed oncogene "addiction") for tumor maintenance (112). (3) Transgenic mice that over-express a mutated Ras (K-Ras^{G12D}) oncogene recapitulate pancreatic tumorigenesis, including spontaneous metastasis and a serum proteomic signature characteristic of human disease (113). In conclusion, previous studies in which human cancers have been modeled in mice have advanced tremendously our knowledge of the biology of cancer. Further investigations are continually developing new genetically modified mouse strains to better model human cancers.

3.1 Creation of Sp2 transgenic mouse lines

As mentioned previously, a link between elevated Sp2 protein expression and the progression of human prostate tumors had been reported (94). As will be detailed in Chapter 4, we noted that the expression of mouse Sp2 is also directly correlated with the progression of carcinogen-induced squamous carcinomas of the skin. To determine if Sp2 over-expression is a "driver" of tumorigenesis or an epiphenomenon in this murine cancer, we decided to generate a transgenic mouse strain in which a wild-type mouse Sp2 (mSp2) cDNA is over-expressed in basal keratinocytes (the cell of origin for squamous carcinomas) via the bovine keratin 5 (K5) promoter. The K5 promoter has been used extensively to express various transgenes within the basal layer of mouse stratified squamous epithelia (114). To determine if the Sp2 DNA-binding domain is required for phenotypes that might result in transgenic animals, we created an independent transgenic strain in which a mutated Sp2 cDNA (termed mSp2-NotI) that encodes a DNA-binding deficient protein is over-expressed in the same cells. Our transgenes were prepared in plasmid pTg1 via the subcloning of the bovine K5 promoter upstream of 5'UTR, splice donor, and splice acceptor sequences derived from the mouse albumin gene. These albumin-derived splicing components were incorporated into our transgene constructs because pre-mRNA processing has been shown to increase the efficiency of transgene expression (115). Full-length, epitope-tagged (*Influenza* hemagglutinin; HA) mSp2 and mSp2-NotI cDNAs were subcloned just downstream of the albumin splice acceptor sequence followed by SV40-derived poly-A sequences. The integrity of these transgene constructs was confirmed by

DNA sequencing, and expression of proteins of the expected sizes was confirmed by Western blotting of extracts prepared from transiently transfected COS-7 cells (Figure 5).

A

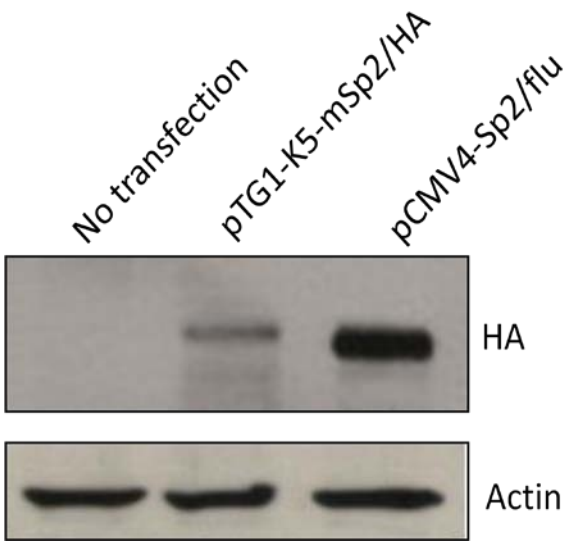

B

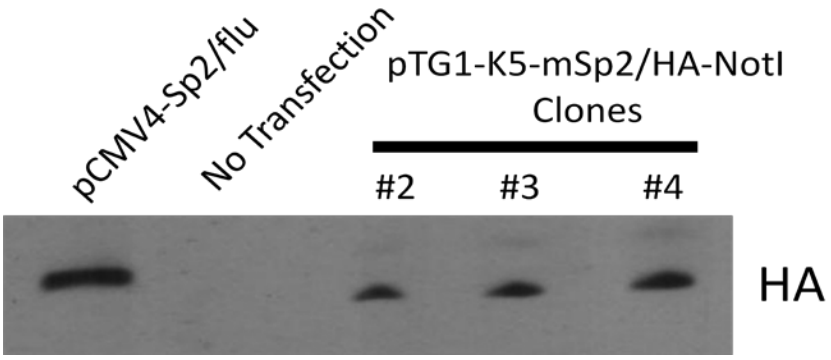

Figure 5 Expression of Sp2 and Sp2-NotI proteins in transiently-transfected COS-7 cells. *A.* COS-7 cells were transfected with pTG1-K5-mSp2/HA (lane 3) or pCVM4-Sp2/flu (positive control; lane 2). Cell extracts prepared from COS-7 cells were used as a negative control (lane 1). Western blotting with an anti-HA antibody detected an HA-tagged protein of the predicted size (80kDa). *B.* COS-7 cells were transfected with three independent pTG1-K5-mSp2/HA-NotI clones (#2-4) or pCMV4-Sp2/flu as a positive control (lane 1).COS-7 cell extracts appear in lane 2 as a negative control. Each transgene clone elicited a truncated HA-tagged protein of the expected size (lane 3-5).

3.2 Microinjection of transgene constructs and identification of founder lines

Transgenic mice are generated via the microinjection of transgenes into the FVB/NJ pronuclei of fertilized eggs by Animal Models Core at University of North Carolina at Chapel Hill. Each transgene was cleaved with Not I restriction endonuclease to liberate the transgene from the plasmid backbone, resulting DNA fragments were gel purified, injected into fertilized eggs, and microinjected eggs were implanted into the oviducts of pseudopregnant females.

Twenty pups were born following the microinjection of the mSp2 transgene into FVB/NJ pronuclei. The PCR was employed to detect potential founder animals. Genomic DNA was prepared from each pup and combined with transgene-specific primers that had been shown to detect the transgene when mixed with a vast excess of mouse chromosomal DNA. Genomic DNAs derived from five animals scored positive in this assay and these animals were designated Sp2-A through Sp2-E. After reaching sexual maturity, each potential founder was inter-bred with wild-type animals to determine if the transgene had been incorporated into the germ line. Three (Sp2-A, C, and E) of five transgene-positive animals transmitted the transgene to their descendants, giving rise to three families of transgenic animals that were characterized further. Following identical procedures, a single Sp2-Not I founder was identified amongst 28 pups resulting from pronuclear microinjections. Each Sp2 and Sp2-Not I founder transmitted their respective transgene to 50% of their descendants indicating that transgene integration had occurred within a single mouse chromosome. Expression of the transgene in the offspring of the founder lines was

investigated by Western blotting using anti-HA antibody and qRT-PCR using primers that bind to both endogenous and exogenous Sp2 transcripts. Once I confirm the expression of transgene in those transgenic animals, I preceded TAIL-PCR (as described in Section 2.9.1) to clone the integration site of transgene in each transgenic line.

3.3 Identification of sites of transgene integration

To determine the integration sites of each transgene, and thus ascertain if transgene integration had disrupted an endogenous gene, a technique termed Thermal Asymmetric Interlaced (TAIL)-PCR was used (detailed methods are described in Section 2.9.1.). This strategy employs a series of PCRs in which a nested set of transgene-specific primers is combined with a set of degenerate primers. Following multiple rounds of DNA amplifications and sequencing of resulting products, the mSp2 transgene was localized to mouse chromosome 6 in Sp2 Family-A members and chromosome 5 in Sp2 Family-C members. In Family-A animals, transgene integration occurred in an intergenic region 40 kbp upstream of exon 1 of mouse *Olr1* (Oxidized low-density lipoprotein receptor1). In Family C animals, transgene integration occurred within the coding region of mouse *Lphn3/CIRL3* (latrophilin 3) resulting in the deletion of 630 nucleotides of intron 15 and 65 nucleotides of exon 16. *Lphn3/CIRL3* encodes a brain-specific G protein-coupled receptor that is expressed most abundantly immediately after birth (116). It is not known if *Lphn3/CIRL3* is an essential gene nor is its physiological significance understood; however a recent study indicates that *LPHN3* is a novel susceptibility gene for Attention Deficit Hyperactivity Disorder (ADHD), the most common childhood behavioral disorder (117).

Additionally, antisense oligonucleotides targeting *Lphn3/CIRL3* have been reported to suppress hypoxia-induced cell death in hippocampal and cortical cell cultures (118). These latter results suggest that latrophilin 3 may be of functional importance in processes leading to neurodegeneration. TAIL-PCR failed to result in the cloning of the Sp2-NotI integration site, and thus its chromosomal location remains uncertain.

Chapter 4

This chapter appeared in Tae-Hyung Kim, Shannon L. Chiera, Keith E. Linder, Carol S. Trempus, Robert C. Smart, and Jonathan M. Horowitz, Overexpression of Transcription Factor Sp2 Inhibits Epidermal Differentiation and Increases Susceptibility to Wound- and Carcinogen-Induced Tumorigenesis, ***Cancer Res***; 70(21) November 1, 2010

4. Over-expression of transcription factor Sp2 inhibits epidermal differentiation and increases susceptibility to wound- and carcinogen-induced tumorigenesis

4.1 Sp2 protein expression increases in concert with DMBA/TPA-induced skin carcinogenesis.

Since Sp2 expression is correlated directly with the progression of human prostate cancers (94), it became of interest to determine if this correlation might extend to additional neoplasms at one or more stages of tumor progression. We chose carcinogen-induced mouse squamous cell carcinomas as our model system for these studies. Protein extracts were prepared from normal whole skin and epidermis, a series of small-, medium-, and large-sized DMBA/TPA-induced papillomas, a mouse cell line derived from a DMBA/TPA-induced squamous cell carcinoma (MT2.6; 18), and a spontaneously-immortalized mouse keratinocyte cell line (BALB/MK2; 22), and equivalent amounts of each extract were examined by Western blotting. As shown in Figure 6, Sp2 expression was below the limit of detection in normal mouse skin (lane 1), epidermis (lane 2), or small-sized papillomas (lanes 3-5). Sp2 expression was barely detectable in medium-sized papillomas (lanes 6-8), was expressed to significant levels in two of three large-sized papillomas (lanes 9-11) and was expressed strongly in BALB/MK2 and MT2.6 cells (lanes 12 and 13, respectively). These results indicate that Sp2 expression is up-regulated in this model system, is correlated directly with the progression of DMBA/TPA-induced neoplasms, and is a feature of immortalized (BALB/MK2) keratinocytes. In contrast, Sp1 expression was not correlated with progression in this model system (Figure 6). Sp2 expression is also elevated in human squamous carcinoma cell lines relative to primary human keratinocytes (Figure 7).

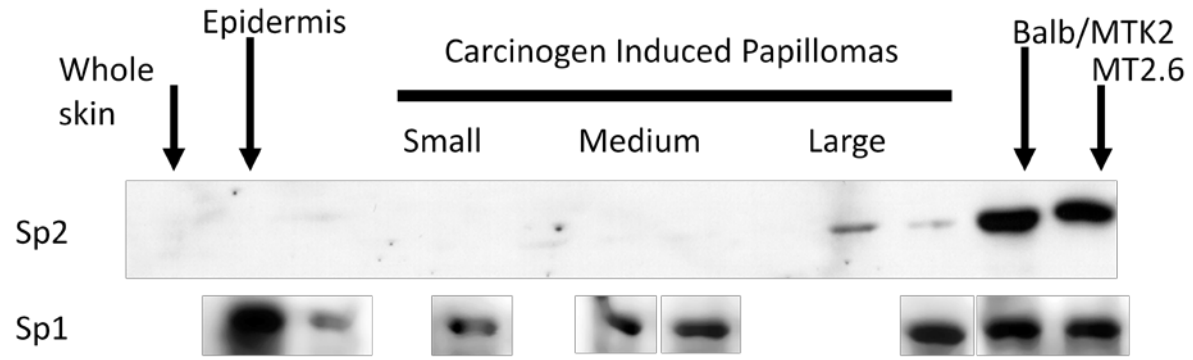

Figure 6 Western blotting of normal and various stages of tumors of mouse epidermis. Extracts from whole skin, epidermis, carcinogen induced papillomas in various sizes, and tumor cells lines were immunoblotted against Sp2 and Sp1. Expression level of Sp1 is consistent regardless of tumorigenesis stages. In contrast, expression level of Sp2 is directly correlated with tumor progression.

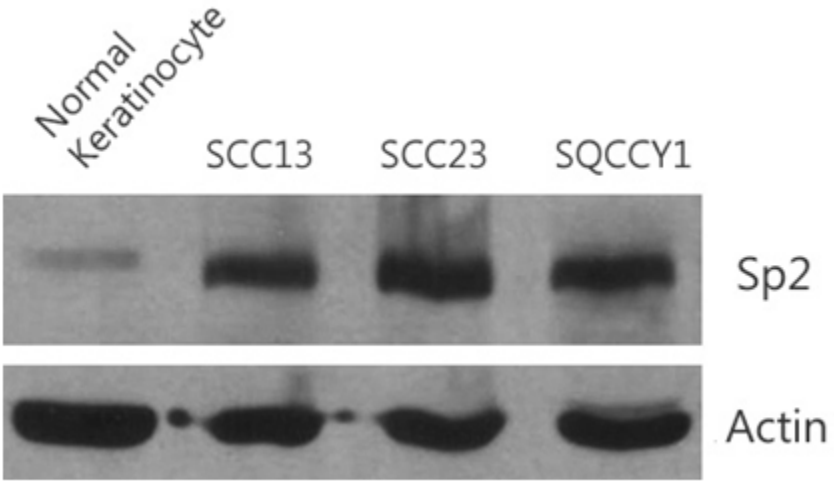

Figure 7 Western blot of human samples with polyclonal antibodies against Sp2 (αSp2) and actin (αActin). Lane 1, primary human keratinocytes; lane 2, SCC13; lane 3, SCC23; lane 4, SQCCY1.

4.2 Sp2 over-expression in basal keratinocytes causes alopecia in hemizygotes and post-natal lethality in homozygotes.

Sp2-A and -C hemizygotes have been bred with FVB/NJ animals for more than 11 generations and exhibit normal life expectancy and fecundity. A majority of Sp2-A hemizygotes develop alopecia and hyperkeratosis beginning at two months of age (Figure 8A). These skin abnormalities can occur at discrete sites, e.g., sites of abrasion or repetitive movement, or extend throughout the dorsal surface and affected regions increase in severity with age. Sp2-C hemizygotes do not exhibit alopecia or other gross phenotypic abnormalities. Homozygous Sp2-A or -C transgenic pups are produced at expected ratios, and the gross appearance of these animals at birth is indistinguishable from wild-type and hemizygous littermates. However, homozygotes perish within the first two weeks of post-natal life. The skin of Sp2-A homozygotes begins to deteriorate on post-natal day three (PD3), becoming increasingly reddened and hyperkeratotic (Figure 8B, asterisks). Such pups become runted and developmentally retarded relative to their littermates and succumb prior to PD13. The skin of Sp2-C homozygotes deteriorates more quickly and pups perish prior to PD3.

A

B

Figure 8 Gross phenotypes of hemizygous and homozygous Sp2-A animals. *A,* alopecia in adult hemizygotes. Representative affected animals are illustrated at 2 to 4 mo of age. *B,* F2 litter of WT, hemizygous, and homozygous animals on PD12. Homozygous animals are indicated with an asterisk.

Histological examinations of PD1 Sp2-A homozygous pups revealed a well-structured stratified epidermis with an intact stratum corneum, as well as developing sebaceous glands and hair follicles similar to wild-type animals. Multifocal apoptosis within the epidermal basal layer was marginally elevated relative to wild-type littermates with scattered disorganization of basal cells that became significantly more pronounced by PD4. A loss of normal epidermal architecture was noted by PD6 with a disorganization of cells in all layers and occasional areas of partial to complete epidermal collapse where the stratum spinosum contacted the dermis. Loss of laminar epidermal architecture was accompanied by scattered apoptosis, hypertrophy and hydropic swelling of keratinocytes, as well as orthokeratotic laminated hyperkeratosis and patchy areas of parakeratosis. The severity and extent of these aforementioned features worsened progressively through PD13. Histological examinations of Sp2-C pups revealed identical epidermal defects.

To assess levels of Sp2 expression in transgenic animals two experiments were performed. First, RNAs were harvested from whole skin of wild-type, hemizygous, and homozygous post-natal pups and Sp2 expression was detected via RT-PCR. As shown in Figure 9, robust levels of Sp2 message were detected in hemizygous and homozygous Sp2-A (left panel) and Sp2-C (right panel) animals relative to wild-type littermates. Second, levels of Sp2 expression were quantified by real-time PCR as a function of animal age. Real-time PCR assays performed with RNAs from whole skin of three-month old hemizygotes indicated that Sp2 expression was nearly 20-fold above endogenous levels in Sp2-A animals and elevated by 200-fold in Sp2-C animals (data not shown). Levels of exogenous Sp2

expression in Sp2-C hemizygotes increased with age whereas transgene expression levels in Sp2-A hemizygotes remained unchanged (data not shown).

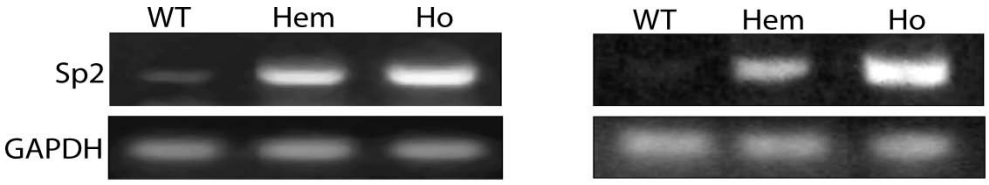

Figure 9 Expression of transgene *in vivo*. Amplification of endogenous and exogenous Sp2 mRNAs in WT and transgenic animals via RT-PCR. Total RNAs were prepared from dorsal whole skin from WT, hemizygous, and homozygous littermates on PD1 and analyzed by RT-PCR with Sp2- or GAPDH-specific primers. Left, Sp2-A; right, Sp2-C.

To determine if proteins of expected sizes were synthesized in transgenic animals, denatured extracts were prepared from whole skin and Western blots were performed using an anti-HA antibody. Consistent with results obtained in transfection experiments (Figure 5), a single protein of 80 kDa was detected (Figure 10). To determine if the bovine keratin 5 promoter directed expression of Sp2 to basal keratinocytes, paraffin-embedded sections were prepared from whole skin harvested from wild-type and homozygous Sp2-A littermates and exogenous Sp2 expression was detected via immunohistochemistry using an anti-HA antibody. As shown in Figure 11, basal cells within the interfollicular epidermis as well as the hair follicle outer root sheath stained strongly with an anti-HA antibody whereas sections prepared from wild-type animals lacked staining. We conclude that the Sp2 transgene is expressed as anticipated, and Sp2 over-expression in basal keratinocytes results in alopecia in Sp2-A hemizygotes and post-natal lethality in Sp2-A and -C homozygotes.

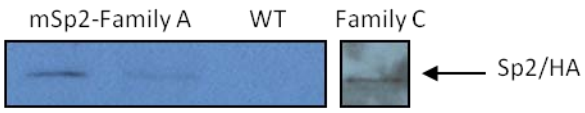

Figure 10 Expression of epitope-tagged Sp2 protein *in vivo*. Lysates from epidermis of transgenic mouse lines, Sp2-A and Sp2-C, were analyzed with anti HA antibody. Extract from wild type epidermis is negative whereas extracts from Sp2-A and Sp2-C epidermis have HA positive band in a correct size (80kDa).

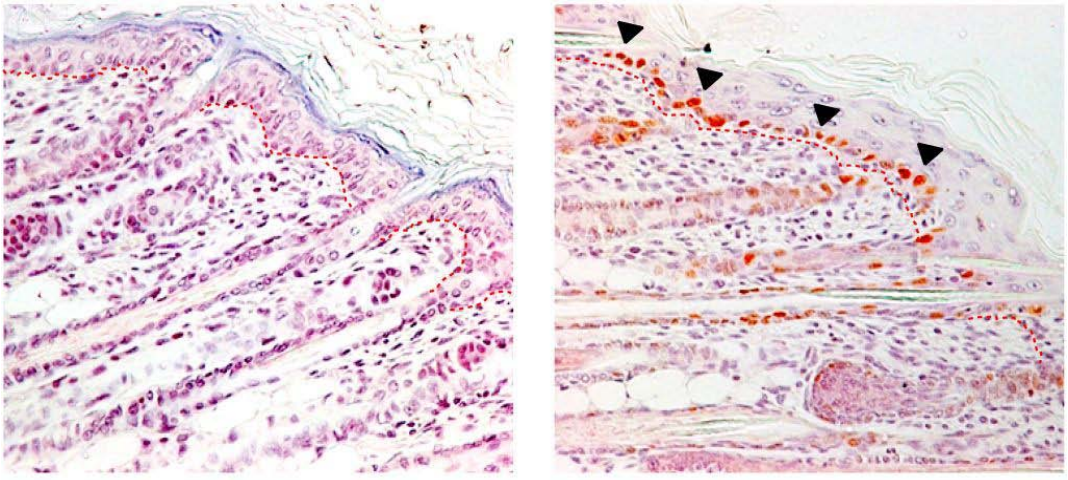

Figure 11 Ectopic expression of mouse Sp2 in basal keratinocytes. Immunohistochemical detection of ectopic mouse Sp2 expression in basal keratinocytes of Sp2A homozygotes. Paraffin-embedded dorsal skin sections prepared from WT (left) and homozygous transgenic (right) littermates on PD6 were analyzed with an anti-HA antibody. HA-positive basal keratinocytes are indicated by a filled arrowhead. The basement membrane separating the epidermis from dermis is indicated by a dotted red line.

4.3 Sp2 over-expression causes arrested differentiation of the interfollicular epidermis.

To determine the consequence of Sp2 over-expression for epidermal differentiation, paraffin-embedded whole skin sections were prepared from Sp2-A homozygotes and wild-type littermates on successive post-natal days. Pups were injected with BRdU one hour prior to euthanasia to label proliferating cells, and skin sections were examined with anti-BRdU antibodies as well as antibodies against differentiation-specific markers. As shown in Figure 12, sections stained with hematoxylin and eosin revealed that the epidermis of wild-type and homozygotes is similar in cell stratification and thickness on PD2 but diverge markedly on subsequent post-natal days. The epidermis of homozygotes thickened increasingly on PD3-4 relative to wild-type littermates with hypertrophic and hydropically swollen cells accumulating in disorganized epidermal layers. To determine whether markers of basal (keratins 5 and 14) and suprabasal (keratin 10) keratinocytes were expressed on these post-natal days, paraffin-embedded sections were analyzed by immunohistochemistry. Keratins 5, 10, and 14 were expressed as expected in wild-type animals (Figure 12, top panels), whereas the expression of these markers was altered profoundly in homozygotes (Figure 12, bottom panels). Basal keratinocytes of homozygotes expressed keratin 5 on PD2 with sporadic keratin 5-stained cells noted in suprabasal layers. The abundance of keratin 5-positive cells in all epidermal cell layers increased significantly on PD3-4. Similarly, keratin 14 expression was detected in basal keratinocytes on PD2 and in all epidermal layers on subsequent days. Keratin 10 expression was detected in all suprabasal layers on PD2, and diminished to low levels or was absent in the granular and cornified layers during subsequent post-natal days.

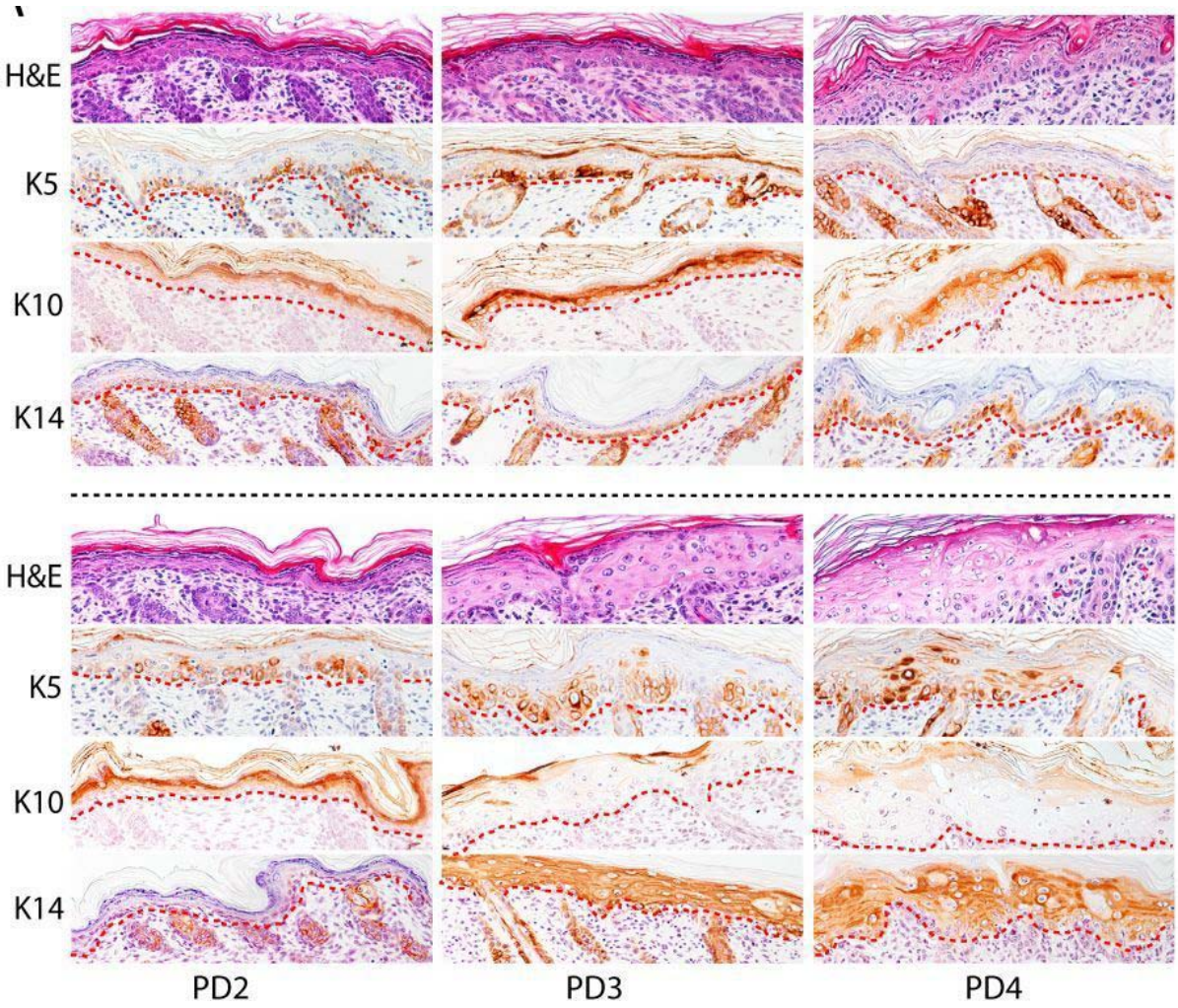

Figure 12 Histochemical and immunohistochemical characterization of postnatal Sp2-A homozygotes. Paraffin-embedded dorsal skin sections from WT (top) and homozygous transgenic (bottom) littermates on PD2 to PD4. Sections were stained with H&E or with antibodies against keratin 5 (K5), 10 (K10), or 14 (K14). Dashed red lines indicate the position of the epidermal basement membrane.

To extend this analysis, paraffin-embedded sections on PD4 were examined for the expression of a bevy of additional markers (Figure 13). The expression of keratin 6, a marker associated with neoplastic, inflamed, and/or wounded epidermis, was detected in the epidermis of homozygotes but not wild-type animals (119, 120). Keratin 8, an alternative heterodimeric partner of keratin 14 and a keratin normally restricted to "simple" epithelia, was detected in the epidermis of homozygotes and absent in wild-type animals (121-124). Finally, a marker characteristic of the stratum corneum, loricrin, was not detected in homozygotes.

To determine if epidermal distress induced the recruitment of stem cells from the hair follicle "bulge" region to the interfollicular epidermis, two experiments were performed. First, PD4 sections were stained for the expression of CD34, a well-characterized marker of this stem cell population (125, 126). Second, a lineage tracing experiment was performed in which Sp2-A mice were inter-crossed with animals that express a transgene, K15-EGFP, restricted to "bulge"-derived stem cells (127, 128). CD34- and EGFP-positive cells were detected within the basal and suprabasal layers of Sp2-A homozygotes, but not wild-type littermates, on PD4 indicating the recruitment of "bulge"-derived cells to the interfollicular epidermis (Figure 13).

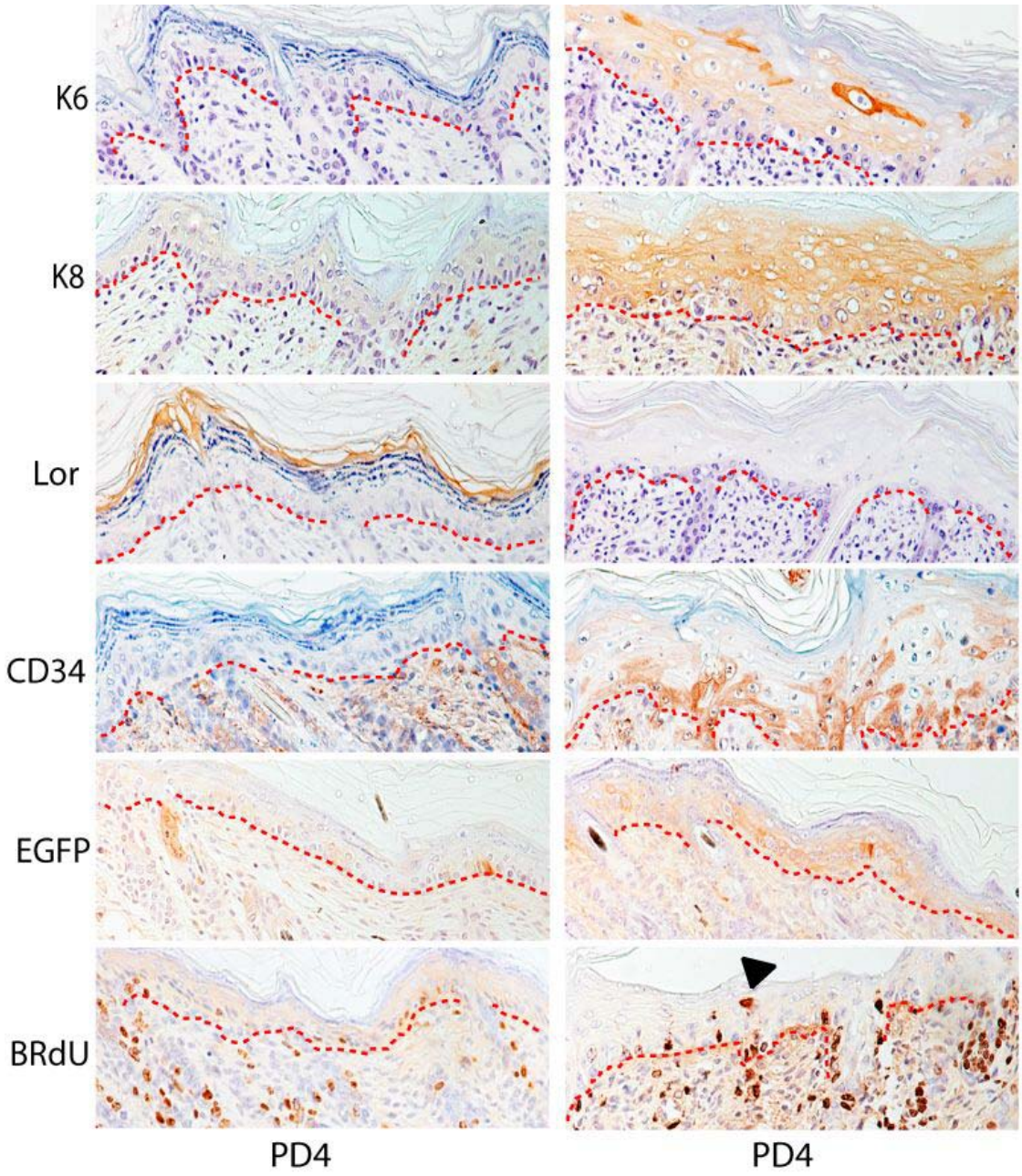

Figure 13 Immunohistochemical characterization of postnatal day 4 Sp2-A homozygotes. Paraffin-embedded dorsal skin sections from K15-EGFP transgenic animals (left) and [K15-EGFP, Sp2-A/Sp2-A] double-transgenic (right) littermates on PD4. Sections were stained with antibodies against keratin 6 (K6) or 8 (K8), loricrin (Lor), CD34, EGFP, or BrdUrd. A filled arrowhead indicates a BrdUrd-positive suprabasal keratinocyte, and dashed red lines indicate the position of the epidermal basement membrane.

Finally, sections were stained with an anti-BRdU antibody to identify proliferating cells. BRdU-positive cells were detected in the basal layers of both wild-type and homozygous animals, however BRdU-positive cells were also noted in suprabasal layers of homozygotes (arrowhead, Figure 13). To quantify basal cell proliferation, BRdU-positive cells within the interfollicular epidermis of wild-type and homozygous post-natal animals were enumerated and compared. As shown in Figure 14, BRdU-positive basal cells were more numerous in homozygotes however this level of increased cell proliferation was not statistically significant ($p<0.1$). Taken together, we conclude from these immunohistochemical analyses that Sp2 over-expression in basal keratinocytes produces a population of phenotypically immature keratinocytes that appear unable to commit to the epidermal differentiation program.

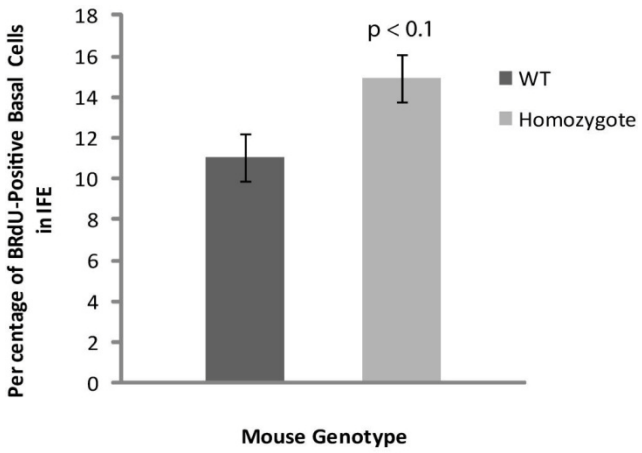

Figure 14 Enumeration of BrdUrd-positive basal keratinocytes. Basal keratinocytes within the interfollicular epidermis of K15-EGFP and [K15-EGFP, Sp2-A/Sp2-A] double-transgenic littermates on PD4. Columns, mean (K15-EGFP, n ≥ 3,400 cells/group; [K15-EGFP, Sp2-A/Sp2-A], n ≥ 7,300 cells/group); bars, SE.

4.4 Sp2 over-expression renders hemizygous animals susceptible to wound-induced neoplasia.

In the course of these studies we noted that Sp2-C hemizygotes developed occasional papillomas at sites of ear punches or minor wounds sustained from littermates. To quantify this apparent susceptibility to wound-induced neoplasia, full-thickness surgical wounds (4 mm diameter) were introduced into the dorsal skin of Sp2-C hemizygotes and wild-type littermates and these animals were monitored for the development of papillomas. As shown in Figure 15, surgery-induced papillomas developed within weeks following wounding of Sp2-C hemizygotes. Whereas surgical wounding of wild-type animals did not induce the formation of a single papilloma, 27% of wounds sustained by Sp2-C hemizygotes induced papillomagenesis (p=0.001; Figure 16A). To determine if the incidence of wound-induced papillomagenesis is influenced by animal age, results presented in Figure 16A were plotted as a function of the age of Sp2-C animals at the time of surgery. Whereas young animals (one to four months of age) were only mildly susceptible to wound-induced papillomas, 70% of animals developed papillomas when wounded at six to ten months of age and this increased incidence of papillomagenesis is statistically significant (p<0.01; Figure 16B). We conclude from these results that Sp2 over-expression in basal keratinocytes induces a marked susceptibility to wound-induced neoplasms. Moreover, this susceptibility to papillomagenesis increases in concert with the age-dependent increase in Sp2 expression noted in these animals.

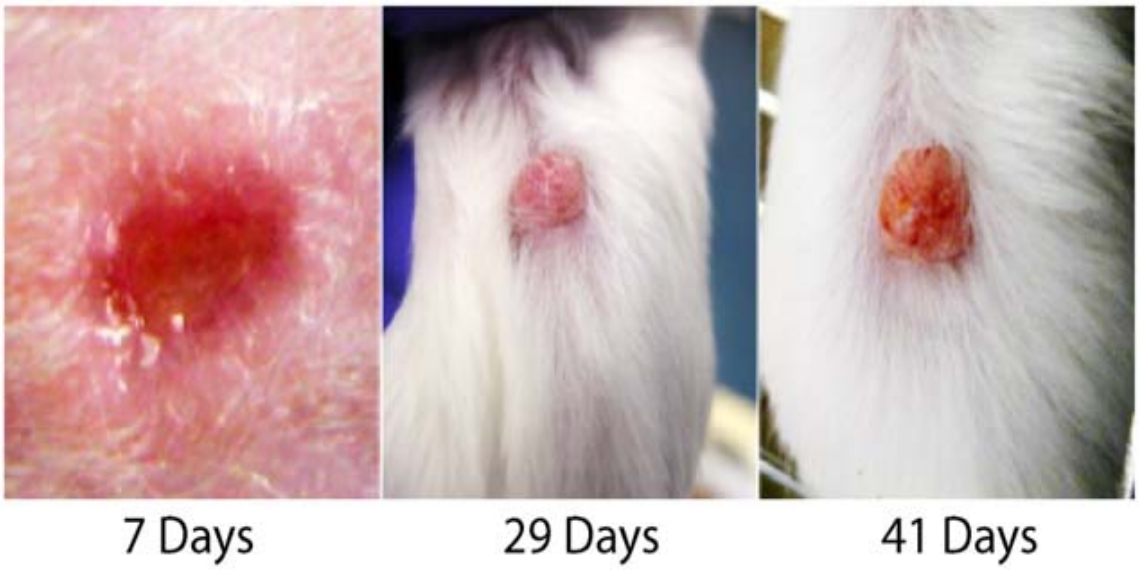

Figure 15 Wound-induced papillomas in Sp2-C hemizygotes. Papilloma development on the dorsal surface of a surgically wounded Sp2-C hemizygote. The number of days following wounding is indicated below each image.

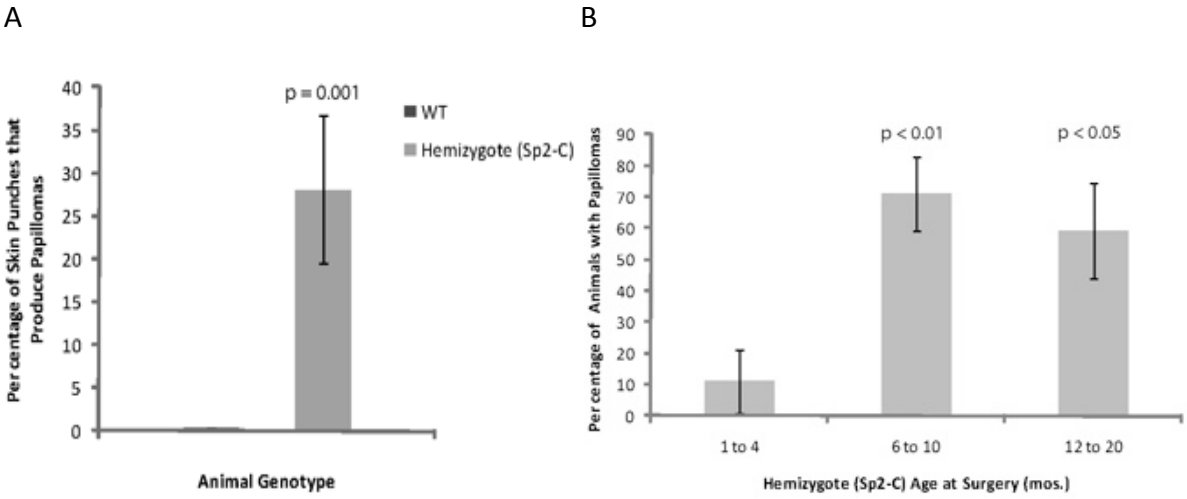

Figure 16 Incidence of wound-induced papillomas in wild-type and Sp2-C hemizygotes. *A,* percentage of surgical wounds that produced papillomas in WT and Sp2-C hemizygous littermates in animals between 1 and 20 mo of age. Columns, mean (WT, n = 11 mice/group; Sp2-C, n = 48 mice/group); bars, SE. *B,* percentage of Sp2-C hemizygotes that developed wound-induced papillomas as a function of age at time of surgery. Columns, mean (1–4 mo, n = 9 mice/group; 6–10 mo, n = 17 mice/group; 12–20 mo, n = 22 mice/group); bars, SE.

Histological examinations of wound-induced lesions revealed them to be pedunculated to sessile cutaneous papillomas, composed of epidermal hyperplasia and fibrovascular stroma that often contained mixed neutrophilic and lymphoplasmacytic inflammation (Figure 17). Multifocal areas of mild epidermal dysplasia were accompanied by mild to moderate keratinocyte apoptosis in the basal and immediate suprabasal layers, where lymphocyte satellitosis was occasionally noted. Skin sections prepared from wound-induced papillomas were examined by immunohistochemistry for markers of cell proliferation (PCNA) and keratinocyte differentiation (keratins 5, 6, 8, 10, 14, 15 and loricrin). Consistent with expectations, only a minority of basal cells within the epidermis at the margins of wound-induced papillomas stained with PCNA antibodies (Figure 18, left column). In stark contrast, PCNA-positive cells were detected throughout wound-induced papillomas in basal as well as suprabasal cell layers (Figure 18, right column). Differentiation markers (keratins 5, 14, and 15) expressed within cells of the basal cell layer in margin tissue were detected largely in suprabasal layers of wound-induced papillomas (Figure 18). Keratin 10 was detected in all suprabasal layers in margin tissue yet was detected weakly in the most superficial suprabasal layers of papillomas (Figure 18). Consistent with results noted earlier for post-natal transgenic homozygotes, keratins 6 and 8 were detected throughout the epidermis of wound-induced neoplasms (Figure 18). Finally, diffuse loricrin expression was detected in papillomas within an expanded suprabasal zone relative to its restricted expression within the cornified layer of margin tissue (Figure 18). We conclude from immunohistochemical results that wound-induced

neoplasms are composed of highly proliferative, phenotypically immature keratinocytes that exhibit a profound disruption of the epidermal differentiation program.

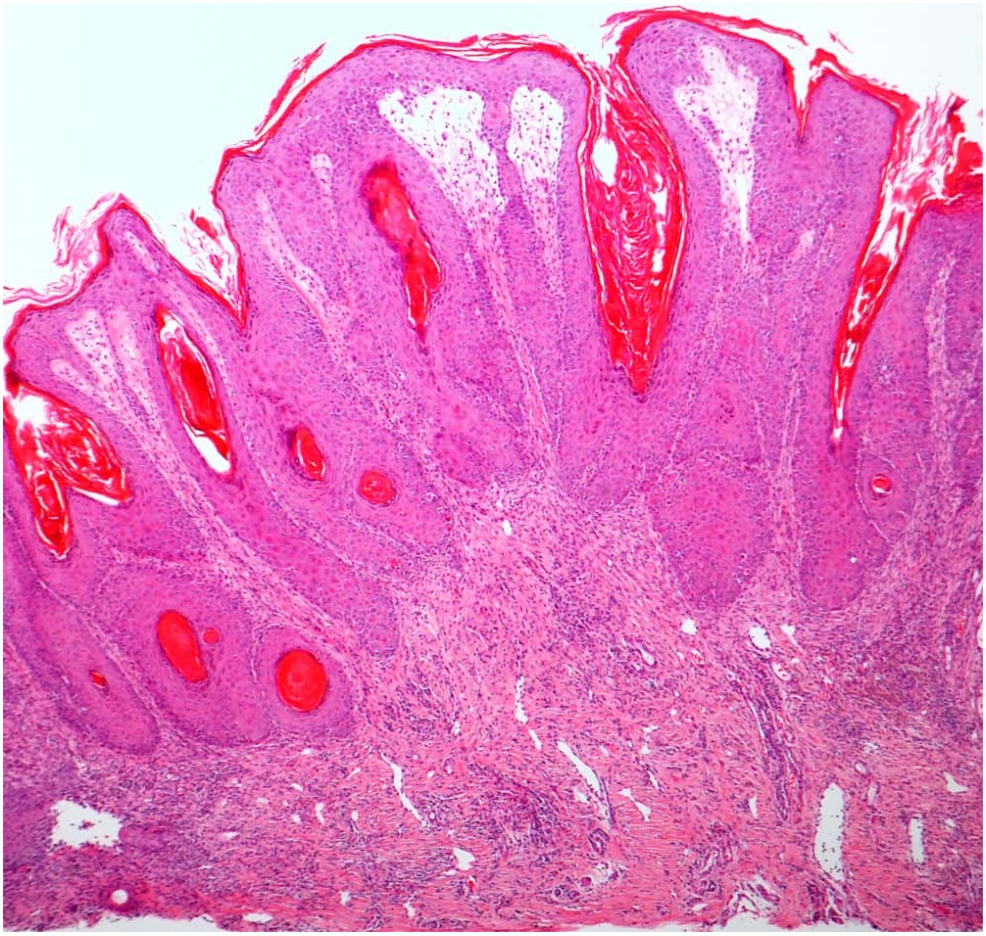

Figure 17 Low-magnification image of wound-induced papilloma. Whole papillomas samples were fixed in 10% formalin and embedded in paraffin, and 10-µm sections were placed on glass slides. Sections were deparaffinized and rehydrated by consecutive incubations in xylene, 100% ethanol, and 95% ethanol and subjected to staining with H&E.

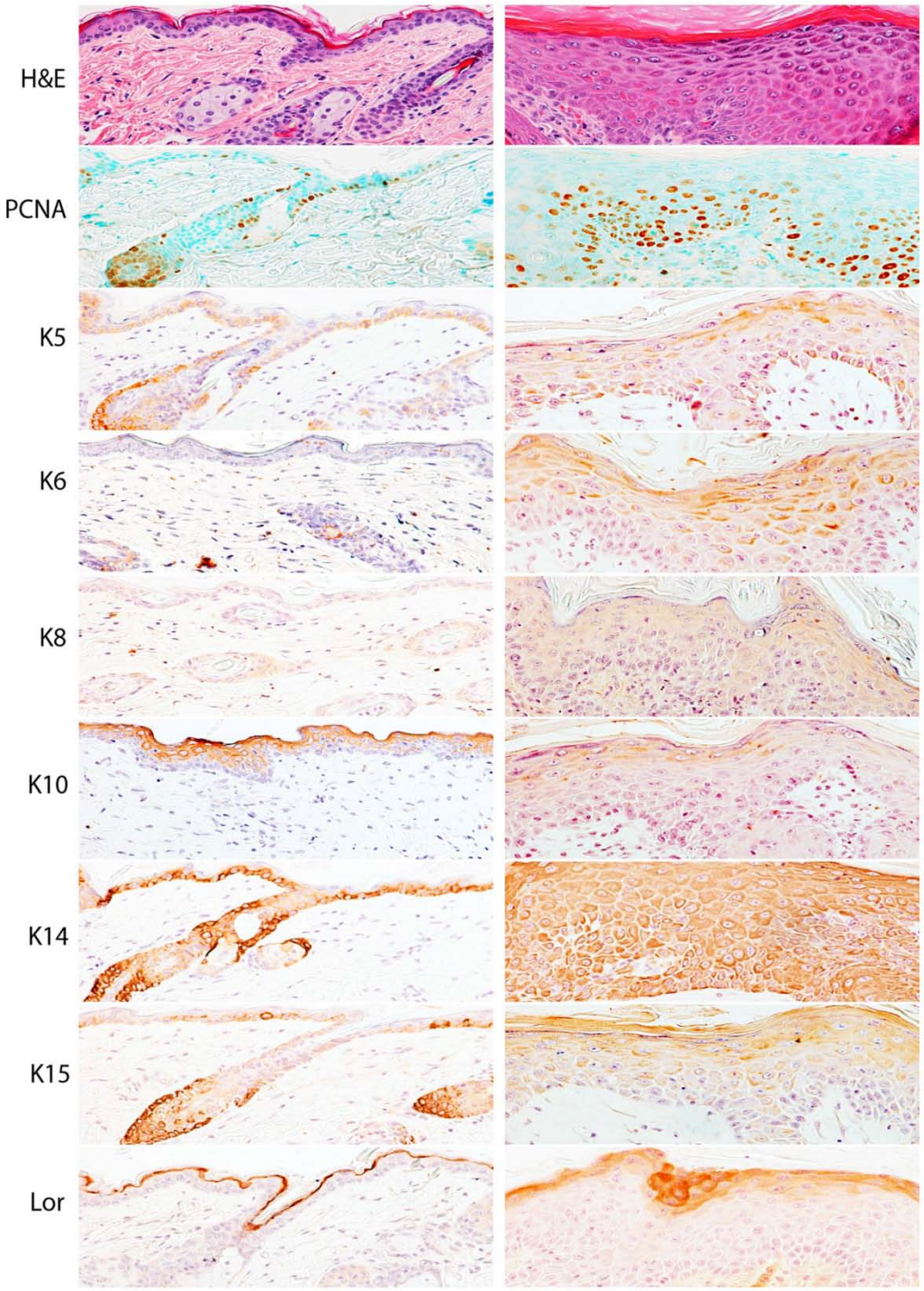

Figure 18 Characterization of wound-induced papillomas in Sp2-C hemizygotes.
Histochemical and immunohistochemical characterization of a wound-induced papilloma. Paraffin-embedded dorsal skin tissue sections from the papilloma margin (left column) and papilloma (right column) were stained with H&E or various antibodies. Antibodies used are indicated as in Figure 13 and 14, with the exception of the addition of antibodies against PCNA and keratin 15 (K15).

4.5 T cell activation is not required for the wound-induced papillomas

Neoplasia following surgical wounding has been noted in a number of animal systems, including humans (129). In some instances the growth of wound-induced neoplastic lesions has been shown to require the infiltration of activated T cells (130). For example, T cell infiltration is required for wound-induced papillomagenesis in transgenic mice that over-express activated MAPK kinase 1 (MEK1) via the human involucrin promoter (130, 131). As a first step towards determining if T cell activation is required for wound-induced papillomagenesis, Sp2-C animals were treated topically with Tacrolimus (Protopic®), a well-characterized T-cell inhibitor. Tacrolimus blocks the dephosphorylation of transcription factor NF-AT (nuclear factor of activated T-cells) by calcineurin and in so doing prevents the expression of genes characteristic of activated T cells, such as IL-2 and related cytokines (132). Tacrolimus was applied topically to the dorsal skin of Sp2-C animals and wild-type littermates three hours before surgical wounding, and every day for five weeks beginning one week after surgery. Interestingly, Tacrolimus treatment in Sp2-C, but not wild-type animals, increased wound-induced papillomagenesis dramatically suggesting that a T-cell mediated immune response limits the outgrowth of wound-induced papillomas in Sp2-C hemizygotes (Figure 19).

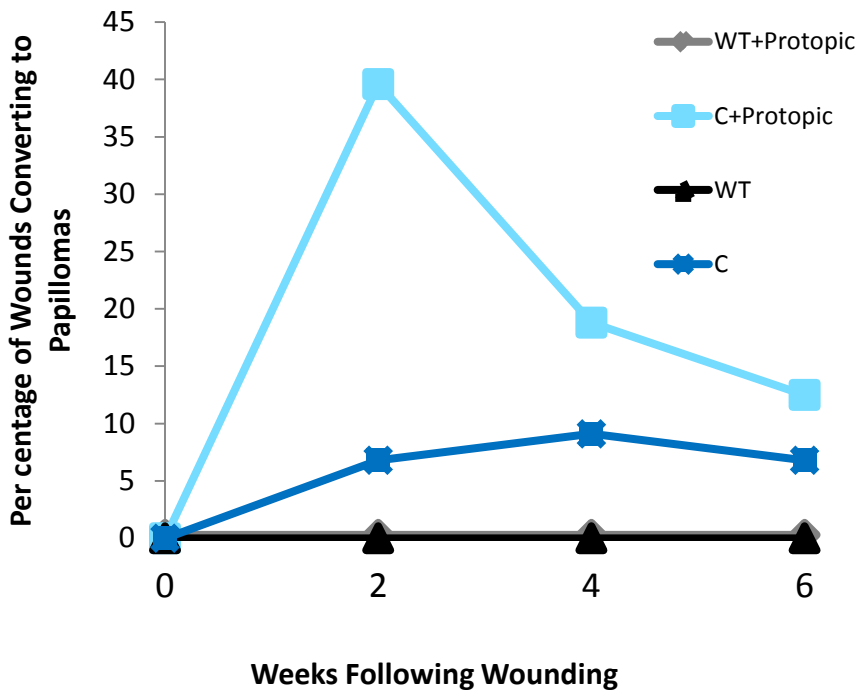

Figure 19 Growth of wound-induced papillomas does not require activation of infiltrating T cells. Sp2 transgenic mice were treated topically with Tacrolimus (Protopic®), a well-characterized inhibitor of T-cells, before and after surgical wounding. Tacrolimus treatment of transgenic, but not wild-type animals, increased wound-induced papillomagenesis dramatically suggesting that infiltration of activated T-cells is not required for papillomagenesis. Instead, T-cells appear to limit the outgrowth of these wound-induced lesions.

4.6 Sp2 over-expression increases the sensitivity of hemizygous animals to skin carcinogenesis.

To determine if Sp2 over-expression increases the sensitivity of basal keratinocytes to transformation by an environmental carcinogen, papillomagenesis in Sp2-C hemizygotes and control animals was analyzed using a "two-stage" model of skin carcinogenesis. Wild-type and hemizygous Sp2-C littermates were treated with a single application of DMBA followed by twice weekly treatments with TPA for 20 weeks. Sp2-C hemizygotes and wild-type littermates developed papillomas 5.5 and 7.5 weeks following DMBA treatment, respectively (data not shown), and DMBA/TPA-treated Sp2-C hemizygotes exhibited greater numbers of papillomas per animal throughout the course of this study (Figure 20). Treated animals were sacrificed prior to the progression of papillomas to squamous cell carcinomas and thus it was not possible to determine whether ectopic Sp2 expression affects the incidence of tumor progression. We conclude from these results that Sp2 over-expression in basal keratinocytes increases their sensitivity to an environmental carcinogen.

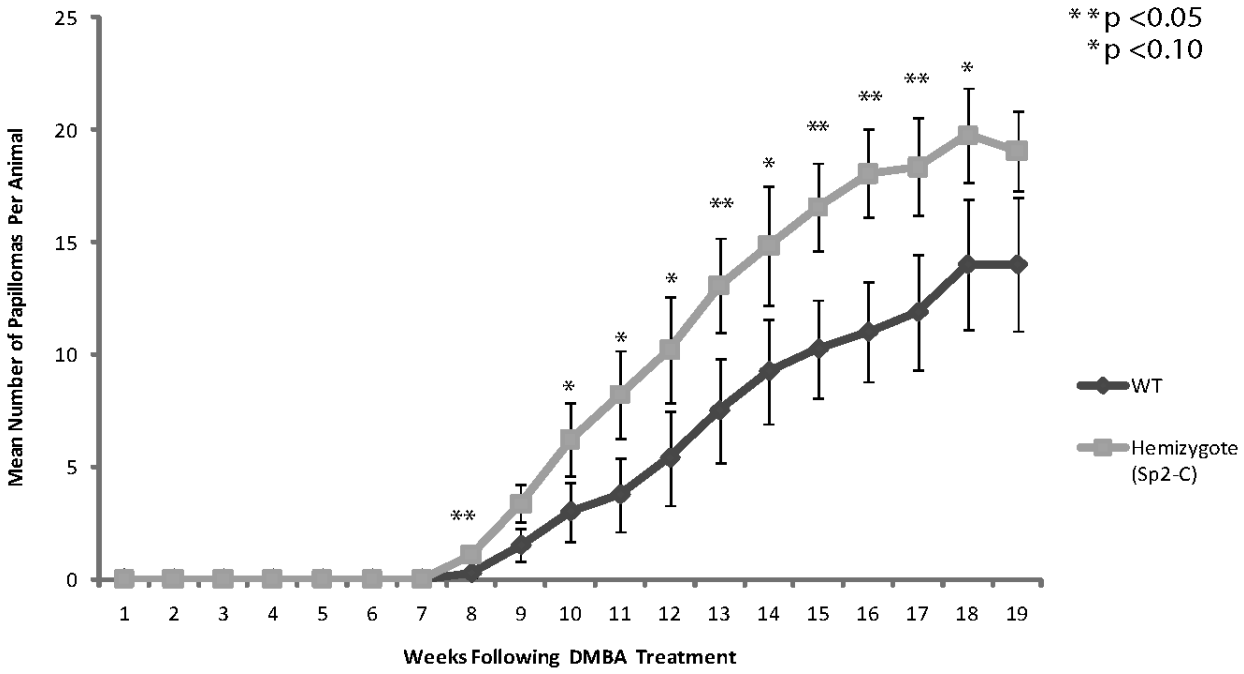

Figure 20 Incidence of DMBA/TPA-induced papillomas in wild-type and Sp2-C hemizygotes. Mean number of DMBA/TPA-induced papillomas per animal (WT, n = 8 mice/group; Sp2-C, n = 14 mice/group) are plotted as a function of age at time of DMBA treatment. Bars, SE.

4.7 Creation of Sp2-NotI mice and characterization of transgene expression

To determine if the phenotypes exhibited by Sp2 transgenic strains require an intact DNA-binding domain, we prepared an analogous transgenic strain in which a DNA-binding deficient Sp2 protein is over-expressed in epidermal progenitor cells. To create this mutant protein, we took advantage of a unique *BspEI* restriction site within the mouse Sp2 cDNA that occurs downstream of the nuclear localization sequence and within the first zinc-"finger" of the DNA-binding domain. We predicted that cleavage with *BspEI*, followed by "filling-in" of resulting "sticky" ends and blunt-end ligation, would lead to a "frame-shift" mutation producing a karyophilic protein lacking DNA-binding activity. Such a mutated protein would be expected to be transported to the nucleus where it could potentially interact with natural Sp2-interacting proteins via the Sp2 *trans*-activation domain. If so, such a protein might be predicted to have "dominant-negative" effects with respect to Sp2-mediated transcription in epidermal progenitor cells. As for the transgenic strains carrying a wild-type Sp2 transgene, transcription of the mutated Sp2 cDNA in this transgene (pTG1-mSp2-NotI/HA) is regulated by the bovine keratin 5 promoter. As presented in the previous chapter, this mutated cDNA was shown to produce a stable, epitope-tagged protein of the predicted size in transfected cells.

To confirm that the expression of the transgene carried by Sp2-NotI mice was as predicted, denatured protein extracts were prepared from the epidermis of transgenic mice and examined by Western blotting with anti-HA and anti-Sp2 antibodies. As shown in Figure 21, a novel HA-tagged Sp2 protein was detected in these extracts and as predicted this

protein is approximately 4.5 kDa smaller in size than endogenous Sp2 protein. It is also apparent that this truncated Sp2 protein is over-expressed relative to levels of the endogenous protein. To quantify this level of expression more precisely, the abundance of Sp2 message was determined by qRT-PCR using oligonucleotide primers that are expected to amplify endogenous and exogenous Sp2 mRNAs. As shown in Figure 22, Sp2 message is 60-fold higher in the epidermis of Sp2-NotI mice than wild-type animals.

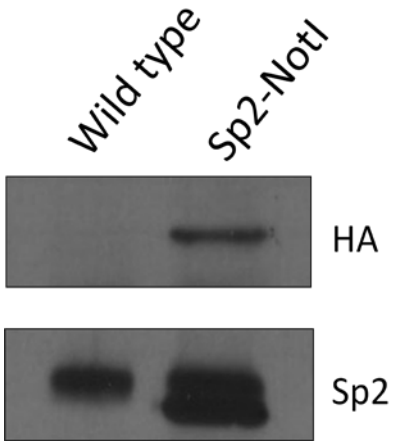

Figure 21 Western blots of Sp2 proteins expressed in the epidermis of wild-type and Sp2-NotI animals. (Top) Denatured epidermal protein extracts were challenged with an anti-HA antibody. (Bottom) A parallel set of denatured extracts were examined with an anti-Sp2 antibody. Note the appearance of a truncated Sp2-derived protein in extracts prepared from Sp2-NotI transgenic animals.

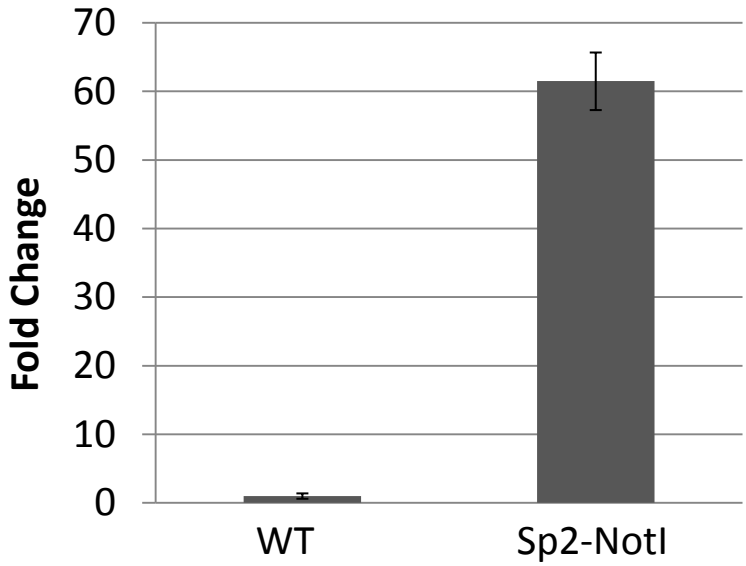

Figure 22 Relative expression levels of Sp2 mRNA in the epidermis of wild-type and Sp2-NotI transgenic animals. Endogenous and exogenous Sp2 transcripts were amplified with primers that bind exons 5 and 6, and message levels were quantified by qRT-PCR. RNAs were prepared from the epidermis of wild-type and Sp2-NotI animals of the same approximate age (3 months old). The expression of Sp2 message in wild-type epidermis is set equal to 1.

4.8 Phenotypes presented by Sp2-NotI transgenic animals.

As mentioned above, Sp2-A hemizygotes begin to exhibit signs of alopecia (hair loss) at weaning and, in general, this phenotype progresses as these animals age. Alopecia in individual Sp2-A animals can be limited to discrete body surfaces, e.g., sites of repetitive movement or sites of repeated scratches, or be more general, e.g., encompassing nearly the entirety of the dorsal surface. Sp2-NotI hemizygotes present with a similar hair loss phenotype; these animals begin to lose hair at approximately three months of age, and their dorsal surface becomes nearly hairless by 11 months of age (Figure 23). Unlike to Sp2-A and Sp2-C animals, I don't have allele specific primers for genotyping of Sp2-NotI animals because the TAIL-PCR failed to clone the integration site of transgene. Due to this lack of primers, Sp2-NotI homozygous animals cannot be distinguished from wild-type and/or hemizygous littermates. Indeed, further phenotypic analysis that might be associated with those Sp2-NotI homozygous animals was not pursued.

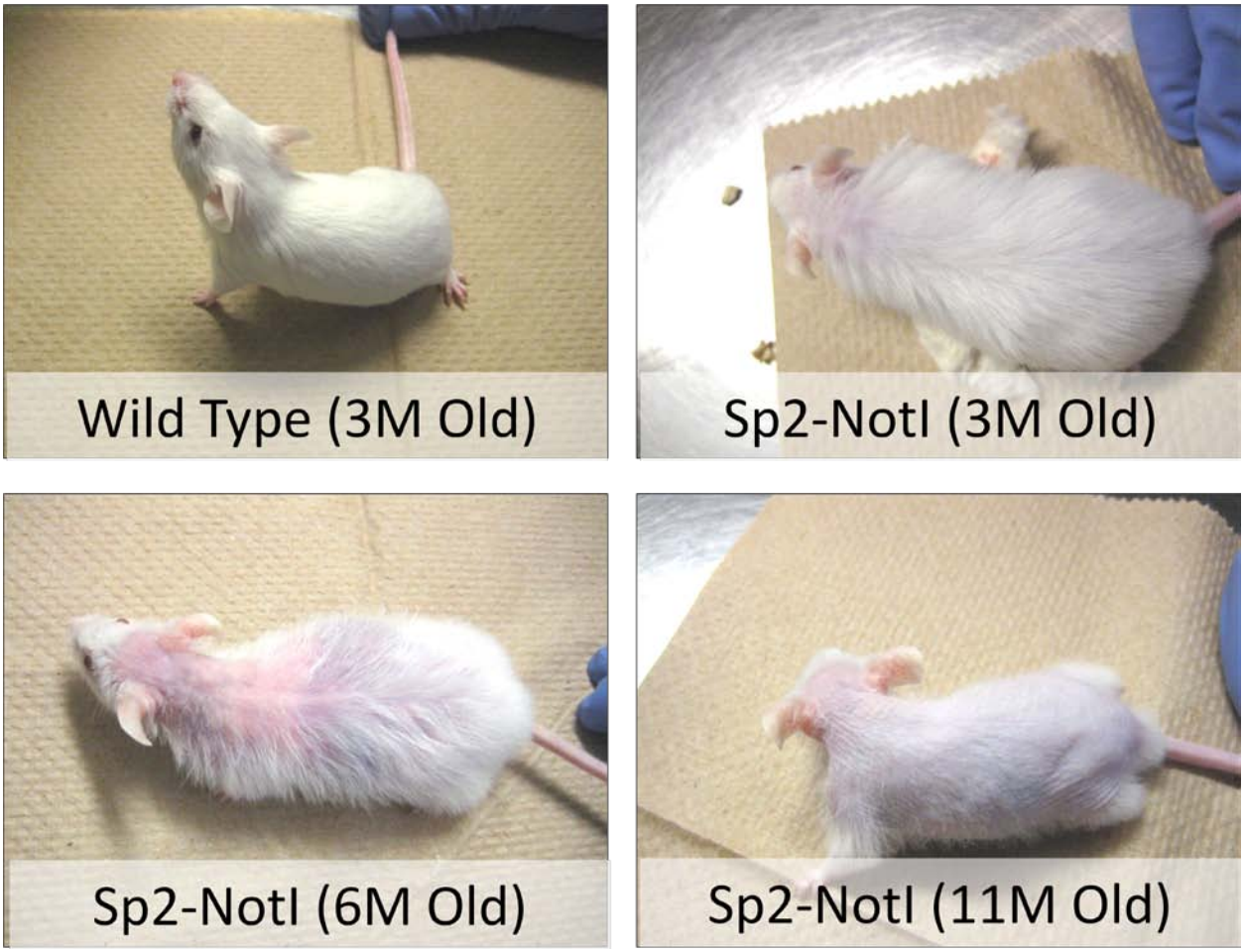

Figure 23 Alopecia in Sp2-NotI mice. Sp2-NotI mice begin to lose their hair at three months of age and this hair loss progresses as these animals age. By 11 months of age the dorsal surface of these animals is nearly devoid of hair.

As discussed above, over-expression of wild-type Sp2 in basal keratinocytes sensitizes animals to wound-induced neoplasia and increases susceptibility to carcinogen-induced tumorigenesis. To determine if the Sp2 DNA-binding domain is required for these effects, Sp2-NotI animals were analyzed in a two-stage carcinogenesis experiment identical to that performed for Sp2-C animals. In stark contrast with results for Sp2-C animals, the incidence of papillomagenesis in Sp2-NotI mice treated with DMBA/TPA is half that of wild-type littermates (Figure 24B; $p<0.01$). In 7.5 weeks after initiation, first papillomas are observed both in wild-type and Sp2-NotI transgenic animals. Even though papillomas are formed around same time, papillomas in Sp2-NotI mice grow slower than those in wild-type animals. Most of the papillomas in Sp2-NotI mice don't grow bigger than 5 mm in diameter whereas most of papillomas in wild-type grow bigger than 5mm and animals are euthanized when papillomas become 1 cm in diameter (Figure 24A). I conclude from this result that over-expression of the Sp2 DNA-binding domain in basal keratinocytes is required for increased susceptibility to carcinogen-induced neoplasia. Given that Sp2-NotI animals are less sensitive to DMBA/TPA-induced tumorigenesis than wild-type animals, these data also suggest that over-expression of the Sp2 *trans*-activation domain interferes with one or more mechanisms underlying carcinogenesis in this system and thus may function as a dominant negative.

A

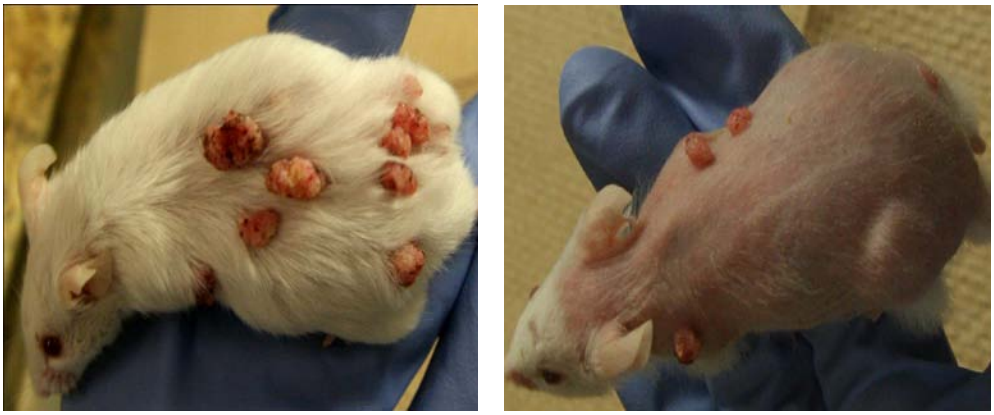

B

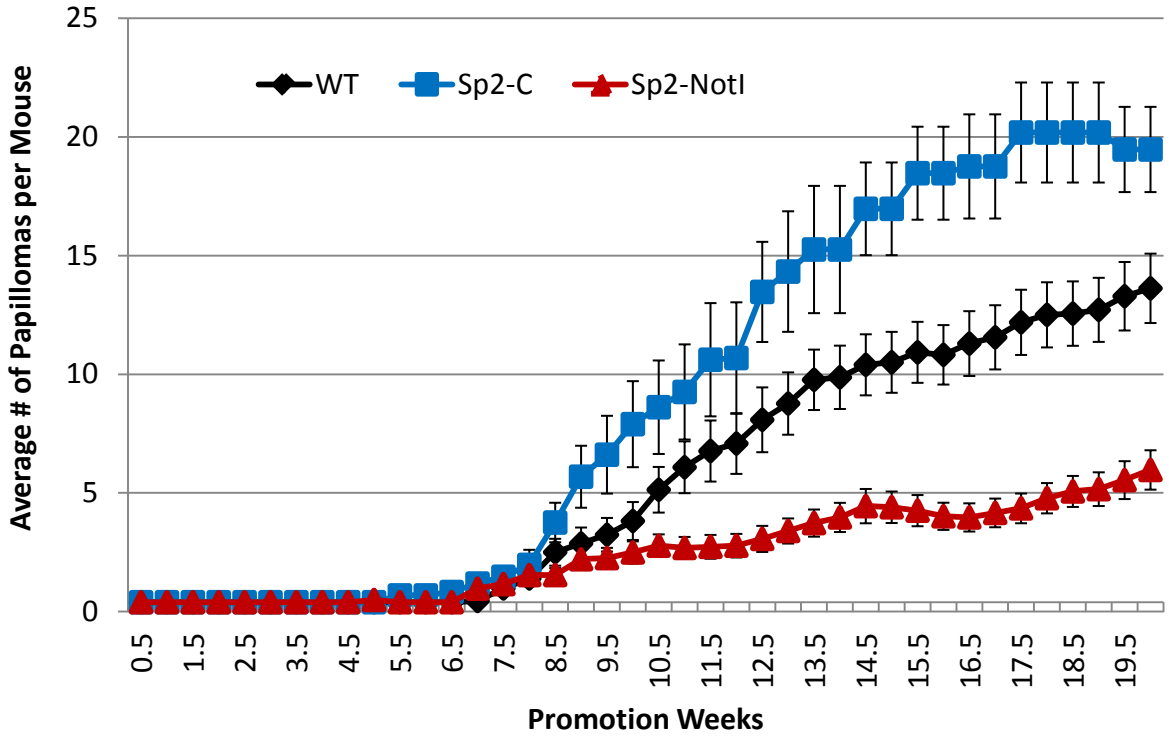

Figure 24 The Sp2 DNA-binding domain is required for increased susceptibility of transgenic animals to tumorigenesis. *A.* Comparison of papilloma size and numbers between wild-type and Sp2-NotI animals. Pictures were taken at post-promotion week 15. Wild-type animals (left) have more and bigger papillomas than Sp2-NotI animals (right) *B.* The incidence of papillomagenesis in Sp2-NotI mice (n=21) treated with DMBA/TPA is half that of wild-type animals. These results indicate that the Sp2 DNA-binding domain is required for increased susceptibility to tumorigenesis and suggests that over-expression of the trans-activation domain may dominantly-interfere with the outgrowth of tumors.

This study establishes that Sp2 over-expression inhibits the differentiation of epidermal keratinocytes, rendering these cells susceptible to oncogenesis. Indeed, the striking incidence of wound-induced papillomagenesis in Sp2-C hemizygotes indicates that Sp2 over-expression is sufficient, in the appropriate physiological milieu, to subvert mechanisms controlling basal cell proliferation and differentiation. Similar susceptibilities to wound-induced neoplasia have been reported in transgenic animals expressing potent oncogenes, e.g., Ha-ras or v-jun, in this same epidermal compartment (133-135). It will be of interest to determine whether wound-induced neoplasms in Sp2-C hemizygotes are dependent on inflammatory growth factors and cytokines released following wounding, as has been noted in other systems (136-139). Since stem cells supporting the interfollicular epidermis are located within the basal layer, our results suggest that Sp2 may regulate the commitment of progenitors in this, and perhaps additional, stem cell compartments. In keeping with this speculation, Sp2 over-expression is associated with the progression of human prostatic carcinoma and thus Sp2 may regulate the proliferation/differentiation of progenitor cells in tissues beyond the epidermis (67). To our knowledge this study provides the first direct evidence that Sp-family members can function as oncogenes and suggests that therapeutic strategies targeting Sp2 may prove efficacious.

Chapter 5

5. Sp2-A and Sp2-NotI transgenic animals exhibit delayed wound healing

Wound healing is a well-orchestrated, stepwise process that requires inflammation, cell proliferation, extracellular matrix deposition, and tissue remodeling (140). In human epidermis, inflammation occurs from the moment of injury and continues for an additional 24-48 hours. During this stage, the wound is hypoxic (ischaemic) and filled with bacteria, neutrophils, and platelets. New tissue formation occurs approximately 2 to 10 days after injury. In this stage, an eschar (scab) is formed on the surface of the wound, new blood vessels are formed, and epithelial cells migrate beneath the scab. In the final stage of healing, tissue remodeling occurs and may last for a year or longer. Fibroblasts are recruited to the wound area and produce an extracellular matrix composed mostly of collagen. The surface of the wound at this stage is fully re-epithelialized and does not contain normal skin appendages such as hair follicles and ducts for sweat glands (141). Despite the complexity of the wound repair process, it is very well controlled following most injuries. Tight control of this process is essential for organismal survival since deficient healing can lead to infection and tissue degeneration, and excessive healing can lead to the uncontrolled expansion of cells in the wounded area. Despite its critical role in tissue and organismal homeostasis, the molecular mechanisms that govern wound healing remain poorly understood.

As indicated in Chapter 4, Sp2-C family mice exhibit a marked sensitivity to wound-induced neoplasia. Interestingly, a very different phenotype, delayed wound healing, was observed for Sp2-A and Sp2-NotI mice. Initial indications that this novel phenotype is a

characteristic of Sp2-A animals came from evidence of delayed healing of ear punches, and this phenotype was explored further and quantified via the introduction of surgical wounds (4 mm diameter) in dorsal skin. Surgical wounds were introduced under anesthesia and the efficiency of wound healing during a two-week recovery period was compared in Sp2-A and Sp2-NotI mice relative to wild-type littermates. Whereas wild-type animals heal their wounds in approximately one week, two-thirds of wounds carried by Sp2-A hemizygotes were still in the process of healing two weeks post-surgery (Figure 25A). Most wounds in Sp2-A animals healed eventually, usually requiring more than one or two months to complete. To determine whether over-expression of the Sp2 DNA-binding domain is required for delayed wound healing, surgical wounds were introduced into the dorsal skin of Sp2-NotI hemizygotes and wild-type littermates and rates of wound healing were compared. Interestingly, Sp2-NotI transgenic animals exhibit delayed wound healing with a time-course similar to that of Sp2-A mice (Figure 25B). These results indicate that over-expression of the Sp2 *trans*-activation domain alone in basal keratinocytes is sufficient to retard wound healing.

A

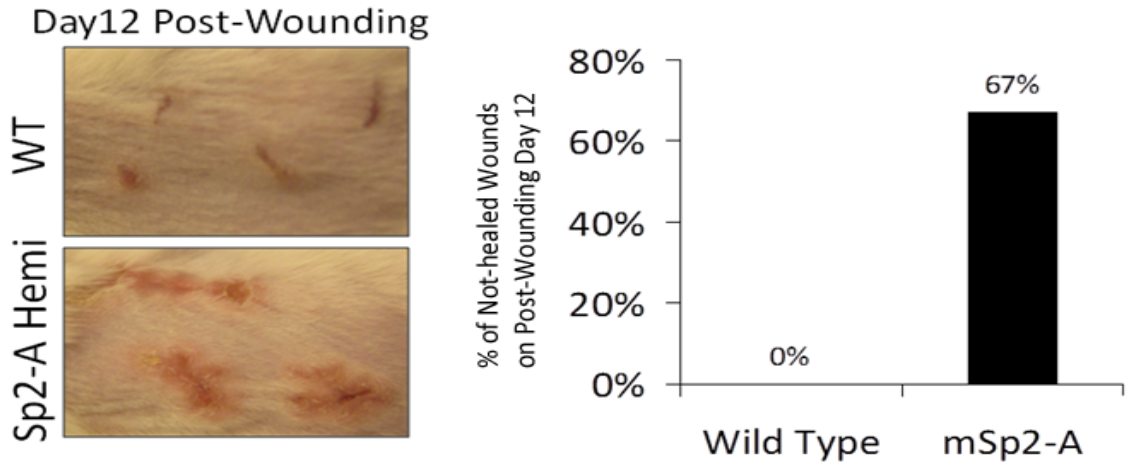

B

Figure 25 Delayed wound healing in Sp2-A and Sp2-NotI mice. *A*. Pictures were taken 12 days after surgical wounding. Wounds in wild-type animals are almost completely healed whereas wounds in Sp2-A hemizygous animals are still healing. As shown graphically, two-thirds of surgical wounds sustained by Sp2-A transgenic animals exhibited not healed completely. *B.* Pictures were taken six days post-wounding. Wounds in 6 months old wild type animals are in the final stages of wound healing and some are completely healed (*). In contrast, wounds in Sp2-NotI animals (at the age of 7 months or 12 months) are still not closed and scabs are still being formed.

5.1 Transcripts levels of endogenous Sp2 in young and old mouse skins

Given that the over-expression of Sp2 in Sp2-A hemizygotes reduced their capacity to heal surgical wounds, it became of interest to determine if Sp2 abundance in the epidermis varies as a function of aging. Delayed wound healing is common in elderly individuals; open wounds in the young rapidly contract and require shorter time to final closure than wounds sustained by older individuals (142). Based on results obtained in Sp2-A animals I speculated that Sp2 message may increase in concert with aging, perhaps accounting for the retardation of wound healing in the elderly. To address this question, I prepared RNA from the epidermis of animals at various ages (from 3 to 18 months of age) and quantified the abundance of endogenous Sp2 transcripts by real-time PCR. In contrast to my expectations, the expression of endogenous Sp2 message was reduced dramatically in the epidermis of older animals relative to expression levels detected in younger animals (Figure 26).

In contrast to Sp2-C animals, the over-expression of Sp2 in Sp2-A and Sp2-NotI transgenic mice results in a profound delay in rates of wound healing. It is not as yet known what stage or stages of wound healing are affected in these animals. It is also not clear why the responses to surgical wounding in Sp2-C and Sp2-A animals are so divergent (papillomagenesis in Sp2-C animals, and delayed wound healing in Sp2-A animals). One possibility is that Sp2 is expressed significantly more abundantly in the epidermis of Sp2 –C mice than Sp2-A mice. Regardless, that Sp2-NotI animals are also susceptible to delayed wound healing indicates that this is a phenotype that does not require over-expression of

the Sp2 DNA-binding domain. Additional studies will be required to determine the mechanistic basis for this effect. Finally, careful quantitation of Sp2 transcript abundance indicates that Sp2 message in mouse epidermis diminishes in concert with the aging of wild-type animals. It is not as yet known if this reflects alterations in the temporal activity of the Sp2 promoter and/or a gradual loss of epidermal progenitors as animals age.

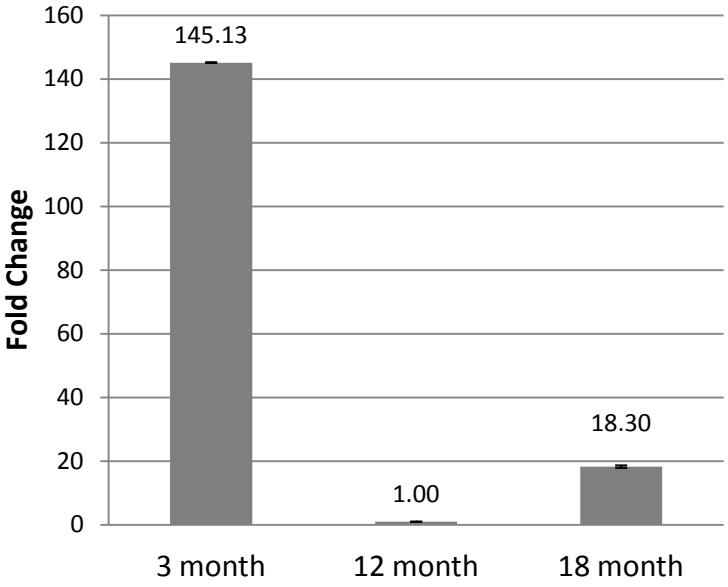

Figure 26 Relative expression level of endogenous mouse Sp2 message in wild-type mice as a function of age. Total skin RNAs were prepared and pooled from three individual animals in each age group and the abundance of Sp2 mRNA was quantified relative to GAPDH at each time point. The expression level of Sp2 message in 12 month old animals was set equal to 1.

Chapter 6

6. Characterization of primary keratinocyte cell cultures prepared from transgenic animals

To begin to explore the mechanisms underlying the *in vivo* phenotypes exhibited by Sp2 transgenic strains, I prepared and characterized primary keratinocyte cultures from newborn animals as described in Section 2.2. Primary epidermal cultures are comprised initially of a mixture of cells, including progenitor cells (basal keratinocytes), their terminally-differentiated descendants (supra-basal keratinocytes), and distinct cell lineages, such as melanocytes. Cells are plated on standard tissue culture dishes in medium that promotes the outgrowth of keratincoytes. Progenitor and terminally-differentiated keratinocytes and melanocytes attach to culture dishes on the first day of culture, terminally-differentiated keratinocytes "slough-off" and are gradually lost from the culture on subsequent days, resulting in cultures predominated by basal keratinocytes and a minor population of melanocytes. Once plated these primary cultures cannot be sub-cultured, and thus *in vitro* studies are limited to sub-confluent cultures that are available within the first week following explant.

Whereas primary cultures prepared from wild-type littermates proliferated as expected, cultures obtained from Sp2-A, Sp2-C, and Sp2-NotI transgenic animals proliferated poorly *in vitro* compared to wild-type keratinocytes (Figure 27). Indeed, cultures prepared from transgenic animals appeared cytostatic and featured cells with abnormal morphologies, some reminiscent of cells undergoing programmed cell death (apoptosis). These results provoked questions from a number of standpoints. First, do cells

cultured from transgenic animals proliferate? Although such cultures appeared not to expand and never reached confluency, it remained possible that these cells were capable of synthesizing DNA and proceeding through mitosis but few daughter cells were capable of surviving. Second, are cells derived from transgenic animals arrested in one or more specific cell-cycle compartments? Finally, are transgenic cultures cytostatic due to the loss of cells via apoptosis? To address these questions I performed a series of standard assays to characterize the proliferative potential of transgenic cell cultures with cultures prepared from wild-type littermates. Three assays (MTT, CyQUANT®, and ^{3}H-Thymidine incorporation) were employed to quantify cell proliferation and DNA synthetic capacity, and flow cytometry was employed to assess the fraction of cells in each cell-cycle compartment. Finally, I compared the numbers of apoptotic cells in transgenic and wild-type cultures via staining for characteristic markers (annexin V and cleaved caspase-3), and assessing the abundance of genomic "DNA laddering". Results from each of these assays will be described below.

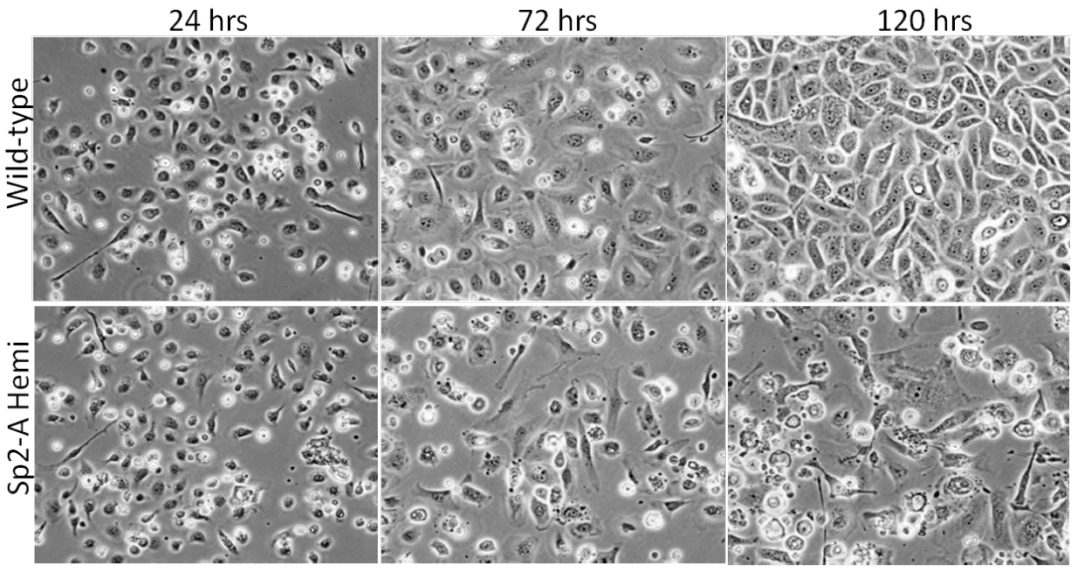

Figure 27 Morphology of primary keratinocytes prepared from wild-type and Sp2-A hemizygous animals. Wild-type and Sp2-A hemizygotes were plated at equivalent cell densities and photographed on successive days in culture.

6.1 Cells cultured from Sp2 transgenic animals proliferate poorly *in vitro*

As a first step towards comparing the proliferative potential of transgenic keratinocyte cultures with wild-type cultures, an MTT assay was performed as described in Section 2.5.2. This assay assesses the overall metabolic activity of populations of cells and is used routinely to quantify cell numbers. Consistent with their expansion in number *in vitro*, cultures of wild-type keratinocytes exhibited increasing levels of metabolic activity on each day post-plating (Figure 28). In stark contrast, keratinocyte cultures prepared from Sp2-A, Sp2-C and Sp2-NotI animals exhibited little or no proliferative activity during the same time course. In detail, wild-type cells show continuous increase of metabolic activity with time in all independent experiments. In Figure 28A, wild-type culture has 3 times higher metabolic activity in post-plating 66 hours than initial culture. In Figure 28B and 28C, similar trends are observed in wild-type cultures. In contrast, the metabolic activities in Sp2-A, Sp2-C, and Sp2-NotI transgenic cultures show little or no increase (Figure 28A, B, and C).

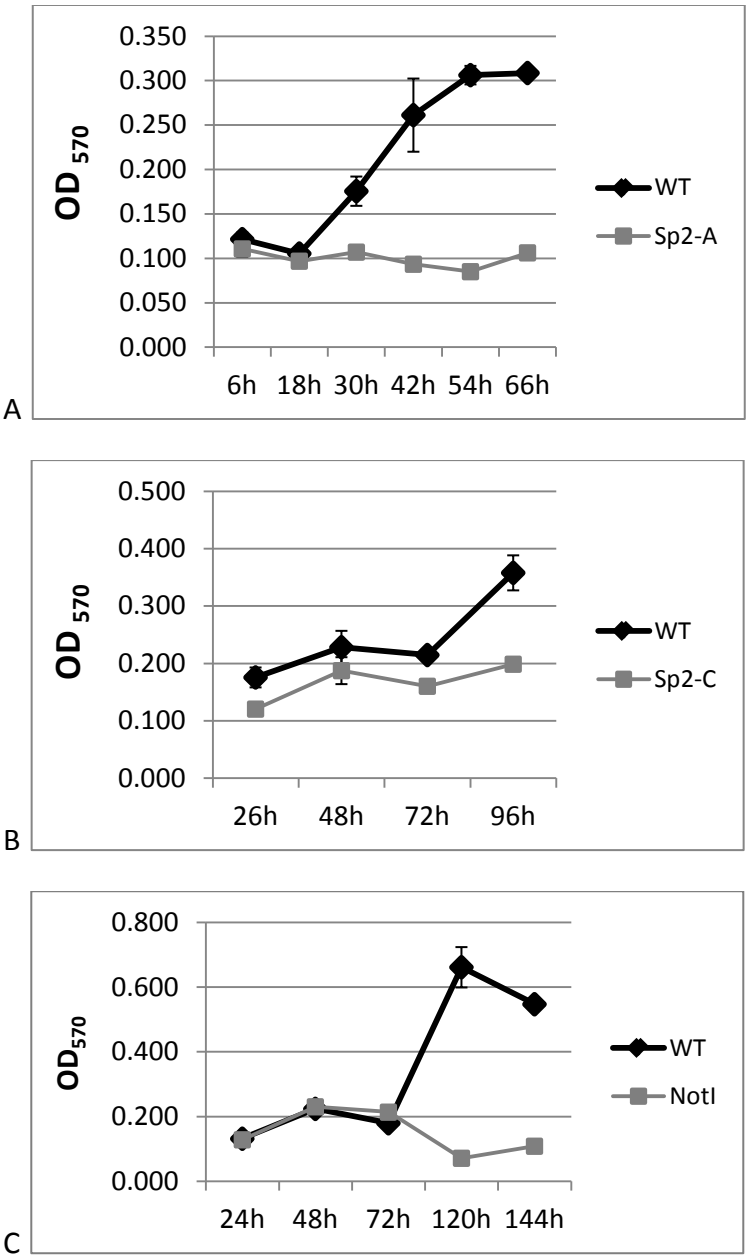

Figure 28 MTT assay of primary keratinocytes prepared from wild-type, Sp2-A, Sp2-C and Sp2-NotI hemizygous animals. *A.* Metabolic activity of wild-type and Sp2-A cultures are measured from post-plating 6 hours through 66 hours. *B.* Metabolic activity of wild-type and Sp2-C cultures are measured from post-plating 26 hours through 96 hours. *C.* Metabolic activity of wild-type and Sp2-NotI cultures are measured from post-plating 24 hours through 144 hours. All graphs are plotted with absorbance at 570 nm of wavelength with time. Bars, SE.

Although results from the aforementioned MTT assays indicated that transgenic cultures are less proliferative than wild-type cultures, we wished to corroborate these findings utilizing an independent assay that did not rely on overall metabolic activity. To this end we employed a commercially available assay (CyQUANT®) that measures the abundance of nucleic acids (RNA and DNA) in culture dishes and is a direct reflection of cell numbers. Consistent with results from MTT assays, we noted that the number of keratinocytes in wild-type cultures increased with each successive day in culture whereas cultures prepared from transgenic cultures exhibited little or no increase in cell numbers during the same time course. As shown in Figure 29, wild-type cells tripled in number by 96 hours post-plating and then slowed as cultures became confluent (usually by day five post-plating). In contrast, keratinocytes prepared from Sp2-A and Sp2-NotI animals were largely cytostatic and cell numbers actually diminished by 96 hours post-plating. Sp2-C animals, unexpectedly, yielded cultures that exhibited a somewhat distinct growth pattern; Sp2-C keratinocytes increased slightly (about 1.5-fold) by 96 hours post-plating.

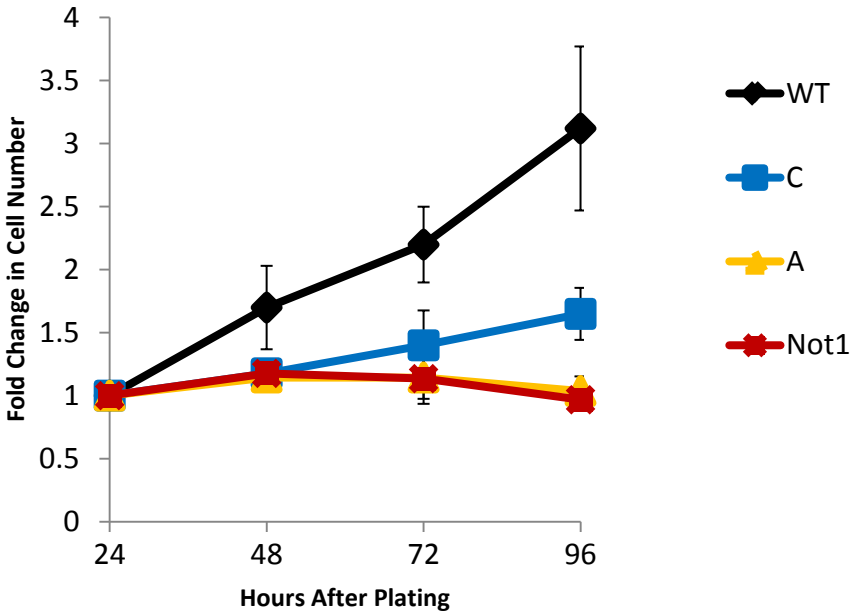

Figure 29 Proliferation of wild-type, Sp2-A, Sp2-C, and Sp2-NotI cultures using CyQUANT® Assay. Initial cell numbers 24 hours post-plating in each culture was set equal to 1.

To quantify relative DNA synthetic capacity of primary keratinocyte cultures directly, wild-type and transgenic cells were cultured on each day post-plating with ^{3}H-thymidine and radiolabeled DNA was quantified following TCA-precipitation. DNA synthetic capacity of transgenic cells was then computed relative to wild-type cells on days 1 to 5 post-plating (Figure 30). Once again, results for transgenic cultures were similar but not identical. Twenty-four hours post-explant, DNA synthesis in Sp2-A cultures was 80% of that exhibited by wild-type cultures. This robust level of DNA synthesis indicates that Sp2-A-derived cells are capable, at least initially, of traversing the restriction point and entering S phase. As shown in Figure 30, however, DNA synthesis in Sp2-A cultures is reduced dramatically (by 70%) within the next 24 hours relative to wild-type cultures and remains at negligible levels throughout the time course of this experiment. Thus, whereas Sp2-A-derived keratinocytes exhibit nearly wild-type levels of DNA synthesis upon plating their capacity to continue to do so is curtailed rapidly. In stark contrast to these results, DNA synthesis in Sp2-C and Sp2-NotI cultures approximated that of wild-type cultures immediately after plating and then diminished gradually on subsequent days in culture. Indeed, DNA synthesis in all transgenic cultures examined was reduced to identical low levels (10% of wild-type) by day 5 post-plating. When results from ^{3}H-thymidine incorporation assays are combined with MTT and CyQUANT® results, two conclusions may be drawn. First, Sp2-A keratinocyte cultures proliferate upon plating akin to cultures prepared from wild-type littermates. Within hours, however, the proliferative potential of transgenic cells is markedly reduced and remains extremely low. Second, cultures prepared from transgenic strains do not proliferate identically. Although cultures prepared from all three transgenic strains proliferate

equivalently initially, Sp2-A cells exhibit a rapid, marked loss of proliferative potential whereas the proliferation of Sp2-C and Sp2-NotI cells diminishes gradually. Given the absence of the Sp2 DNA-binding domain in Sp2-NotI-derived cells, this latter result indicates that expression of the Sp2 *trans*-activation domain is sufficient to block keratinocyte proliferation *in vitro*.

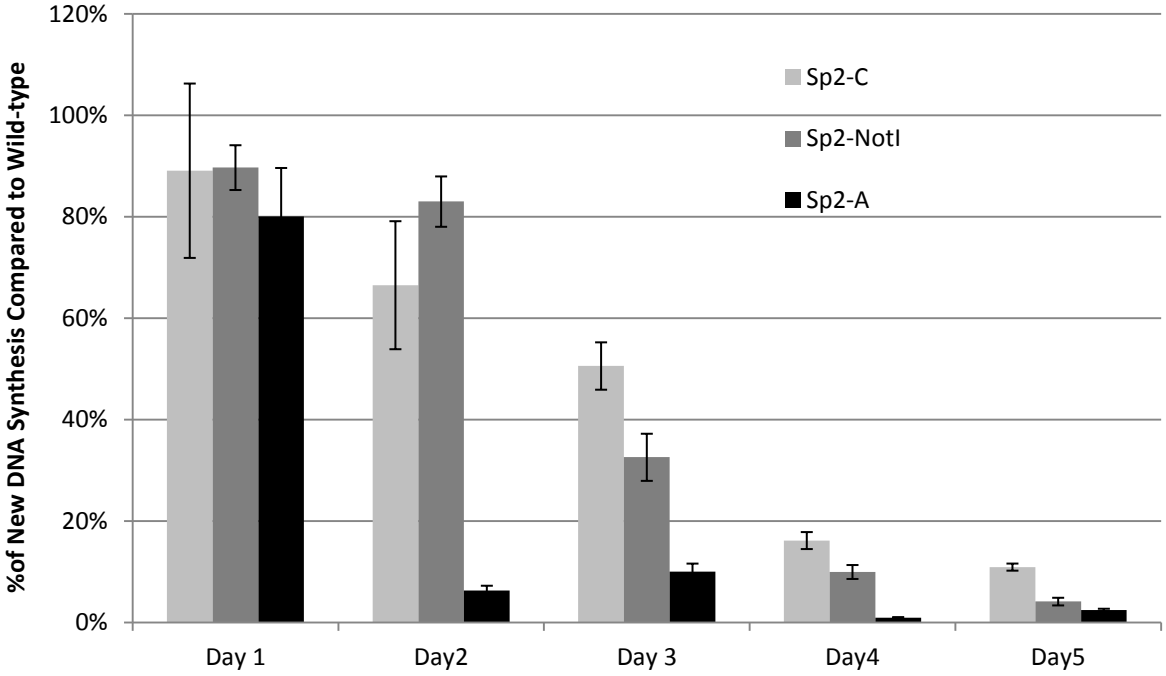

Figure 30 ^{3}H-Thymidine incorporation by Sp2-A, Sp2-C, and Sp2-NotI cultures. The amount of DNA synthesis in each transgenic culture is expressed relative to that of wild-type cultures (set equal to 100 per cent on each day in culture).

6.2 Cells derived from Sp2 transgenic animals arrest in all cell-cycle phases

Results from MTT, CyQUANT®, and ^{3}H-thymidine assays indicate that keratinocytes derived from Sp2 transgenic animals proliferate poorly *in vitro*. With these results in hand it became of interest to determine whether Sp2 over-expression causes the arrest of keratinocytes in one or more cell-cycle compartments. To address this issue wild-type and transgenic cultures were harvested on days 1 and 3 post-plating, stained with propidium iodide (PI), and the fraction of cells in each cell-cycle compartment was determined by flow cytometry. The change in the percentages of cells in each cell-cycle compartment between days 1 and 3 is plotted in Figure 31. As previously reported (143), the majority (71%) of wild-type keratinocytes were in G1 24 hours post-plating with a minority of cells in S (7%) and G2/M (21%). A large fraction of the wild-type cell population had entered the cell cycle by day 3 post-plating as cells in G1 diminished significantly (to 40% of the total cell population) and resulting in a commensurate increase in cells in S (22%) and G2/M (35%). In contrast to wild-type keratinocytes, 66% of Sp2-A cells remained in G1 3 days post-plating (a 9% decrease relative the G1 fraction on day 1) and the fraction of cells in S and G2/M increased only marginally (6% and 2%, respectively). Thus, whereas a substantial portion (30%) of wild-type cells had entered the cell-cycle by day 3, less than 10% of Sp2-A cells had done so during the same time course. It is worth noting that whereas there was an equivalent increase in the percentages of wild-type cells in S and G2/M phases by day 3 post-plating, a smaller fraction of Sp2-A cells accumulated in G2/M than S phase. These results suggest that Sp2 over-expression in Sp2-A cells may perturb the length of time spent in latter stages of the cell cycle (*e.g.*, S phase may be somewhat longer and/or G2/M phase may be

somewhat shorter in length). In contrast to results for Sp2-A cultures, flow cytometric profiles for Sp2-C and Sp2-NotI cultures largely paralleled those of wild-type cells. It is worth noting, however, that a greater fraction of Sp2-C cells (42%) accumulated in G2/M relative to wild-type (35%) cultures.

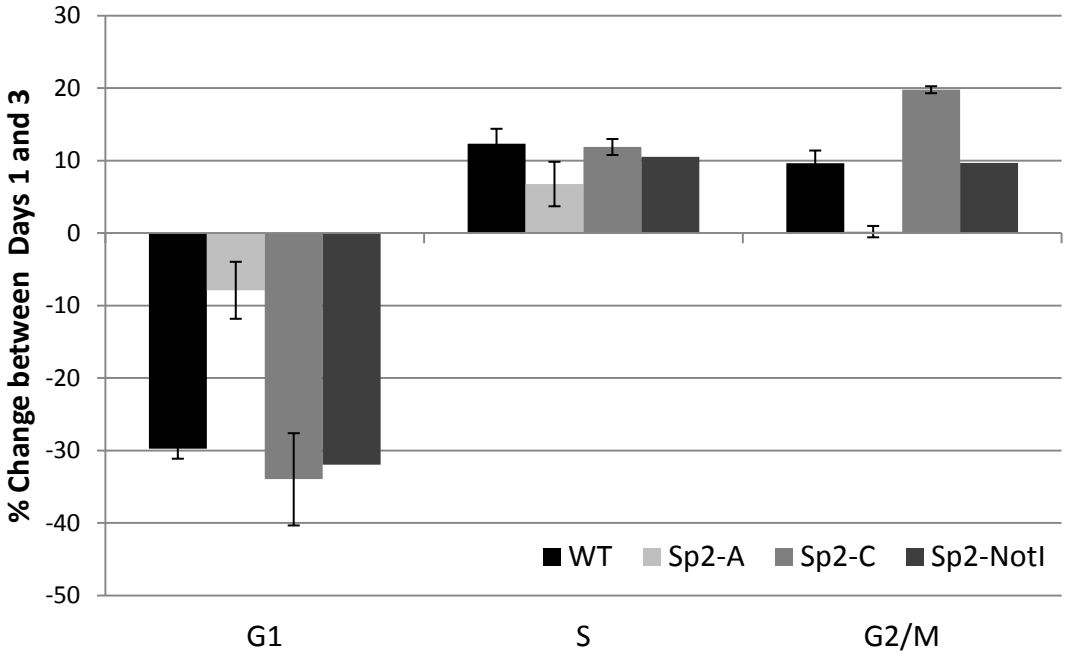

Figure 31 Flow cytometric analysis of wild-type and transgenic keratinocyte cultures between days 1 and 3 post-plating. The per cent change of cells in each cell cycle compartment is plotted.

The flow cytometric results presented thus far represent "snapshots" of the fractions of cells in particular cell-cycle compartments on each day analyzed. Since cell populations can enter and move through the cell cycle at different rates we were interested in comparing the percentages of cells in each cell population (wild-type and transgenic) that progressed through each cell-cycle phase. To address this question I treated wild-type and transgenic keratinocyte cultures with nocodazole, a potent inhibitor of mitosis. Nocodazole blocks the polymerization of microtubules required for the formation of the mitotic spindle, resulting in the arrest of cells in G2/M. Primary keratinocyte cultures were treated with 20 μM nocodazole or DMSO for 24 hours on day 3 post-plating, and cells were stained with PI and analyzed by flow cytometry. As expected, treatment of wild-type cells with nocodazole resulted in a 25% reduction in cells in G1, a 2% reduction of cells in S phase, and the accumulation of cells in G2/M (18% increase; Figure 32). In contrast, treatment of Sp2-A and Sp2-C cultures resulted in little change in the fraction of cells in each cell-cycle compartment (Figure 32). Indeed, nocodazole treatment resulted in only a minor accumulation of cells in G2/M (Sp2-A, 5% increase); Sp2-C, 9% increase). Thus, results from nocodazole-treated cultures indicate that only a minor fraction (5 to 9%) of Sp2 transgenic cells actively progress through the cell cycle. Indeed, these data indicate that transgenic keratinocytes progress through the cell cycle inefficiently and accumulate in all cell cycle compartments.

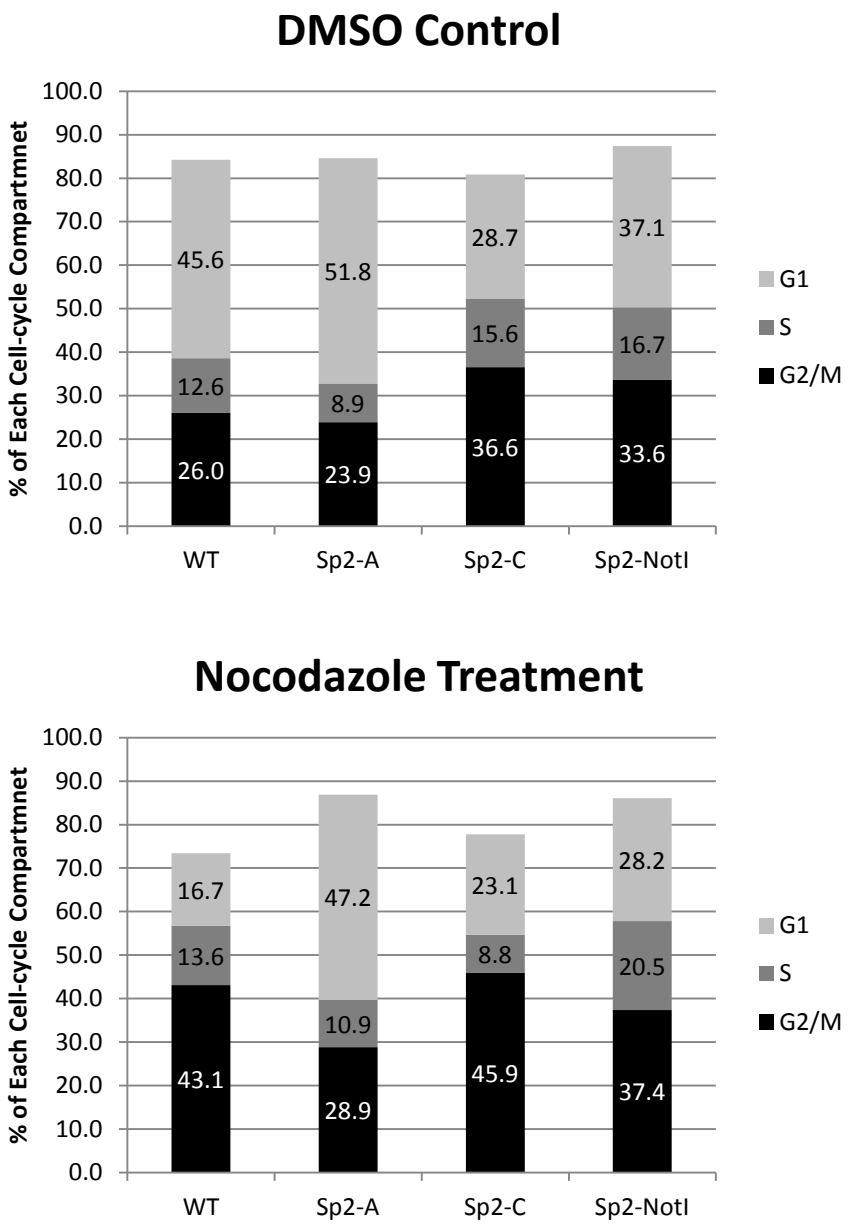

Figure 32 Cell-cycle progression of wild-type and transgenic cultures following treatment with nocodazole. On day 3post-plating, keratinocyte cultures were treated with 20µM nocodazole or DMSO for 24 hours. Cultures were then stained with PI and analyzed by flow cytometry.

6.3 Transgenic cultures exhibit elevated numbers of apoptotic cells

As mentioned above, Sp2 transgenic keratinocyte cultures featured cells with abnormal morphologies as well as cells that appeared to be undergoing programmed cell death. Indeed, such apoptotic cells were readily visualized in Sp2 transgenic keratinocyte cultures expressing fluorescent proteins. For example, Sp2-A transgenic mice were inter-crossed with a transgenic mouse line in which enhanced green fluorescent protein (EGFP) is expressed via the keratin 5 promoter. Primary cultures prepared from compound hemizygotes (Sp2-A/+, K5-EGFP/+) revealed many keratinocytes with “blebs” characteristic of apoptotic cells whereas their presence was less frequent in control cultures (+/+, K5-EGFP/+; Figure 33). To assess the abundance of apoptotic cells in wild-type and Sp2 transgenic keratinocyte cultures, three traditional assays for apoptotic cells were performed: (1) keratinocyte cultures were stained for annexin V, (2) keratinocyte cultures were stained for cleaved (activated) caspase-3, and (3) the abundance of apoptotic DNA "ladders" was determined.

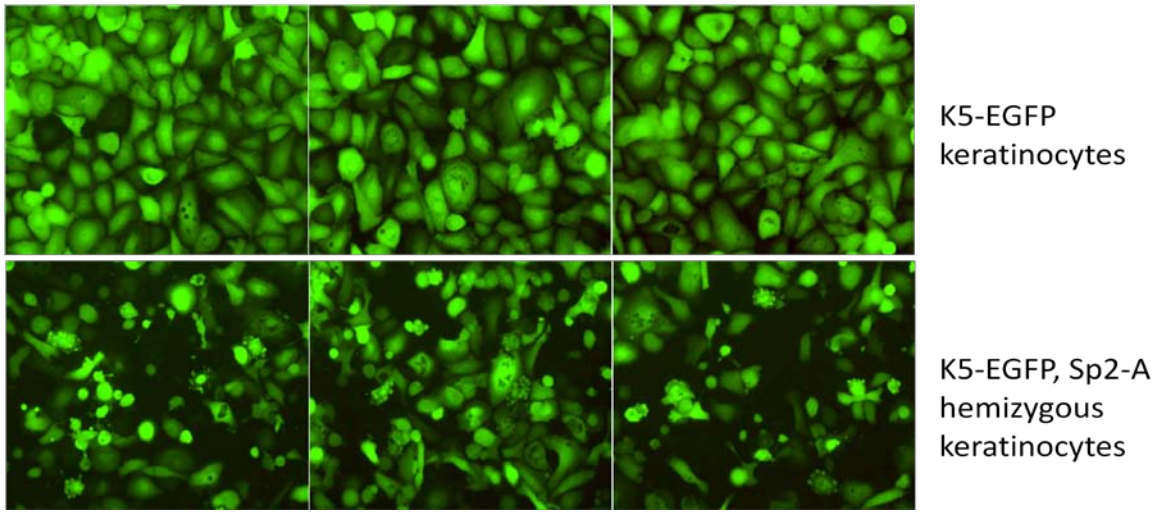

Figure 33 Morphology of K5-EGFP and [K5-EGFP, Sp2-A] hemizygous keratinocytes. Cells were photographed on day 3 post-plating. Cells in wild-type cultures are nearly confluent whereas cultures prepared from Sp2-A mice contain many irregularly shaped cells as well as cells with morphological characteristics of apoptotic cells.

Cells undergoing apoptosis and other forms of cell death express phosphatidylserine (PS) on the outer leaflet of the plasma membrane, whereas PS is located on the cytoplasmic surface of the cell membrane in normal cells. This exposure of PS to the external cellular environment marks dying cells for recognition and phagocytosis by macrophages. Annexin V is a Ca^{2+}-dependent phospholipid binding protein that binds to PS with high affinity. Consequently, annexin V protein that has been conjugated to a fluorophore can be used to identify apoptotic cells. Since annexin V is displayed on the surface of necrotic cells as well, staining for annexin V is often combined with a vital dye, such as PI, to distinguish live, necrotic, and apoptotic cells in a population. Cells stained with annexin V alone are considered to be "early stage" apoptotic cells, cells stained by both annexin V and PI are considered to be necrotic or "late stage" apoptotic cells, and cells that do not stain with either annexin V or PI are live cells. Sp2-A and Sp2-C cells were stained with annexin V and PI on days 1 through 5 post-plating (Figure 34A). Following an initial burst of apoptotic cells in wild-type cultures, numbers of apoptotic cells decreased as the culture stabilizes. In contrast, numbers of apoptotic cells in Sp2-A cultures increased continuously throughout the same time course. Similar to Sp2-A cultures, numbers of apoptotic cells in Sp2-C cultures increased from day 1 though day 4 post-plating and then diminished (Figure 34B). Numbers of apoptotic cells in Sp2-NotI cultures increased continuously on days 1, 2, 3, 4, and 7 post-plating (Figure 34C). In summary, keratinocyte cultures prepared from Sp2 transgenic mice contain significant numbers of annexin V-positive cells and their numbers increased with each day in culture. In contrast, wild-type keratinocyte cultures contain

fewer annexin V-positive cells and their numbers decrease as basal keratinocytes proliferate and dominate the cell population.

A

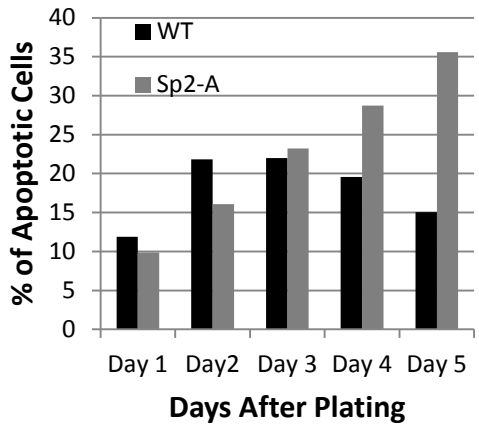

B

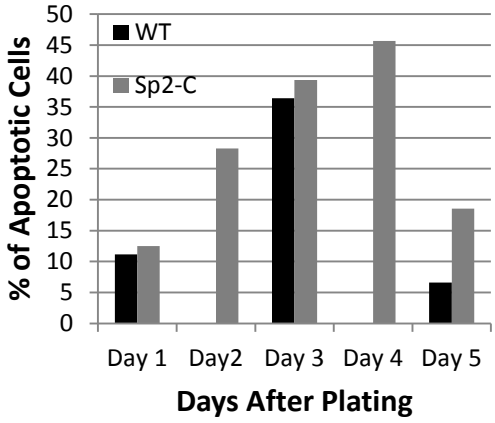

C

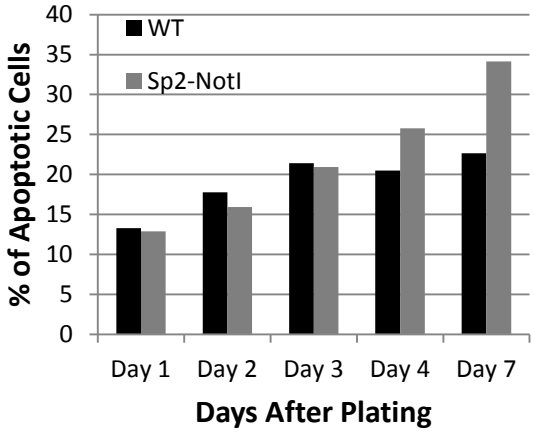

Figure 34 Annexin V-stained cells in wild-type and transgenic keratinocyte cultures. Cells were stained with annexin V and PI and quantified by flow cytometry. The percentage of cells stained with annexin V only was calculated on each day of culture and plotted. *A*. Percentage of annexin V-stained cells in wild-type and Sp2-A cultures. *B.* Percentage of annexin V-stained cells in wild-type and Sp2-C cultures. *C.* Percentage of annexin V-stained cells in wild-type and Sp2-NotI cultures.

Apoptosis induces a proteolytic cascade in which cysteine proteases, termed caspases, are activated and function as cellular executioners. Caspase-3 is one of the final caspases in the proteolytic cascade and thus an excellent biomarker of apoptotic cells. Antibodies specific for cleaved forms of caspases-3 have been developed and their use in conjunction with fluorescently-labeled secondary antibodies provides a means to enumerate apoptotic cells *in situ*. Primary keratinocyte cultures prepared from wild-type or transgenic animals were stained on various days after plating with an anti-cleaved caspase-3 antibody (Figure 35A). Cells were counter-stained with fluorescent dyes that bind to DNA (DAPI) and actin (phalloidin). The numbers of cleaved caspase 3-positive cells as well as cells stained only with DAPI and phalloidin were enumerated in 20x microscopic fields and the percentage of cleaved caspase-3 positive cells in each keratinocyte culture was calculated. Wild-type and Sp2-A cultures were stained with anti-cleaved caspase-3 on days 2, 3, and 4 post-plating. As shown in Figure 35B, statistically significant differences in the numbers of cleaved caspase-3-positive cells were noted on day 4 (wild-type 25%; Sp2-A 42%; $p < 0.05$). Similar numbers of cleaved caspase-3-positive cells were noted in cultures of wild-type and Sp2-NotI cells on days 2 and 3 post-plating. By day 7, however, only 10% of wild-type cells were stained with an anti-cleaved caspase-3 antibody whereas more than 43% of Sp2-NotI cells were stained ($p < 0.001$; Figure 35C).

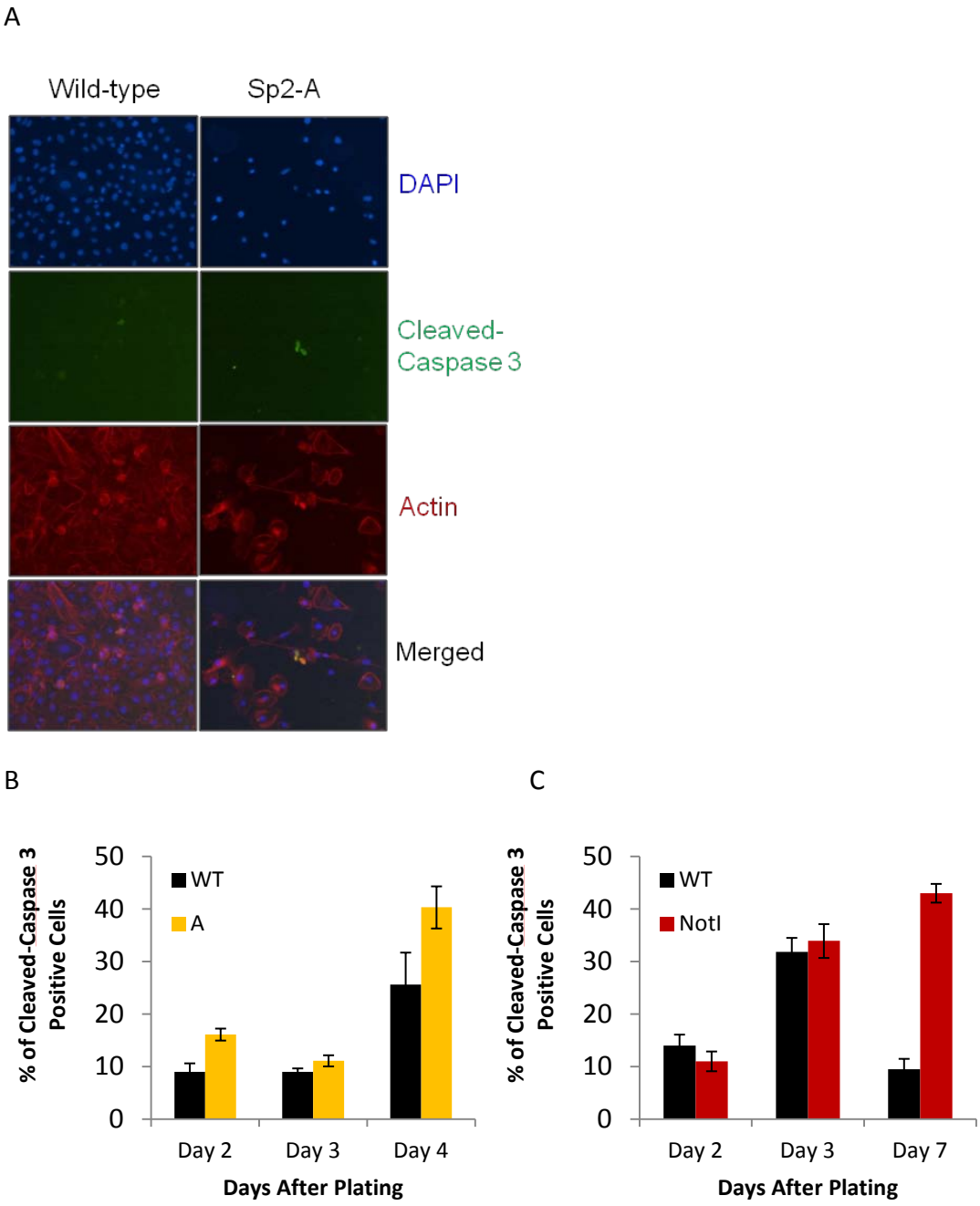

Figure 35 Staining of keratinocytes prepared from wild-type and Sp2-A hemizygous animals with an antibody against cleaved caspases-3. *A.*Micrographs of wild-type and Sp2-A cells stained with an anti-cleaved caspase-3 antibody, DAPI, and phalloidin (Alexa Fluor 595). *B*. Comparison of cleaved caspase-3-positive cells in cultures of wild-type and Sp2-A keratinocytes. The percentages of stained cells on each day in culture are illustrated. *C*. Comparison of cleaved caspase-3-positive cells in cultures of wild-type and Sp2-NotI keratinocytes. The percentages of stained cells on each day in culture are illustrated.

Endonucleases are activated during apoptosis resulting in the degradation of genomic DNA where readily exposed, such as between nucleosomes. Such internucleosomal cleavages produce DNA fragments of 180 base pairs, as well as fragments representing multimers of 180 base pairs, and appear as a DNA "ladder" following agarose gel electrophoresis. To determine if such characteristic DNA "ladders" are present in cultures of primary keratinocytes from transgenic and wild-type animals, nuclei were collected selectively from apoptotic cells, genomic DNA was prepared, and resolved on ethidum bromide-stained agarose gels. As shown in Figure 36, at early time-points post-plating (*e.g.*, day 3) DNA "ladders" were detected in cultures of wild-type and transgenic keratinocytes (Figure 36). Following stabilization of wild-type keratinocyte cultures (*e.g.*, by day 6 post-plating), however, DNA "laddering" diminished significantly whereas robust levels of DNA "ladders" continued to be detected in cultures of Sp2-A cells. In conclusion, each apoptosis assay employed revealed greater numbers of apoptotic cells in Sp2 transgenic cultures than cultures prepared from wild-type animals. Differences between wild-type and transgenic cultures were most pronounced at later time points (days 5 to 7 post-plating), with 35 to 45% of transgenic cells expressing characteristic apoptotic markers (annexin V or cleaved caspase-3). Interestingly, this induction of apoptotic cells is not dependent on an intact Sp2 DNA-binding domain since statistically significant numbers of apoptotic cells were noted in Sp2-NotI cultures relative to wild-type cultures analyzed in parallel.

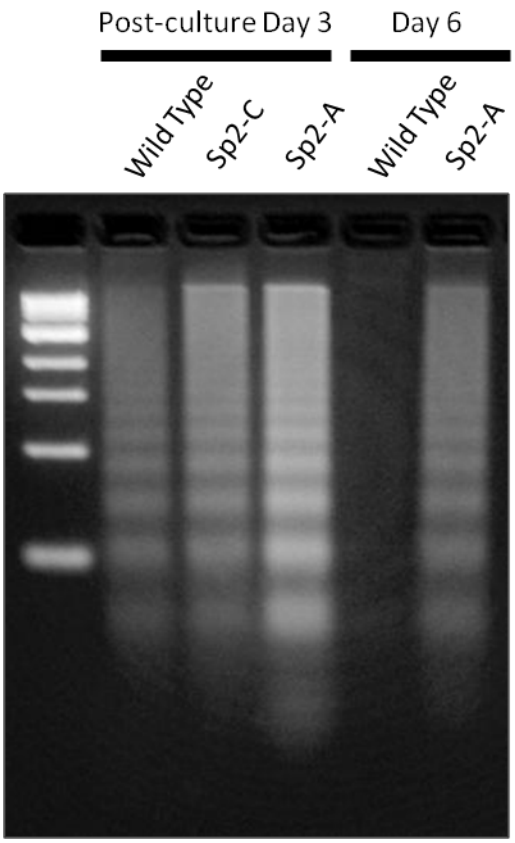

Figure 36 Apoptotic DNA "ladders" prepared from primary keratinocyte cultures. Apoptotic nuclei were selectively harvested from wild-type and transgenic keratinocyte cultures, genomic DNAs were prepared and resolved on 1.8% agarose gels.

Chapter 7

7. Discussion

Transcription in mammalian cells is controlled by a constellation of proteins, including sequence-specific DNA-binding proteins. The Sp-family of sequence-specific DNA-binding proteins regulate the expression of a diverse set of genes responsible for cell-cycle control, differentiation, and development. As a consequence, de-regulation of Sp protein abundance and/or activity would be predicted to perturb organismal development, cell and tissue physiology, and the outgrowth of tumorigenic cells. Correlations between specific Sp-family members and various human cancers have been reported by numerous studies. However, direct evidence that any given Sp protein can be oncogenic has been lacking.

Previous evidence from the Horowitz laboratory had indicated that the abundance of one particular Sp-family member, Sp2, is correlated directly with the progression of murine squamous cell carcinomas of the skin. To determine if this correlation is functionally significant, I created transgenic mouse lines in which a mouse Sp2 cDNA is over-expressed in the cell of origin of this skin cancer. I then characterized the gross phenotypes of these animals, characterized their susceptibility to tumorigenesis, and undertook a series of molecular and biochemical studies to reveal mechanisms underlying phenotypes presented by these mice. As a consequence of my efforts I have shown that over-expression of Sp2 in epidermal progenitor cells is oncogenic and associated with a profound block in the epidermal differentiation program. I showed further that Sp2 over-expression retards wound-healing and blocks the proliferation of basal keratinocytes *in vitro*. Finally, I showed that the Sp2 DNA-binding domain is required for some, but not all, of the *in vivo* and *in vitro*

phenotypes associated with Sp2 transgenic mice. Taken together, my results indicate that Sp2 over-expression plays an important role in the regulation of keratinocyte proliferation, differentiation, and tumorigenesis.

7.1 Sp2 over-expression in epidermal progenitor cells is lethal and associated with a block in the epidermal differentiation program

A major finding of this study is that Sp2 over-expression in basal keratinocytes leads to post-natal lethality. Sp2-A and Sp2-C transgenic homozygotes are developmentally retarded, their skin is hairless, scaly, and overly reddened, and these animals perish within weeks after birth. Exogenous Sp2 expression in Sp2-C animals is ten-fold greater than that of Sp2-A animals, and in keeping with these differences in expression levels Sp2-C animals rarely survive past post-natal day two whereas Sp2-A homozygotes often survive until post-natal day 13. Careful examination of skin sections prepared Sp2-A and -C transgenic homozygotes revealed that the epidermis of these animals is comprised of an expanded population of immature (keratins 5 and 14-positive) keratinocytes. Cells expressing standard markers of differentiated keratinocytes, such as keratins 1 and 10 as well as loricrin, were identified in the epidermis of some early post-natal animals (post-natal day two), however such cells diminished in numbers during subsequent days and were virtually absent within a week of birth. This de-regulation of the epidermal differentiation program was also associated with the expression of markers, such as keratin 6, that are normally restricted to "simple" epithelia and markers, such as keratin 8, that are commonly expressed in neoplastic or distressed epithelium. Taken together, these results indicate that Sp2 over-

expression in basal keratinocytes antagonizes the induction and/or maintenance of the normal epidermal differentiation program and results in an expanded pool of progenitor cells that inundate basal and supra-basal cell layers.

7.2 Sp2 over-expression in epidermal progenitor cells is oncogenic

Given that Sp2 over-expression expands the pool of cycling epidermal progenitors it is perhaps not surprising that over-expression of Sp2 is oncogenic. Hints that Sp2 over-expression might play a role in tumorigenesis were first reported for human prostate cancers (94). Sp2 abundance, detected by immunohistochemical staining of tissue sections, was shown to be elevated in concert with prostate tumor progression. A second line of evidence was obtained by experiments in our lab focusing on murine squamous cell carcinomas. As described in Chapter 4, the abundance of Sp2 protein was shown to be correlated directly with the progression of DMBA/TPA-induced tumorigenesis. It is also worth mentioning that earlier work from our lab had established that Sp2 is over-expressed uniformly in more than 30 human and mouse cell lines examined (26). Taken together, these three results suggested that Sp2 over-expression might be oncogenic and required for the step-wise progression of human and murine cancers. Yet, the possibility that Sp2 over-expression is a consequence of transformation, as opposed to being functionally significant, remained equally plausible. The characterization of Sp2 transgenic mouse lines has provided strong evidence that Sp2 over-expression is indeed oncogenic and a cause, not a consequence, of tumorigenesis.

Over-expression of Sp2 in basal keratinocytes increased susceptibility to carcinogen-induced cancers, and induced sensitivity to wound-induced neoplasia. Indeed, treatment of Sp2-C hemizygotes with DMBA/TPA induced more average papillomas per animal than wild-type littermates and lesions in hemizygotes developed more rapidly. These results indicate that Sp2 over-expression provides a cellular milieu that increases the likelihood of the initiation and/or expansion of progenitor cells carrying carcinogen-induced oncogenic mutations. What might be the nature of such oncogenic mutations? H-ras and K-ras mutations are associated with epithelial malignancies, such as squamous cell carcinomas (144, 145), and are found uniformly in many chemically induced mouse skin tumors. My results suggest that Sp2 over-expression may increase the pool of progenitor cells available for mutational activation and/or collaborate with signals promoted by activated Ras genes to expand this pre-malignant cell population.

Since Sp2-C hemizygotes are at significant risk of developing wound-induced neoplasms, Sp2 over-expression must also de-regulate the response to proliferative signals encountered by normal progenitor cells. Indeed, I observed that the frequency of wound-induced papillomas increases in concert with the aging of Sp2-C mice and is correlated directly with the age-dependent increase in Sp2 expression levels in this transgenic strain. What mechanism(s) might underlie the susceptibility of Sp2-C hemizygotes to wound-induced neoplasms? Under homeostatic conditions basal keratinocytes proliferate to provide cells required for tissue maintenance and wound repair. Cell proliferation in response to tissue damage is well-controlled under normal conditions, and proliferation is

halted when wounds are healed and/or sufficient numbers of differentiated keratinocytes are produced. One could imagine that if Sp2 antagonizes keratinocyte differentiation that epidermal progenitors in Sp2-C hemizygotes may undergo excessive rounds of replication in an attempt to generate sufficient numbers of differentiated descendants. One could imagine further that excessive replication increases the likelihood that inadvertent oncogenic mutations will occur. If so, are activated Ras genes associated with the outgrowth of wound-induced papillomas? Three hot spots for mutations, codons 12, 13, and 61, have been identified in Ras genes (146-148). To determine if Sp2 over-expression increases the likelihood of Ras mutations following surgical wounding, I used Ras mutation-specific PCR as well as pyrosequencing to search for activated Ras genes in wound-induced neoplasms. It had previously been established that neoplasms resulting from DMBA/TPA treatment are frequently associated with a particular A to T mutation at codon 61 of the H-Ras gene (149). I employed allele-specific oligonucleotide primers that give rise to amplification products only in instances in which codon 61 mutations are present to search for activated H-Ras genes in wound-induced neoplasms. As an alternative method, all three Ras gene hotspots (codon 12, 13, and 61) were sequenced directly by pyrosequencing. Six wound-induced papillomas were examined using both techniques and Ras mutations were not detected. These results indicate that wound-induced papillomas arise independently of mutations that are commonplace in carcinogen-induced squamous carcinomas. In this vein, it is worth noting that wound-induced papillomas that arose in Sp2-C mice invariably degenerated, perhaps due to the absence of oncogenic mutations required to sustain their progression.

Regardless, the uniform degeneration of wound-induced papillomas indicates that Sp2 over-expression is insufficient to promote tumor progression.

7.3 Sp2 over-expression retards would healing

In addition to increasing the susceptibility to wound- and carcinogen-induced tumorigenesis, over-expression of Sp2 resulted in the retardation of wound healing. Whereas surgical wounds introduced into the dorsal skin of wild-type mice are healed within a week, two-thirds of surgical wounds in Sp2-A mice are not healed after two weeks and many wounds require up to two months to heal completely. Interestingly, wound healing by Sp2-NotI animals is equally defective indicating that over-expression of the Sp2 DNA-binding domain is not required for this phenotype.

Given that Sp2 over-expression antagonizes the epidermal differentiation program, it is perhaps not surprising that delayed wound healing is a feature of Sp2 transgenic mice. Basal keratinocytes are recruited into the cell cycle in response to wounding, and are charged with the responsibility of producing more of themselves, as well as spawning transit-amplifying cells and terminally-differentiated descendants required for tissue repair. Yet, the differential response of Sp2-A and -C animals to surgical wounding is puzzling. Each strain expresses the same transgene, yet wounds in one strain (Sp2-A) heal poorly whereas wounds in the other (Sp2-C) convert to neoplastic lesions. How might these apparently contradictory responses be reconciled? One possibility is that the differential responses of Sp2-A and -C animals depend on the levels of the transgene expressed in each strain. Western blotting and quantitative real-time PCR experiments indicate that Sp2 expression

levels in Sp2-C animals are ten-fold higher than steady-state levels in Sp2-A animals, and three-fold greater than levels in another strain (Sp2-NotI) that exhibits delayed wound healing. As will be detailed below, I speculate that the relatively modest elevation of the abundance of the Sp2 *trans*-activation domain in the epidermal progenitors of Sp2-A and Sp2-NotI animals is sufficient to antagonize the epidermal differentiation program and retard wound healing but insufficient to sensitize these same cells to wound-induced neoplasia.

7.4 A model for the differential roles of the Sp2 DNA-binding and *trans*-activation domains in tumorigenesis and wound healing

Our lab reported that the Sp2 DNA-binding and *trans*-activation domains are each regulated negatively in mammalian cells by as yet unknown mechanisms (26). Using a series of chimeric proteins carrying complementary portions of the Sp1 and Sp2 proteins, Moorefield *et al.* reported that linkage of the Sp2 *trans*-activation domain to the Sp1 DNA-binding domain reduced resulting transcription dramatically without affecting DNA-binding activity. This result suggests that the Sp2 *trans*-activation domain interacts with one or more cellular proteins that collaborate to restrict transcription. Similarly, linkage of the Sp2 DNA-binding domain to the Sp1 *trans*-activation domain reduced DNA-binding activity and *trans*-activation. This result suggests that the Sp2 DNA-binding domain interacts with one or more cellular proteins that antagonize its association with DNA thereby preventing *trans*-activation. Although the identities of the cellular proteins that interact with the Sp2 *trans*-

activation and DNA-binding domains remain unknown, I speculate that these protein-protein interactions underlie the phenotypes exhibited by Sp2 transgenic strains.

I propose that a protein critical for the induction and/or maintenance of the epidermal differentiation program, termed "protein A", interacts with Sp2 via the Sp2 *trans*-activation domain. Modest over-expression of this domain, as in epidermal progenitor cells of Sp2-A or Sp2-NotI animals, results in the sequestration of "protein A" and antagonism of the epidermal differentiation program. As a consequence of the reduced numbers of terminally-differentiated keratinocytes, Sp2-A and Sp2-NotI animals exhibit alopecia and delayed wound healing. I propose further that another Sp2-interacting protein, termed "protein B", has tumor-suppressive functions and associates with Sp2 via the Sp2 DNA-binding domain. "Protein B" may be less abundant than "protein A" and/or bind less efficiently to Sp2, however, at the elevated levels of Sp2 achieved in Sp2-C animals both proteins are bound and sequestered by Sp2. As a consequence of these combined protein-protein interactions epidermal differentiation is blocked, the proliferative potential of progenitor cells in Sp2-C animals is increased significantly, and Sp2-C animals are at increased risk of wound- and carcinogen-induced neoplasia. One phenotype that is not accounted for by this model is the absence of alopecia in Sp2-C mice. At levels of expression encountered in Sp2-C animals, I would have expected that physical interactions between the Sp2 *trans*-activation domain and "protein A" would have resulted in alopecia in hemizygotes. A possible explanation for this result is that interactions of Sp2 with "protein A" that antagonize the epidermal differentiation program are negated by interactions of the

DNA-binding domain with "protein B". In this scenario, interactions of the DNA-binding domain with "protein B" cause the amplification of epidermal progenitors and transit-amplifying cells and provide enough terminally-differentiated keratinocytes to counter-balance the sequestration of "protein A" by the *trans*-activation domain (Figure 37).

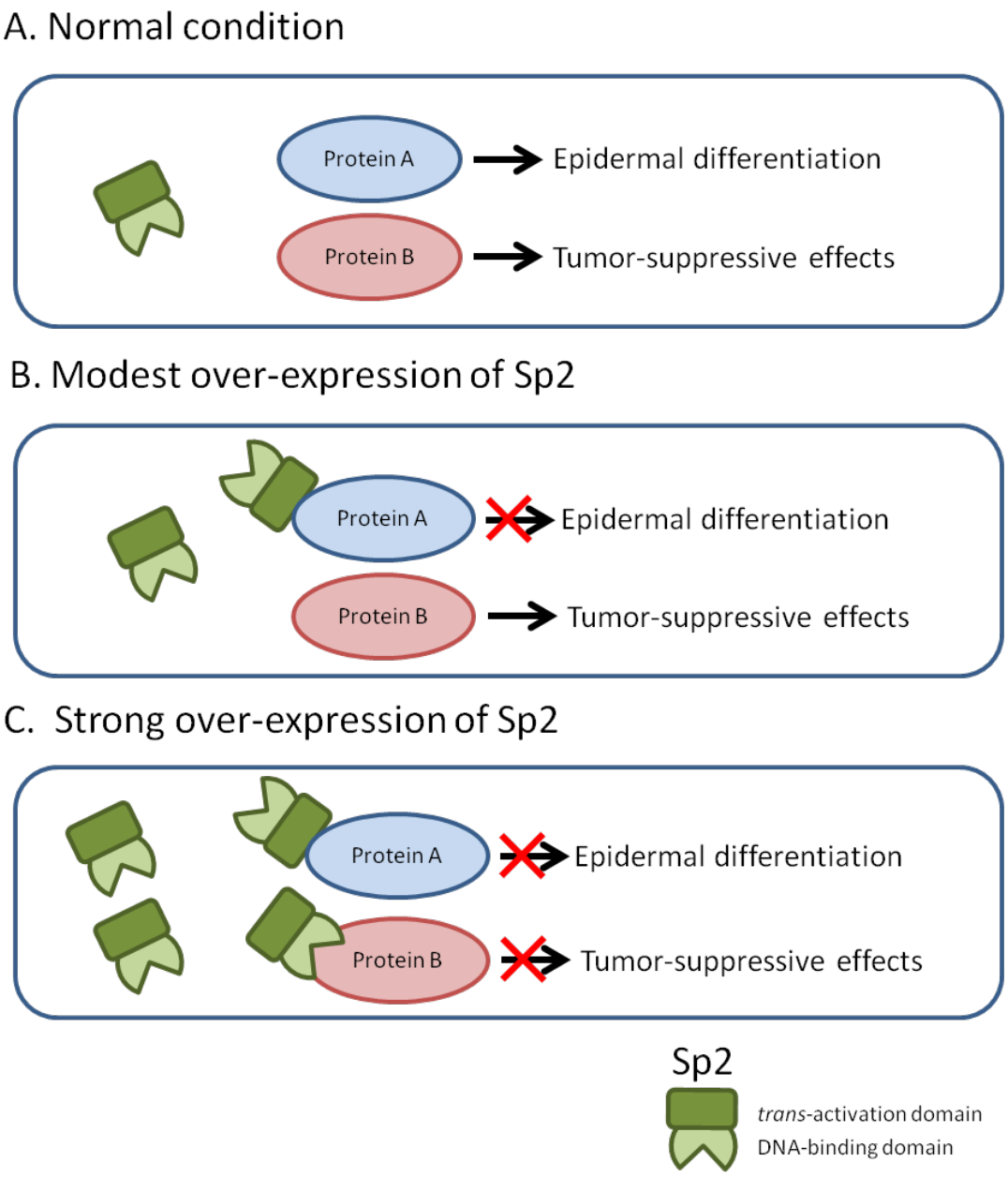

Figure 37 A model for the differential roles of the Sp2 DNA-binding and *trans*-activation domains in tumorigenesis and wound healing.

7.5 Sp2 over-expressing mouse as a useful tool for the studies of tumorigenesis and stem cell differentiation

Perhaps the most surprising result to spring from my research is the apparent disparity in the proliferative potential of transgenic epidermal progenitors *in vivo* and *in vitro*. Although Sp2-A and Sp2-NotI hemizygotes exhibit alopecia as adults, these animals and Sp2-C mice are born with a healthy epidermis that protects them from the environment for years. In stark contrast to these results, as well as the oncogenic effects of Sp2 over-expression in Sp2-C mice, basal keratinocyte cultures prepared from these animals exhibit limited proliferative potential. Sp2 over-expression in Sp2-A, Sp2-C, and Sp2-NotI cultures results in an arrest of cell-cycle progression in all cell-cycle compartments and a marked increase in the percentage of apoptotic cells. These effects are most striking for Sp2-A cultures. At 24 hours post-plating Sp2-A cultures are difficult to distinguish from cultures prepared from wild-type littermates. Indeed, their DNA synthetic capacity is 80% of that of wild-type cultures and they are indistinguishable morphologically. Yet, with 24 hours DNA synthesis plummets to 10% of that of wild-type cultures and percentages of apoptotic cells rise dramatically. To explain the apparent contradictory growth of transgenic keratinocytes, I reasoned that environmental differences encountered by transgenic progenitor cells *in vivo* and *in vitro* might account for these disparate results. In an attempt to define key environmental differences, I performed a number of experiments in which key parameters of *in vitro* keratinocyte cultivation were adjusted. Each will be discussed in turn.

First, I considered that interactions between transgenic keratinocytes and the extracellular matrix (basement membrane) *in vivo* might supply one or more factors required for their growth. It is well known that such interactions can play an important role in the regulation of the proliferation and differentiation of epidermal stem cells. Four major epidermal stem cell populations have been identified *in vivo*: (1) interfollicular epidermal stem cells, (2) hair follicle "bulge" stem cells, (3) sebaceous gland stem cells, and (4) follicular isthmus stem cells (150). Among these stem cell populations, interfollicular epidermal stem cells and the stem cells derived from the hair follicle "bulge" region have been shown to be the origin of epidermal tumors and the source of cells for skin homeostasis. These two major stem cell populations reside in the epidermal basal layer attached to the basement membrane. Ghalbzouri *et al.* reported that the attachment of basal keratinocytes to the basement membrane is mediated by integrins α1β1 and α2β1 *in vivo* (151). Recently, Spichkina *et al.* reported that basal keratinocytes can be isolated specifically from the skin by attachment to type I collagen and fibronectin (152). In an attempt to support the growth of Sp2 transgenic keratinocytes *in vitro*, I coated tissue culture dishes with type I collagen and fibronectin prior to plating and compared their attachment and proliferation with cells prepared from wild-type littermates. Despite these efforts, transgenic cells plated on collagen- or fibronectin-treated dishes proliferated poorly and underwent apoptosis at increased rates. Although I cannot rule-out that other components of extracellular matrix may be able to rescue these transgenic cells, I conclude at least type I collagen and fibronectin are not sufficient.

Second, I reasoned that transgenic keratinocyte cultures one or more growth factors required for their proliferation *in vitro*. To examine this possibility, I performed two experiments: (1) I co-cultivated transgenic and wild-type keratinocytes with the hope that wild-type keratinocytes would support the survival of transgenic keratinocytes. In order to distinguish transgenic keratinocytes from the wild-type cells, I inter-crossed Sp2-A hemizygotes with transgenic mice that express EGFP in basal keratinocytes via the bovine K5 promoter. Wild-type keratinocytes were co-cultivated with [Sp2-A/+, K5-EGFP/+] keratinocytes and the proliferation of [Sp2-A/+, K5-EGFP/+] was monitored by fluorescence microscopy on each day post-plating. This experiment resulted in cultures that were quickly dominated by wild-type keratinocytes, indicating that the growth of [Sp2-A/+, K5-EGFP/+] cells was not favored under these culture conditions. (2) It has been reported that fibroblasts can support the proliferation of stem cells co-cultures (153). Given that basal keratinocytes are in intimate contact with dermal fibroblasts *in vivo*, I reasoned that their addition to keratinocyte cultures might support the proliferation of transgenic cells. Primary fibroblasts that had been irradiated to prevent their proliferation were obtained from Dr. Jorge Piedrahita in the Department of Molecular Biomedical Sciences at North Carolina State University, and these cells were co-cultivated with primary keratinocytes prepared from Sp2 transgenic animals. Once again, addition of these cells to keratinocyte cultures did not rescue their proliferative capacity.

It is well-established that under homeostatic conditions the concentration of oxygen in the epidermis is 3% (154). Under standard growth conditions *in vitro*, ambient oxygen concentrations are 21% and the proliferation of primary mouse cells has been reported to

be limited under these conditions (155). I reasoned that perhaps Sp2 transgenic keratinocytes were extremely sensitive to ambient oxygen conditions. To address this possible explanation for the poor growth of transgenic keratinocytes *in vitro*, I plated primary keratinocytes from wild-type and transgenic animals in a chamber held at an oxygen concentration of 3% for five days and quantified the proliferation of keratinocytes on each day. Although wild-type keratinocytes proliferated well, transgenic keratinocytes remained poorly proliferative throughout the time course of this experiment.

Although these attempts to modify conditions of *in vitro* cultivation did not identify conditions under which the proliferation of transgenic keratinocytes was supported, these experiments were helpful in eliminating a handful of obvious possibilities. Yet, many others remain to be examined. For example, it is conceivable that Sp2 transgenic keratinocytes are deficient in one or more proteins that provide for the stable attachment of cells to each other. A previous report concluded that the over-expression of Sp2 in prostatic epithelia was inversely correlated with the expression of CEACAM1, a cell-cell adhesion protein (94). Should this correlation extend to basal keratinocytes, it is possible that the plating of transgenic keratinocytes at high densities might overcome this intrinsic defect and facilitate cell survival if not proliferation. Regardless, it is clear that Sp2 over-expression in basal keratinocytes produces a cellular milieu in which programmed cell death is triggered *in vitro*. Much is known about oncogenic mechanisms that illicit this response in primary cells. Indeed, when normal cells are forced to proliferate by the expression of activated oncogenes such as Ras, Myc, or E2f-1, this "oncogenic stress" triggers self-defense

mechanisms that result in cellular senescence or apoptosis. The Rb and p53 pathways are major players in the induction of these two mechanisms of terminal growth arrest. For example, excess E2F-1 expression causes the transcription of $p19^{ARF}$ and this leads to the inactivation of Mdm2, an inhibitor of p53 function. p53 triggers the expression of many target genes resulting in various outcomes depending on the cell and tissue type and the convergence of different signaling pathways (156). I speculate that over-expression of Sp2 causes "oncogenic stress" in basal keratinocytes both *in vivo* and *in vitro*, however, the cellular response to this "stress" is negated or diminished *in vivo* (Figure 38). In contrast, when the same cells are removed from the epidermis and cultured *in vitro* the response to this "oncogenic stress" is revealed resulting in cell-cycle arrest and apoptosis. Should this be the case, Sp2 transgenic mice may help identify the signals/pathways that suppress "oncogenic stress" *in vivo*. Identification of such an "anti-oncogenic stress mechanism" may have significant therapeutic implications. For example, drugs that block the "anti-oncogenic stress mechanism" may serve as chemotherapeutic agents alone or in conjunction with current frontline therapies.

Although much has been learned by my research efforts, including that Sp2 is a regulator of progenitor cell proliferation, differentiation, and tumorigenesis, it is fair to say that much remains to be discovered. Sp2 target genes, if any, have yet to be identified and the identities of binding proteins, such as the hypothetical "proteins A and B", must be defined. Given these limitations it is difficult to speculate on the precise mechanisms that underlie the control of progenitor cell fate by Sp2. It is known that p63, a p53-related

protein, is a master regulator of epithelial cell development (157). The p63 gene is controlled by two promoters that produce two classes of proteins, TAp63 and ΔNp63, and due to alternative splicing each has three variants with different carboxy-termini (α, β, and γ). One of these isoforms, ΔNp63α, is expressed predominantly in basal keratinocytes and it plays a pivotal role in the maintenance of stemness. To determine if Sp2 over-expression impacts the expression of ΔNp63α and/or TAp63, I used qRT-PCR to quantify the abundance of each transcript in the skin of transgenic mice at various ages. These experiments did not detect correlations between Sp2 expression level and the abundance of ΔNp63α and/or TAp63 messages, however it is conceivable that these key regulators of epithelial biology are regulated by Sp2 at the post-transcriptional level.

Yet, there are additional potential mechanisms that may underlie the regulation of progenitor cells by Sp2. It is possible that Sp2 may be involved in cell-fate decisions by controlling the symmetry of basal keratinocyte divisions. Our lab reported that the majority of Sp2 protein is associated with the nuclear matrix, and it is at least conceivable that the over-expression of Sp2 recruits proteins that control the polarity of cell division to the nuclear matrix. In so doing Sp2 may determine whether cell divisions are symmetric or asymmetric. Several proteins are known to be asymmetrically distributed at the cell cortex during mitosis: the Par complex—consisting of Bazooka(Par3), Par6 and atypical protein kinase C (aPKC)—functions as a master polarity determinant, while Gαi, Pins(LGN/AGS3), Mud(NuMA) and p150glued(Dctn1), regulate spindle positioning (158). Disruption of the distribution of these proteins by Sp2 protein could result in the de-regulation of division

symmetry, resulting in the production of too few or too many cells of the wrong type. Components of the Notch signaling pathway are additional candidates for regulation by Sp2 as they play important roles in progenitor cell-fate decisions. For example, Hes1 and Hes5 are required for the repression of several genes (e.g., Mash1) that are required for neuronal cell differentiation (159, 160). Should de-regulated expression of Sp2 result in the induction of Hes1 and Hes5 transcription in epidermal stem cells, one would predict that differentiation would be blocked in this system. Regardless of the precise mechanisms involved, Sp2 transgenic mice will undoubtedly prove to be useful research tools.

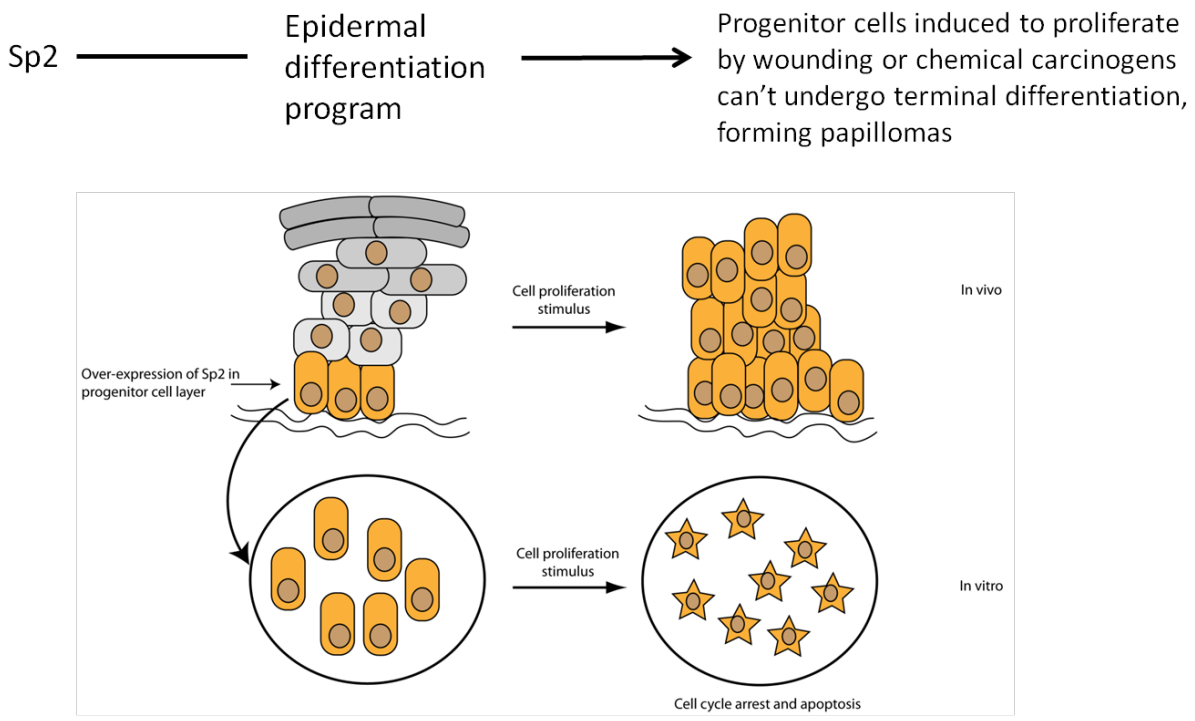

Figure 38 Summary of results obtained from Sp2 over-expressing model *in vivo* and *in vitro*.

REFERENCES

1. International Human Genome Sequencing Consortium. Finishing the euchromatic sequence of the human genome. *Nature.* 2004 Oct 21; 431(7011): 931-945.

2. Lander ES, Linton LM, Birren B, Nusbaum C, Zody MC, Baldwin J, Devon K, Dewar K, Doyle M, FitzHugh W, Funke R, Gage D, Harris K, Heaford A, Howland J, Kann L, Lehoczky J, LeVine R, McEwan P, McKernan K, Meldrim J, Mesirov JP, Miranda C, Morris W, Naylor J, Raymond C, Rosetti M, Santos R, Sheridan A, Sougnez C, Stange-Thomann N, Stojanovic N, Subramanian A, Wyman D, Rogers J, Sulston J, Ainscough R, Beck S, Bentley D, Burton J, Clee C, Carter N, Coulson A, Deadman R, Deloukas P, Dunham A, Dunham I, Durbin R, French L, Grafham D, Gregory S, Hubbard T, Humphray S, Hunt A, Jones M, Lloyd C, McMurray A, Matthews L, Mercer S, Milne S, Mullikin JC, Mungall A, Plumb R, Ross M, Shownkeen R, Sims S, Waterston RH, Wilson RK, Hillier LW, McPherson JD, Marra MA, Mardis ER, Fulton LA, Chinwalla AT, Pepin KH, Gish WR, Chissoe SL, Wendl MC, Delehaunty KD, Miner TL, Delehaunty A, Kramer JB, Cook LL, Fulton RS, Johnson DL, Minx PJ, Clifton SW, Hawkins T, Branscomb E, Predki P, Richardson P, Wenning S, Slezak T, Doggett N, Cheng JF, Olsen A, Lucas S, Elkin C, Uberbacher E, Frazier M, Gibbs RA, Muzny DM, Scherer SE, Bouck JB, Sodergren EJ, Worley KC, Rives CM, Gorrell JH, Metzker ML, Naylor SL, Kucherlapati RS, Nelson DL, Weinstock GM, Sakaki Y, Fujiyama A, Hattori M, Yada T, Toyoda A, Itoh T, Kawagoe C, Watanabe H, Totoki Y, Taylor T, Weissenbach J, Heilig R, Saurin W, Artiguenave F, Brottier P, Bruls T, Pelletier E, Robert C, Wincker P, Smith DR, Doucette-Stamm L, Rubenfield M, Weinstock K, Lee HM, Dubois J, Rosenthal A, Platzer M, Nyakatura G, Taudien S, Rump A, Yang H, Yu J, Wang J, Huang G, Gu J, Hood L, Rowen L, Madan A, Qin S, Davis RW, Federspiel NA, Abola AP, Proctor MJ, Myers RM, Schmutz J, Dickson M, Grimwood J, Cox DR, Olson MV, Kaul R, Raymond C, Shimizu N, Kawasaki K, Minoshima S, Evans GA, Athanasiou M, Schultz R, Roe BA, Chen F, Pan H, Ramser J, Lehrach H, Reinhardt R, McCombie WR, de la Bastide M, Dedhia N, Blocker H, Hornischer K, Nordsiek G, Agarwala R, Aravind L, Bailey JA, Bateman A, Batzoglou S, Birney E, Bork P, Brown DG, Burge CB, Cerutti L, Chen HC, Church D, Clamp M, Copley RR, Doerks T, Eddy SR, Eichler EE, Furey TS, Galagan J, Gilbert JG, Harmon C, Hayashizaki Y, Haussler D, Hermjakob H, Hokamp K, Jang W, Johnson LS, Jones TA, Kasif S, Kaspryzk A, Kennedy S, Kent WJ, Kitts P, Koonin EV, Korf I, Kulp D, Lancet D, Lowe TM, McLysaght A, Mikkelsen T, Moran JV, Mulder N, Pollara VJ, Ponting CP, Schuler G, Schultz J, Slater G, Smit AF, Stupka E, Szustakowski J, Thierry-Mieg D, Thierry-Mieg J, Wagner L, Wallis J, Wheeler R, Williams A, Wolf YI, Wolfe KH, Yang SP, Yeh RF, Collins F, Guyer MS, Peterson J, Felsenfeld A, Wetterstrand KA, Patrinos A, Morgan MJ, de Jong P, Catanese JJ, Osoegawa K, Shizuya H, Choi S, Chen YJ, International Human Genome Sequencing Consortium. Initial sequencing and analysis of the human genome. *Nature.* 2001 Feb 15; 409(6822): 860-921.

3. Schmidt D, Durrett R. Adaptive evolution drives the diversification of zinc-finger binding domains. *Mol Biol Evol.* 2004 Dec; 21(12): 2326-2339.

4. Hoovers JM, Mannens M, John R, Bliek J, van Heyningen V, Porteous DJ, Leschot NJ, Westerveld A, Little PF. High-resolution localization of 69 potential human zinc finger protein genes: A number are clustered. *Genomics.* 1992 Feb; 12(2): 254-263.

5. Tupler R, Perini G, Green MR. Expressing the human genome. *Nature.* 2001 Feb 15; 409(6822): 832-833.

6. Swamynathan SK. Kruppel-like factors: Three fingers in control. *Hum Genomics.* 2010 Apr; 4(4): 263-270. PMCID: PMC2975451.

7. Kaczynski J, Cook T, Urrutia R. Sp1- and kruppel-like transcription factors. *Genome Biol.* 2003; 4(2): 206. PMCID: PMC151296.

8. Dynan WS, Tjian R. Isolation of transcription factors that discriminate between different promoters recognized by RNA polymerase II. *Cell.* 1983 Mar; 32(3): 669-680.

9. Kadonaga JT, Carner KR, Masiarz FR, Tjian R. Isolation of cDNA encoding transcription factor Sp1 and functional analysis of the DNA binding domain. *Cell.* 1987 Dec 24; 51(6): 1079-1090.

10. Philipsen S, Suske G. A tale of three fingers: The family of mammalian Sp/XKLF transcription factors. *Nucleic Acids Res.* 1999 Aug 1; 27(15): 2991-3000. PMCID: PMC148522.

11. Hagen G, Muller S, Beato M, Suske G. Cloning by recognition site screening of two novel GT box binding proteins: A family of Sp1 related genes. *Nucleic Acids Res.* 1992 Nov 11; 20(21): 5519-5525. PMCID: PMC334381.

12. Kingsley C, Winoto A. Cloning of GT box-binding proteins: A novel Sp1 multigene family regulating T-cell receptor gene expression. *Mol Cell Biol.* 1992 Oct; 12(10): 4251-4261. PMCID: PMC360348.

13. Harrison SM, Houzelstein D, Dunwoodie SL, Beddington RS. Sp5, a new member of the Sp1 family, is dynamically expressed during development and genetically interacts with brachyury. *Dev Biol.* 2000 Nov 15; 227(2): 358-372.

14. Scohy S, Gabant P, Van Reeth T, Hertveldt V, Dreze PL, Van Vooren P, Riviere M, Szpirer J, Szpirer C. Identification of KLF13 and KLF14 (SP6), novel members of the SP/XKLF transcription factor family. *Genomics.* 2000 Nov 15; 70(1): 93-101.

15. Nakashima K, Zhou X, Kunkel G, Zhang Z, Deng JM, Behringer RR, de Crombrugghe B. The novel zinc finger-containing transcription factor osterix is required for osteoblast differentiation and bone formation. *Cell.* 2002 Jan 11; 108(1): 17-29.

16. Milona MA, Gough JE, Edgar AJ. Genomic structure and cloning of two transcript isoforms of human Sp8. *BMC Genomics.* 2004 Nov 8; 5: 86. PMCID: PMC534095.

17. Kawakami Y, Esteban CR, Matsui T, Rodriguez-Leon J, Kato S, Izpisua Belmonte JC. Sp8 and Sp9, two closely related buttonhead-like transcription factors, regulate Fgf8 expression and limb outgrowth in vertebrate embryos. *Development.* 2004 Oct; 131(19): 4763-4774.

18. Treichel D, Schock F, Jackle H, Gruss P, Mansouri A. mBtd is required to maintain signaling during murine limb development. *Genes Dev.* 2003 Nov 1; 17(21): 2630-2635. PMCID: PMC280612.

19. Saffer JD, Jackson SP, Annarella MB. Developmental expression of Sp1 in the mouse. *Mol Cell Biol.* 1991 Apr; 11(4): 2189-2199. PMCID: PMC359911.

20. Zhao C, Meng A. Sp1-like transcription factors are regulators of embryonic development in vertebrates. *Dev Growth Differ.* 2005 May; 47(4): 201-211.

21. Yin H, Nichols TD, Horowitz JM. Transcription of mouse Sp2 yields alternatively spliced and sub-genomic mRNAs in a tissue- and cell-type-specific fashion. *Biochim Biophys Acta.* 2010 Jul; 1799(7): 520-531. PMCID: PMC2893284.

22. Suske G, Bruford E, Philipsen S. Mammalian SP/KLF transcription factors: Bring in the family. *Genomics.* 2005 May; 85(5): 551-556.

23. Black AR, Black JD, Azizkhan-Clifford J. Sp1 and kruppel-like factor family of transcription factors in cell growth regulation and cancer. *J Cell Physiol.* 2001 Aug; 188(2): 143-160.

24. Pavletich NP, Pabo CO. Zinc finger-DNA recognition: Crystal structure of a Zif268-DNA complex at 2.1 A. *Science.* 1991 May 10; 252(5007): 809-817.

25. Letovsky J, Dynan WS. Measurement of the binding of transcription factor Sp1 to a single GC box recognition sequence. *Nucleic Acids Res.* 1989 Apr 11; 17(7): 2639-2653. PMCID: PMC317648.

26. Moorefield KS, Fry SJ, Horowitz JM. Sp2 DNA binding activity and trans-activation are negatively regulated in mammalian cells. *J Biol Chem.* 2004 Apr 2; 279(14): 13911-13924.

27. Kolell KJ, Crawford DL. Evolution of sp transcription factors. *Mol Biol Evol.* 2002 Mar; 19(3): 216-222.

28. Shields JM, Yang VW. Two potent nuclear localization signals in the gut-enriched kruppel-like factor define a subfamily of closely related kruppel proteins. *J Biol Chem.* 1997 Jul 18; 272(29): 18504-18507. PMCID: PMC2268085.

29. Song A, Patel A, Thamatrakoln K, Liu C, Feng D, Clayberger C, Krensky AM. Functional domains and DNA-binding sequences of RFLAT-1/KLF13, a kruppel-like transcription factor of activated T lymphocytes. *J Biol Chem.* 2002 Aug 16; 277(33): 30055-30065.

30. Courey AJ, Tjian R. Analysis of Sp1 in vivo reveals multiple transcriptional domains, including a novel glutamine-rich activation motif. *Cell.* 1988 Dec 2; 55(5): 887-898.

31. Suske G. The sp-family of transcription factors. *Gene.* 1999 Oct 1; 238(2): 291-300.

32. Roos MD, Su K, Baker JR, Kudlow JE. O glycosylation of an Sp1-derived peptide blocks known Sp1 protein interactions. *Mol Cell Biol.* 1997 Nov; 17(11): 6472-6480. PMCID: PMC232500.

33. Yang X, Su K, Roos MD, Chang Q, Paterson AJ, Kudlow JE. O-linkage of N-acetylglucosamine to Sp1 activation domain inhibits its transcriptional capability. *Proc Natl Acad Sci U S A.* 2001 Jun 5; 98(12): 6611-6616. PMCID: PMC34401.

34. Kadonaga JT, Carner KR, Masiarz FR, Tjian R. Isolation of cDNA encoding transcription factor Sp1 and functional analysis of the DNA binding domain. *Cell.* 1987 Dec 24; 51(6): 1079-1090.

35. Pascal E, Tjian R. Different activation domains of Sp1 govern formation of multimers and mediate transcriptional synergism. *Genes Dev.* 1991 Sep; 5(9): 1646-1656.

36. Safe S, Abdelrahim M. Sp transcription factor family and its role in cancer. *Eur J Cancer.* 2005 Nov; 41(16): 2438-2448.

37. Lee JA, Suh DC, Kang JE, Kim MH, Park H, Lee MN, Kim JM, Jeon BN, Roh HE, Yu MY, Choi KY, Kim KY, Hur MW. Transcriptional activity of Sp1 is regulated by molecular interactions between the zinc finger DNA binding domain and the inhibitory domain with corepressors, and this interaction is modulated by MEK. *J Biol Chem.* 2005 Jul 29; 280(30): 28061-28071.

38. Murata Y, Kim HG, Rogers KT, Udvadia AJ, Horowitz JM. Negative regulation of Sp1 trans-activation is correlated with the binding of cellular proteins to the amino terminus of the Sp1 trans-activation domain. *J Biol Chem.* 1994 Aug 12; 269(32): 20674-20681.

39. Majello B, De Luca P, Lania L. Sp3 is a bifunctional transcription regulator with modular independent activation and repression domains. *J Biol Chem.* 1997 Feb 14; 272(7): 4021-4026.

40. Dennig J, Beato M, Suske G. An inhibitor domain in Sp3 regulates its glutamine-rich activation domains. *EMBO J.* 1996 Oct 15; 15(20): 5659-5667. PMCID: PMC452310.

41. Courey AJ, Holtzman DA, Jackson SP, Tjian R. Synergistic activation by the glutamine-rich domains of human transcription factor Sp1. *Cell.* 1989 Dec 1; 59(5): 827-836.

42. Pore N, Liu S, Shu HK, Li B, Haas-Kogan D, Stokoe D, Milanini-Mongiat J, Pages G, O'Rourke DM, Bernhard E, Maity A. Sp1 is involved in akt-mediated induction of VEGF expression through an HIF-1-independent mechanism. *Mol Biol Cell.* 2004 Nov; 15(11): 4841-4853. PMCID: PMC524732.

43. Jackson SP, Tjian R. O-glycosylation of eukaryotic transcription factors: Implications for mechanisms of transcriptional regulation. *Cell.* 1988 Oct 7; 55(1): 125-133.

44. Huang W, Zhao S, Ammanamanchi S, Brattain M, Venkatasubbarao K, Freeman JW. Trichostatin A induces transforming growth factor beta type II receptor promoter activity and acetylation of Sp1 by recruitment of PCAF/p300 to a Sp1.NF-Y complex. *J Biol Chem.* 2005 Mar 18; 280(11): 10047-10054.

45. Su K, Roos MD, Yang X, Han I, Paterson AJ, Kudlow JE. An N-terminal region of Sp1 targets its proteasome-dependent degradation in vitro. *J Biol Chem.* 1999 May 21; 274(21): 15194-15202.

46. Spengler ML, Brattain MG. Sumoylation inhibits cleavage of Sp1 N-terminal negative regulatory domain and inhibits Sp1-dependent transcription. *J Biol Chem.* 2006 Mar 3; 281(9): 5567-5574.

47. Pugh BF, Tjian R. Mechanism of transcriptional activation by Sp1: Evidence for coactivators. *Cell.* 1990 Jun 29; 61(7): 1187-1197.

48. Kennett SB, Udvadia AJ, Horowitz JM. Sp3 encodes multiple proteins that differ in their capacity to stimulate or repress transcription. *Nucleic Acids Res.* 1997 Aug 1; 25(15): 3110-3117. PMCID: PMC146854.

49. Sapetschnig A, Koch F, Rischitor G, Mennenga T, Suske G. Complexity of translationally controlled transcription factor Sp3 isoform expression. *J Biol Chem.* 2004 Oct 1; 279(40): 42095-42105.

50. Ross S, Best JL, Zon LI, Gill G. SUMO-1 modification represses Sp3 transcriptional activation and modulates its subnuclear localization. *Mol Cell.* 2002 Oct; 10(4): 831-842.

51. Valin A, Gill G. Regulation of the dual-function transcription factor Sp3 by SUMO. *Biochem Soc Trans.* 2007 Dec; 35(Pt 6): 1393-1396.

52. Spengler ML, Kennett SB, Moorefield KS, Simmons SO, Brattain MG, Horowitz JM. Sumoylation of internally initiated Sp3 isoforms regulates transcriptional repression via a trichostatin A-insensitive mechanism. *Cell Signal.* 2005 Feb; 17(2): 153-166.

53. Braun H, Koop R, Ertmer A, Nacht S, Suske G. Transcription factor Sp3 is regulated by acetylation. *Nucleic Acids Res.* 2001 Dec 15; 29(24): 4994-5000. PMCID: PMC97549.

54. Ammanamanchi S, Freeman JW, Brattain MG. Acetylated sp3 is a transcriptional activator. *J Biol Chem.* 2003 Sep 12; 278(37): 35775-35780.

55. Kingsley C, Winoto A. Cloning of GT box-binding proteins: A novel Sp1 multigene family regulating T-cell receptor gene expression. *Mol Cell Biol.* 1992 Oct; 12(10): 4251-4261. PMCID: PMC360348.

56. Lin SY, Black AR, Kostic D, Pajovic S, Hoover CN, Azizkhan JC. Cell cycle-regulated association of E2F1 and Sp1 is related to their functional interaction. *Mol Cell Biol.* 1996 Apr; 16(4): 1668-1675. PMCID: PMC231153.

57. Moorefield KS, Yin H, Nichols TD, Cathcart C, Simmons SO, Horowitz JM. Sp2 localizes to subnuclear foci associated with the nuclear matrix. *Mol Biol Cell.* 2006 Apr; 17(4): 1711-1722. PMCID: PMC1415311.

58. Letourneur M, Valentino L, Travagli-Gross J, Bertoglio J, Pierre J. Sp2 regulates interferon-gamma-mediated socs1 gene expression. *Mol Immunol.* 2009 Jul; 46(11-12): 2151-2160.

59. Endo TA, Masuhara M, Yokouchi M, Suzuki R, Sakamoto H, Mitsui K, Matsumoto A, Tanimura S, Ohtsubo M, Misawa H, Miyazaki T, Leonor N, Taniguchi T, Fujita T, Kanakura Y, Komiya S, Yoshimura A. A new protein containing an SH2 domain that inhibits JAK kinases. *Nature.* 1997 Jun 26; 387(6636): 921-924.

60. Naka T, Narazaki M, Hirata M, Matsumoto T, Minamoto S, Aono A, Nishimoto N, Kajita T, Taga T, Yoshizaki K, Akira S, Kishimoto T. Structure and function of a new STAT-induced STAT inhibitor. *Nature.* 1997 Jun 26; 387(6636): 924-929.

61. Cawley S, Bekiranov S, Ng HH, Kapranov P, Sekinger EA, Kampa D, Piccolboni A, Sementchenko V, Cheng J, Williams AJ, Wheeler R, Wong B, Drenkow J, Yamanaka M, Patel S, Brubaker S, Tammana H, Helt G, Struhl K, Gingeras TR. Unbiased mapping of transcription factor binding sites along human chromosomes 21 and 22 points to widespread regulation of noncoding RNAs. *Cell.* 2004 Feb 20; 116(4): 499-509.

62. Finkenzeller G, Sparacio A, Technau A, Marme D, Siemeister G. Sp1 recognition sites in the proximal promoter of the human vascular endothelial growth factor gene are essential for platelet-derived growth factor-induced gene expression. *Oncogene.* 1997 Aug 7; 15(6): 669-676.

63. Rhee I, Bachman KE, Park BH, Jair KW, Yen RW, Schuebel KE, Cui H, Feinberg AP, Lengauer C, Kinzler KW, Baylin SB, Vogelstein B. DNMT1 and DNMT3b cooperate to silence genes in human cancer cells. *Nature.* 2002 Apr 4; 416(6880): 552-556.

64. Jinawath A, Miyake S, Yanagisawa Y, Akiyama Y, Yuasa Y. Transcriptional regulation of the human DNA methyltransferase 3A and 3B genes by Sp3 and Sp1 zinc finger proteins. *Biochem J.* 2005 Jan 15; 385(Pt 2): 557-564. PMCID: PMC1134729.

65. Marin M, Karis A, Visser P, Grosveld F, Philipsen S. Transcription factor Sp1 is essential for early embryonic development but dispensable for cell growth and differentiation. *Cell.* 1997 May 16; 89(4): 619-628.

66. Xie J, Yin H, Nichols TD, Yoder JA, Horowitz JM. Sp2 is a maternally inherited transcription factor required for embryonic development. *J Biol Chem.* 2010 Feb 5; 285(6): 4153-4164. PMCID: PMC2823555.

67. Baur F, Nau K, Sadic D, Allweiss L, Elsasser HP, Gillemans N, de Wit T, Kruger I, Vollmer M, Philipsen S, Suske G. Specificity protein 2 (Sp2) is essential for mouse development and autonomous proliferation of mouse embryonic fibroblasts. *PLoS One.* 2010 Mar 8; 5(3): e9587. PMCID: PMC2833205.

68. Bouwman P, Gollner H, Elsasser HP, Eckhoff G, Karis A, Grosveld F, Philipsen S, Suske G. Transcription factor Sp3 is essential for post-natal survival and late tooth development. *EMBO J.* 2000 Feb 15; 19(4): 655-661. PMCID: PMC305603.

69. Bouwman P, Gollner H, Elsasser HP, Eckhoff G, Karis A, Grosveld F, Philipsen S, Suske G. Transcription factor Sp3 is essential for post-natal survival and late tooth development. *EMBO J.* 2000 Feb 15; 19(4): 655-661. PMCID: PMC305603.

70. Gollner H, Dani C, Phillips B, Philipsen S, Suske G. Impaired ossification in mice lacking the transcription factor Sp3. *Mech Dev.* 2001 Aug; 106(1-2): 77-83.

71. Van Loo PF, Bouwman P, Ling KW, Middendorp S, Suske G, Grosveld F, Dzierzak E, Philipsen S, Hendriks RW. Impaired hematopoiesis in mice lacking the transcription factor Sp3. *Blood.* 2003 Aug 1; 102(3): 858-866.

72. Supp DM, Witte DP, Branford WW, Smith EP, Potter SS. Sp4, a member of the Sp1-family of zinc finger transcription factors, is required for normal murine growth, viability, and male fertility. *Dev Biol.* 1996 Jun 15; 176(2): 284-299.

73. Gollner H, Bouwman P, Mangold M, Karis A, Braun H, Rohner I, Del Rey A, Besedovsky HO, Meinhardt A, van den Broek M, Cutforth T, Grosveld F, Philipsen S, Suske G. Complex phenotype of mice homozygous for a null mutation in the Sp4 transcription factor gene. *Genes Cells.* 2001 Aug; 6(8): 689-697.

74. Treichel D, Becker MB, Gruss P. The novel transcription factor gene Sp5 exhibits a dynamic and highly restricted expression pattern during mouse embryogenesis. *Mech Dev.* 2001 Mar; 101(1-2): 175-179.

75. Hertveldt V, De Mees C, Scohy S, Van Vooren P, Szpirer J, Szpirer C. The Sp6 locus uses several promoters and generates sense and antisense transcripts. *Biochimie.* 2007 Nov; 89(11): 1381-1387.

76. Nakamura T, de Vega S, Fukumoto S, Jimenez L, Unda F, Yamada Y. Transcription factor epiprofin is essential for tooth morphogenesis by regulating epithelial cell fate and tooth number. *J Biol Chem.* 2008 Feb 22; 283(8): 4825-4833.

77. Hertveldt V, Louryan S, van Reeth T, Dreze P, van Vooren P, Szpirer J, Szpirer C. The development of several organs and appendages is impaired in mice lacking Sp6. *Dev Dyn.* 2008 Apr; 237(4): 883-892.

78. Milona MA, Gough JE, Edgar AJ. Expression of alternatively spliced isoforms of human Sp7 in osteoblast-like cells. *BMC Genomics.* 2003 Nov 7; 4: 43. PMCID: PMC280673.

79. Gao Y, Jheon A, Nourkeyhani H, Kobayashi H, Ganss B. Molecular cloning, structure, expression, and chromosomal localization of the human osterix (SP7) gene. *Gene.* 2004 Oct 27; 341: 101-110.

80. Bell SM, Schreiner CM, Waclaw RR, Campbell K, Potter SS, Scott WJ. Sp8 is crucial for limb outgrowth and neuropore closure. *Proc Natl Acad Sci U S A.* 2003 Oct 14; 100(21): 12195-12200. PMCID: PMC218735.

81. Zhao C, Meng A. Sp1-like transcription factors are regulators of embryonic development in vertebrates. *Dev Growth Differ.* 2005 May; 47(4): 201-211.

82. Lania L, Majello B, De Luca P. Transcriptional regulation by the sp family proteins. *Int J Biochem Cell Biol.* 1997 Dec; 29(12): 1313-1323.

83. Wang L, Wei D, Huang S, Peng Z, Le X, Wu TT, Yao J, Ajani J, Xie K. Transcription factor Sp1 expression is a significant predictor of survival in human gastric cancer. *Clin Cancer Res.* 2003 Dec 15; 9(17): 6371-6380.

84. Shi Q, Le X, Abbruzzese JL, Peng Z, Qian CN, Tang H, Xiong Q, Wang B, Li XC, Xie K. Constitutive Sp1 activity is essential for differential constitutive expression of vascular endothelial growth factor in human pancreatic adenocarcinoma. *Cancer Res.* 2001 May 15; 61(10): 4143-4154.

85. Yao JC, Wang L, Wei D, Gong W, Hassan M, Wu TT, Mansfield P, Ajani J, Xie K. Association between expression of transcription factor Sp1 and increased vascular

endothelial growth factor expression, advanced stage, and poor survival in patients with resected gastric cancer. *Clin Cancer Res.* 2004 Jun 15; 10(12 Pt 1): 4109-4117.

86. Zannetti A, Del Vecchio S, Carriero MV, Fonti R, Franco P, Botti G, D'Aiuto G, Stoppelli MP, Salvatore M. Coordinate up-regulation of Sp1 DNA-binding activity and urokinase receptor expression in breast carcinoma. *Cancer Res.* 2000 Mar 15; 60(6): 1546-1551.

87. Kitadai Y, Yasui W, Yokozaki H, Kuniyasu H, Haruma K, Kajiyama G, Tahara E. The level of a transcription factor Sp1 is correlated with the expression of EGF receptor in human gastric carcinomas. *Biochem Biophys Res Commun.* 1992 Dec 30; 189(3): 1342-1348.

88. Liang H, O'Reilly S, Liu Y, Abounader R, Laterra J, Maher VM, McCormick JJ. Sp1 regulates expression of MET, and ribozyme-induced down-regulation of MET in fibrosarcoma-derived human cells reduces or eliminates their tumorigenicity. *Int J Oncol.* 2004 May; 24(5): 1057-1067.

89. Chiefari E, Brunetti A, Arturi F, Bidart JM, Russo D, Schlumberger M, Filetti S. Increased expression of AP2 and Sp1 transcription factors in human thyroid tumors: A role in NIS expression regulation? *BMC Cancer.* 2002 Dec 10; 2: 35. PMCID: PMC139985.

90. Hosoi Y, Watanabe T, Nakagawa K, Matsumoto Y, Enomoto A, Morita A, Nagawa H, Suzuki N. Up-regulation of DNA-dependent protein kinase activity and Sp1 in colorectal cancer. *Int J Oncol.* 2004 Aug; 25(2): 461-468.

91. Kumar AP, Butler AP. Enhanced Sp1 DNA-binding activity in murine keratinocyte cell lines and epidermal tumors. *Cancer Lett.* 1999 Apr 1; 137(2): 159-165.

92. Lou Z, O'Reilly S, Liang H, Maher VM, Sleight SD, McCormick JJ. Down-regulation of overexpressed sp1 protein in human fibrosarcoma cell lines inhibits tumor formation. *Cancer Res.* 2005 Feb 1; 65(3): 1007-1017.

93. Guan H, Cai J, Zhang N, Wu J, Yuan J, Li J, Li M. Sp1 is upregulated in human glioma, promotes MMP-2-mediated cell invasion and predicts poor clinical outcome. *Int J Cancer.* 2011 Apr 5.

94. Phan D, Cheng CJ, Galfione M, Vakar-Lopez F, Tunstead J, Thompson NE, Burgess RR, Najjar SM, Yu-Lee LY, Lin SH. Identification of Sp2 as a transcriptional repressor of carcinoembryonic antigen-related cell adhesion molecule 1 in tumorigenesis. *Cancer Res.* 2004 May 1; 64(9): 3072-3078.

95. Pu YS, Luo W, Lu HH, Greenberg NM, Lin SH, Gingrich JR. Differential expression of C-CAM cell adhesion molecule in prostate carcinogenesis in a transgenic mouse model. *J Urol.* 1999 Sep; 162(3 Pt 1): 892-896.

96. Busch C, Hanssen TA, Wagener C, OBrink B. Down-regulation of CEACAM1 in human prostate cancer: Correlation with loss of cell polarity, increased proliferation rate, and gleason grade 3 to 4 transition. *Hum Pathol.* 2002 Mar; 33(3): 290-298.

97. Maurer GD, Leupold JH, Schewe DM, Biller T, Kates RE, Hornung HM, Lau-Werner U, Post S, Allgayer H. Analysis of specific transcriptional regulators as early predictors of independent prognostic relevance in resected colorectal cancer. *Clin Cancer Res.* 2007 Feb 15; 13(4): 1123-1132.

98. Essafi-Benkhadir K, Grosso S, Puissant A, Robert G, Essafi M, Deckert M, Chamorey E, Dassonville O, Milano G, Auberger P, Pages G. Dual role of Sp3 transcription factor as an inducer of apoptosis and a marker of tumour aggressiveness. *PLoS ONE.* 2009; 4(2): e4478. PMCID: PMC2636865.

99. Essafi-Benkhadir K, Grosso S, Puissant A, Robert G, Essafi M, Deckert M, Chamorey E, Dassonville O, Milano G, Auberger P, Pages G. Dual role of Sp3 transcription factor as an inducer of apoptosis and a marker of tumour aggressiveness. *PLoS One.* 2009; 4(2): e4478. PMCID: PMC2636865.

100. Abdelrahim M, Safe S. Cyclooxygenase-2 inhibitors decrease vascular endothelial growth factor expression in colon cancer cells by enhanced degradation of Sp1 and Sp4 proteins. *Mol Pharmacol.* 2005 Aug; 68(2): 317-329.

101. Pines A, Backendorf C. Matched cultures of keratinocytes and fibroblasts derived from normal and NER-deficient mouse models. *Methods Mol Biol.* 2010; 585: 45-57.

102. Jensen KB, Driskell RR, Watt FM. Assaying proliferation and differentiation capacity of stem cells using disaggregated adult mouse epidermis. *Nat Protoc.* 2010; 5(5): 898-911.

103. Yeung MC. Accelerated apoptotic DNA laddering protocol. *BioTechniques.* 2002 Oct; 33(4): 734, 736.

104. Pillai MM, Venkataraman GM, Kosak S, Torok-Storb B. Integration site analysis in transgenic mice by thermal asymmetric interlaced (TAIL)-PCR: Segregating multiple-integrant founder lines and determining zygosity. *Transgenic Res.* 2008 Aug; 17(4): 749-754.

105. Owens DM, Wei S, Smart RC. A multihit, multistage model of chemical carcinogenesis. *Carcinogenesis.* 1999 Sep; 20(9): 1837-1844.

106. Mouse Genome Sequencing Consortium, Waterston RH, Lindblad-Toh K, Birney E, Rogers J, Abril JF, Agarwal P, Agarwala R, Ainscough R, Alexandersson M, An P, Antonarakis SE, Attwood J, Baertsch R, Bailey J, Barlow K, Beck S, Berry E, Birren B, Bloom T, Bork P, Botcherby M, Bray N, Brent MR, Brown DG, Brown SD, Bult C, Burton J, Butler J, Campbell RD, Carninci P, Cawley S, Chiaromonte F, Chinwalla AT, Church DM, Clamp M, Clee C, Collins

FS, Cook LL, Copley RR, Coulson A, Couronne O, Cuff J, Curwen V, Cutts T, Daly M, David R, Davies J, Delehaunty KD, Deri J, Dermitzakis ET, Dewey C, Dickens NJ, Diekhans M, Dodge S, Dubchak I, Dunn DM, Eddy SR, Elnitski L, Emes RD, Eswara P, Eyras E, Felsenfeld A, Fewell GA, Flicek P, Foley K, Frankel WN, Fulton LA, Fulton RS, Furey TS, Gage D, Gibbs RA, Glusman G, Gnerre S, Goldman N, Goodstadt L, Grafham D, Graves TA, Green ED, Gregory S, Guigo R, Guyer M, Hardison RC, Haussler D, Hayashizaki Y, Hillier LW, Hinrichs A, Hlavina W, Holzer T, Hsu F, Hua A, Hubbard T, Hunt A, Jackson I, Jaffe DB, Johnson LS, Jones M, Jones TA, Joy A, Kamal M, Karlsson EK, Karolchik D, Kasprzyk A, Kawai J, Keibler E, Kells C, Kent WJ, Kirby A, Kolbe DL, Korf I, Kucherlapati RS, Kulbokas EJ, Kulp D, Landers T, Leger JP, Leonard S, Letunic I, Levine R, Li J, Li M, Lloyd C, Lucas S, Ma B, Maglott DR, Mardis ER, Matthews L, Mauceli E, Mayer JH, McCarthy M, McCombie WR, McLaren S, McLay K, McPherson JD, Meldrim J, Meredith B, Mesirov JP, Miller W, Miner TL, Mongin E, Montgomery KT, Morgan M, Mott R, Mullikin JC, Muzny DM, Nash WE, Nelson JO, Nhan MN, Nicol R, Ning Z, Nusbaum C, O'Connor MJ, Okazaki Y, Oliver K, Overton-Larty E, Pachter L, Parra G, Pepin KH, Peterson J, Pevzner P, Plumb R, Pohl CS, Poliakov A, Ponce TC, Ponting CP, Potter S, Quail M, Reymond A, Roe BA, Roskin KM, Rubin EM, Rust AG, Santos R, Sapojnikov V, Schultz B, Schultz J, Schwartz MS, Schwartz S, Scott C, Seaman S, Searle S, Sharpe T, Sheridan A, Shownkeen R, Sims S, Singer JB, Slater G, Smit A, Smith DR, Spencer B, Stabenau A, Stange-Thomann N, Sugnet C, Suyama M, Tesler G, Thompson J, Torrents D, Trevaskis E, Tromp J, Ucla C, Ureta-Vidal A, Vinson JP, Von Niederhausern AC, Wade CM, Wall M, Weber RJ, Weiss RB, Wendl MC, West AP, Wetterstrand K, Wheeler R, Whelan S, Wierzbowski J, Willey D, Williams S, Wilson RK, Winter E, Worley KC, Wyman D, Yang S, Yang SP, Zdobnov EM, Zody MC, Lander ES. Initial sequencing and comparative analysis of the mouse genome. *Nature.* 2002 Dec 5; 420(6915): 520-562.

107. Rosenthal N, Brown S. The mouse ascending: Perspectives for human-disease models. *Nat Cell Biol.* 2007 Sep; 9(9): 993-999.

108. Frese KK, Tuveson DA. Maximizing mouse cancer models. *Nat Rev Cancer.* 2007 Sep; 7(9): 645-658.

109. Palmiter RD, Brinster RL, Hammer RE, Trumbauer ME, Rosenfeld MG, Birnberg NC, Evans RM. Dramatic growth of mice that develop from eggs microinjected with metallothionein-growth hormone fusion genes. *Nature.* 1982 Dec 16; 300(5893): 611-615.

110. Cheon DJ, Orsulic S. Mouse models of cancer. *Annu Rev Pathol.* 2011 Feb 28; 6: 95-119.

111. Orsulic S, Li Y, Soslow RA, Vitale-Cross LA, Gutkind JS, Varmus HE. Induction of ovarian cancer by defined multiple genetic changes in a mouse model system. *Cancer Cell.* 2002 Feb; 1(1): 53-62. PMCID: PMC2267863.

112. Chin L, Tam A, Pomerantz J, Wong M, Holash J, Bardeesy N, Shen Q, O'Hagan R, Pantginis J, Zhou H, Horner JW,2nd, Cordon-Cardo C, Yancopoulos GD, DePinho RA.

Essential role for oncogenic ras in tumour maintenance. *Nature.* 1999 Jul 29; 400(6743): 468-472.

113. Hingorani SR, Petricoin EF, Maitra A, Rajapakse V, King C, Jacobetz MA, Ross S, Conrads TP, Veenstra TD, Hitt BA, Kawaguchi Y, Johann D, Liotta LA, Crawford HC, Putt ME, Jacks T, Wright CV, Hruban RH, Lowy AM, Tuveson DA. Preinvasive and invasive ductal pancreatic cancer and its early detection in the mouse. *Cancer Cell.* 2003 Dec; 4(6): 437-450.

114. Ramirez A, Bravo A, Jorcano JL, Vidal M. Sequences 5' of the bovine keratin 5 gene direct tissue- and cell-type-specific expression of a lacZ gene in the adult and during development. *Differentiation.* 1994 Nov; 58(1): 53-64.

115. Brinster RL, Allen JM, Behringer RR, Gelinas RE, Palmiter RD. Introns increase transcriptional efficiency in transgenic mice. *Proc Natl Acad Sci U S A.* 1988 Feb; 85(3): 836-840. PMCID: PMC279650.

116. Ichtchenko K, Bittner MA, Krasnoperov V, Little AR, Chepurny O, Holz RW, Petrenko AG. A novel ubiquitously expressed alpha-latrotoxin receptor is a member of the CIRL family of G-protein-coupled receptors. *J Biol Chem.* 1999 Feb 26; 274(9): 5491-5498.

117. Arcos-Burgos M, Jain M, Acosta MT, Shively S, Stanescu H, Wallis D, Domene S, Velez JI, Karkera JD, Balog J, Berg K, Kleta R, Gahl WA, Roessler E, Long R, Lie J, Pineda D, Londono AC, Palacio JD, Arbelaez A, Lopera F, Elia J, Hakonarson H, Johansson S, Knappskog PM, Haavik J, Ribases M, Cormand B, Bayes M, Casas M, Ramos-Quiroga JA, Hervas A, Maher BS, Faraone SV, Seitz C, Freitag CM, Palmason H, Meyer J, Romanos M, Walitza S, Hemminger U, Warnke A, Romanos J, Renner T, Jacob C, Lesch KP, Swanson J, Vortmeyer A, Bailey-Wilson JE, Castellanos FX, Muenke M. A common variant of the latrophilin 3 gene, LPHN3, confers susceptibility to ADHD and predicts effectiveness of stimulant medication. *Mol Psychiatry.* 2010 Nov; 15(11): 1053-1066.

118. Bin Sun H, Ruan Y, Xu ZC, Yokota H. Involvement of the calcium-independent receptor for alpha-latrotoxin in brain ischemia. *Brain Res Mol Brain Res.* 2002 Aug 15; 104(2): 246-249.

119. Moll R, Franke WW, Schiller DL, Geiger B, Krepler R. The catalog of human cytokeratins: Patterns of expression in normal epithelia, tumors and cultured cells. *Cell.* 1982 Nov; 31(1): 11-24.

120. Lane EB, McLean WH. Keratins and skin disorders. *J Pathol.* 2004 Nov; 204(4): 355-366.

121. Oshima RG, Baribault H, Caulin C. Oncogenic regulation and function of keratins 8 and 18. *Cancer Metastasis Rev.* 1996 Dec; 15(4): 445-471.

122. Lu H, Hesse M, Peters B, Magin TM. Type II keratins precede type I keratins during early embryonic development. *Eur J Cell Biol.* 2005 Aug; 84(8): 709-718.

123. Yamada S, Wirtz D, Coulombe PA. Pairwise assembly determines the intrinsic potential for self-organization and mechanical properties of keratin filaments. *Mol Biol Cell.* 2002 Jan; 13(1): 382-391. PMCID: PMC65095.

124. Omary MB, Ku NO, Strnad P, Hanada S. Toward unraveling the complexity of simple epithelial keratins in human disease. *J Clin Invest.* 2009 Jul; 119(7): 1794-1805. PMCID: PMC2701867.

125. Trempus CS, Morris RJ, Bortner CD, Cotsarelis G, Faircloth RS, Reece JM, Tennant RW. Enrichment for living murine keratinocytes from the hair follicle bulge with the cell surface marker CD34. *J Invest Dermatol.* 2003 Apr; 120(4): 501-511.

126. Trempus CS, Morris RJ, Ehinger M, Elmore A, Bortner CD, Ito M, Cotsarelis G, Nijhof JG, Peckham J, Flagler N, Kissling G, Humble MM, King LC, Adams LD, Desai D, Amin S, Tennant RW. CD34 expression by hair follicle stem cells is required for skin tumor development in mice. *Cancer Res.* 2007 May 1; 67(9): 4173-4181. PMCID: PMC2121659.

127. Liu Y, Lyle S, Yang Z, Cotsarelis G. Keratin 15 promoter targets putative epithelial stem cells in the hair follicle bulge. *J Invest Dermatol.* 2003 Nov; 121(5): 963-968.

128. Ito M, Liu Y, Yang Z, Nguyen J, Liang F, Morris RJ, Cotsarelis G. Stem cells in the hair follicle bulge contribute to wound repair but not to homeostasis of the epidermis. *Nat Med.* 2005 Dec; 11(12): 1351-1354.

129. Bogden AE, Moreau JP, Eden PA. Proliferative response of human and animal tumours to surgical wounding of normal tissues: Onset, duration and inhibition. *Br J Cancer.* 1997; 75(7): 1021-1027. PMCID: PMC2222742.

130. Arwert EN, Lal R, Quist S, Rosewell I, van Rooijen N, Watt FM. Tumor formation initiated by nondividing epidermal cells via an inflammatory infiltrate. *Proc Natl Acad Sci U S A.* 2010 Nov 16; 107(46): 19903-19908. PMCID: PMC2993377.

131. Hobbs RM, Silva-Vargas V, Groves R, Watt FM. Expression of activated MEK1 in differentiating epidermal cells is sufficient to generate hyperproliferative and inflammatory skin lesions. *J Invest Dermatol.* 2004 Sep; 123(3): 503-515.

132. Musson RE, Smit NP. Regulatory mechanisms of calcineurin phosphatase activity. *Curr Med Chem.* 2011; 18(2): 301-315.

133. Schuh AC, Keating SJ, Monteclaro FS, Vogt PK, Breitman ML. Obligatory wounding requirement for tumorigenesis in v-jun transgenic mice. *Nature.* 1990 Aug 23; 346(6286): 756-760.

134. Battalora MS, Spalding JW, Szczesniak CJ, Cape JE, Morris RJ, Trempus CS, Bortner CD, Lee BM, Tennant RW. Age-dependent skin tumorigenesis and transgene expression in the tg.AC (v-ha-ras) transgenic mouse. *Carcinogenesis.* 2001 Apr; 22(4): 651-659.

135. Cannon RE, Spalding JW, Trempus CS, Szczesniak CJ, Virgil KM, Humble MC, Tennant RW. Kinetics of wound-induced v-ha-ras transgene expression and papilloma development in transgenic tg.AC mice. *Mol Carcinog.* 1997 Sep; 20(1): 108-114.

136. Sieweke MH, Thompson NL, Sporn MB, Bissell MJ. Mediation of wound-related rous sarcoma virus tumorigenesis by TGF-beta. *Science.* 1990 Jun 29; 248(4963): 1656-1660.

137. Vassar R, Fuchs E. Transgenic mice provide new insights into the role of TGF-alpha during epidermal development and differentiation. *Genes Dev.* 1991 May; 5(5): 714-727.

138. Martins-Green M, Boudreau N, Bissell MJ. Inflammation is responsible for the development of wound-induced tumors in chickens infected with rous sarcoma virus. *Cancer Res.* 1994 Aug 15; 54(16): 4334-4341.

139. Stuelten CH, Barbul A, Busch JI, Sutton E, Katz R, Sato M, Wakefield LM, Roberts AB, Niederhuber JE. Acute wounds accelerate tumorigenesis by a T cell-dependent mechanism. *Cancer Res.* 2008 Sep 15; 68(18): 7278-7282. PMCID: PMC2766858.

140. Grose R, Werner S. Wound-healing studies in transgenic and knockout mice. *Mol Biotechnol.* 2004 Oct; 28(2): 147-166.

141. Gurtner GC, Werner S, Barrandon Y, Longaker MT. Wound repair and regeneration. *Nature.* 2008 May 15; 453(7193): 314-321.

142. Goodson WH,3rd, Hunt TK. Wound healing and aging. *J Invest Dermatol.* 1979 Jul; 73(1): 88-91.

143. D'Souza SJ, Vespa A, Murkherjee S, Maher A, Pajak A, Dagnino L. E2F-1 is essential for normal epidermal wound repair. *J Biol Chem.* 2002 Mar 22; 277(12): 10626-10632.

144. Burns PA, Bremner R, Balmain A. Genetic changes during mouse skin tumorigenesis. *Environ Health Perspect.* 1991 Jun; 93: 41-44. PMCID: PMC1568051.

145. Ray KC, Bell KM, Yan J, Gu G, Chung CH, Washington MK, Means AL. Epithelial tissues have varying degrees of susceptibility to kras(G12D)-initiated tumorigenesis in a mouse model. *PLoS One.* 2011 Feb 2; 6(2): e16786. PMCID: PMC3032792.

146. Bos JL. Ras oncogenes in human cancer: A review. *Cancer Res.* 1989 Sep 1; 49(17): 4682-4689.

147. Capella G, Cronauer-Mitra S, Pienado MA, Perucho M. Frequency and spectrum of mutations at codons 12 and 13 of the c-K-ras gene in human tumors. *Environ Health Perspect.* 1991 Jun; 93: 125-131. PMCID: PMC1568052.

148. Corominas M, Sloan SR, Leon J, Kamino H, Newcomb EW, Pellicer A. Ras activation in human tumors and in animal model systems. *Environ Health Perspect.* 1991 Jun; 93: 19-25. PMCID: PMC1568045.

149. Nelson MA, Futscher BW, Kinsella T, Wymer J, Bowden GT. Detection of mutant ha-ras genes in chemically initiated mouse skin epidermis before the development of benign tumors. *Proc Natl Acad Sci U S A.* 1992 Jul 15; 89(14): 6398-6402. PMCID: PMC49508.

150. Blanpain C, Fuchs E. Epidermal homeostasis: A balancing act of stem cells in the skin. *Nat Rev Mol Cell Biol.* 2009 Mar; 10(3): 207-217. PMCID: PMC2760218.

151. El Ghalbzouri A, Jonkman MF, Dijkman R, Ponec M. Basement membrane reconstruction in human skin equivalents is regulated by fibroblasts and/or exogenously activated keratinocytes. *J Invest Dermatol.* 2005 Jan; 124(1): 79-86.

152. Spichkina OG, Kalmykova NV, Kukhareva LV, Voronkina IV, Blinova MI, Pinaev GP. Isolation of human basal keratinocytes by selective adhesion to extracellular matrix proteins. *Tsitologiia.* 2006; 48(10): 841-847.

153. Prunieras M. Recent advances in epidermal cell cultures. *Arch Dermatol Res.* 1979 Mar 31; 264(2): 243-247.

154. Roy S, Khanna S, Bickerstaff AA, Subramanian SV, Atalay M, Bierl M, Pendyala S, Levy D, Sharma N, Venojarvi M, Strauch A, Orosz CG, Sen CK. Oxygen sensing by primary cardiac fibroblasts: A key role of p21(Waf1/Cip1/Sdi1). *Circ Res.* 2003 Feb 21; 92(3): 264-271.

155. Lin TP, Hom YK, Richards J, Nandi S. Effects of antioxidants and reduced oxygen tension on rat mammary epithelial cells in culture. *In Vitro Cell Dev Biol.* 1991 Mar; 27A(3 Pt 1): 191-196.

156. Sherr CJ. Divorcing ARF and p53: An unsettled case. *Nat Rev Cancer.* 2006 Sep; 6(9): 663-673.

157. Candi E, Cipollone R, Rivetti di Val Cervo P, Gonfloni S, Melino G, Knight R. P63 in epithelial development. *Cell Mol Life Sci.* 2008 Oct; 65(20): 3126-3133.

158. Williams SE, Beronja S, Pasolli HA, Fuchs E. Asymmetric cell divisions promote notch-dependent epidermal differentiation. *Nature.* 2011 Feb 17; 470(7334): 353-358. PMCID: PMC3077085.

159. Cau E, Gradwohl G, Casarosa S, Kageyama R, Guillemot F. Hes genes regulate sequential stages of neurogenesis in the olfactory epithelium. *Development.* 2000 Jun; 127(11): 2323-2332.

160. Baek JH, Hatakeyama J, Sakamoto S, Ohtsuka T, Kageyama R. Persistent and high levels of Hes1 expression regulate boundary formation in the developing central nervous system. *Development.* 2006 Jul; 133(13): 2467-2476.